



UNIVERSIDADE ESTADUAL DE CAMPINAS

FACULDADE DE ENGENHARIA ELÉTRICA E DE COMPUTAÇÃO

CARINA MARCONI GERMER

**EVALUATION OF THE EFFECTS OF SINUSOIDAL VIBROTACTILE STIMULATION ON  
THE NEUROPHYSIOLOGICAL CONTROL OF MUSCLE FORCE**

AVALIAÇÃO DOS EFEITOS DA ESTIMULAÇÃO VIBROTÁTIL SENOIDAL NO CONTROLE  
NEUROFISIOLÓGICO DA FORÇA MUSCULAR

CAMPINAS

2019

CARINA MARCONI GERMER

**EVALUATION OF THE EFFECTS OF SINUSOIDAL VIBROTACTILE STIMULATION ON  
THE NEUROPHYSIOLOGICAL CONTROL OF MUSCLE FORCE**

AVALIAÇÃO DOS EFEITOS DA ESTIMULAÇÃO VIBROTÁTIL SENOIDAL NO CONTROLE  
NEUROFISIOLÓGICO DA FORÇA MUSCULAR

Thesis submitted to the School of Electrical and Computer Engineering,  
University of Campinas, in partial fulfillment of the requirements for the  
degree of Doctor in Electrical Engineering, in the area of Biomedical  
Engineering.

*Tese apresentada à Faculdade de Engenharia Elétrica e de  
Computação da Universidade Estadual de Campinas como parte dos  
requisitos exigidos para a obtenção do título Doutora em Engenharia  
Elétrica, na área de Engenharia Biomédica.*

SUPERVISOR: LEONARDO ABDALA ELIAS

ESTE TRABALHO CORRESPONDE À VERSÃO  
FINAL DA TESE DEFENDIDA PELA ALUNA  
CARINA MARCONI GERMER, E ORIENTADA  
PELO PROF. DR. LEONARDO ABDALA ELIAS.

CAMPINAS

2019

Ficha catalográfica  
Universidade Estadual de Campinas  
Biblioteca da Área de Engenharia e Arquitetura  
Rose Meire da Silva - CRB 8/5974

G317e Germer, Carina Marconi, 1990-  
Evaluation of the effects of sinusoidal vibrotactile stimulation on the neurophysiological control of muscle force / Carina Marconi Germer. – Campinas, SP : [s.n.], 2019.

Orientador: Leonardo Abdala Elias.  
Tese (doutorado) – Universidade Estadual de Campinas, Faculdade de Engenharia Elétrica e de Computação.

1. Neurônios motores. 2. Mecanorreceptores. I. Elias, Leonardo Abdala, 1985-. II. Universidade Estadual de Campinas. Faculdade de Engenharia Elétrica e de Computação. III. Título.

Informações para Biblioteca Digital

**Título em outro idioma:** Avaliação dos efeitos da estimulação vibrotátil senoidal no controle neurofisiológico da força muscular

**Palavras-chave em inglês:**

Motor neurons

Mechanoreceptors

**Área de concentração:** Engenharia Biomédica

**Titulação:** Doutora em Engenharia Elétrica

**Banca examinadora:**

Leonardo Abdala Elias [Orientador]

Fernando Henrique Magalhães

Renato Naville Watanabe

Carlos Julio Tierra Criollo

Antônio Augusto Fasolo Quevedo

**Data de defesa:** 02-09-2019

**Programa de Pós-Graduação:** Engenharia Elétrica

Identificação e informações acadêmicas do(a) aluno(a)

- ORCID do autor: <https://orcid.org/0000-0002-7323-3767>

- Currículo Lattes do autor: <http://lattes.cnpq.br/8205284377032041>

## COMISSÃO JULGADORA – TESE DE DOUTORADO

**Candidata:** Carina Marconi Germer RA:086305

**Data da Defesa:** 2 de setembro de 2019

**Título da Tese:** “Evaluation of the effects of sinusoidal vibrotactile stimulation on the neurophysiological control of muscle force”.

**Título em outro idioma:** Avaliação dos efeitos da estimulação vibrotátil senoidal no controle neurofisiológico da força muscular

PROF. DR. LEONARDO ABDALA ELIAS

PROF. DR. CARLOS JULIO TIERRA CRIOLLO

PROF. DR. FERNANDO HENRIQUE MAGALHÃES

PROF. DR. RENATO NAVILLE WATANABE

PROF. DR. ANTÔNIO AUGUSTO FASOLO QUEVEDO

A ata da defesa, com as respectivas assinaturas dos membros da Comissão Julgadora, encontra-se no SIGA (Sistema de Fluxo de Dissertação/Tese) e na Secretaria de Pós-Graduação da Faculdade de Engenharia Elétrica e de Computação.

## ACKNOWLEDGMENTS

---

First and foremost, I would like to thank my supervisor Dr. Leonardo A. Elias for his unconditional support, continuous encouragement, and advice throughout this work. Thank you also to Dr. Dario Farina for the opportunity to work in one of the most significant research groups in the field of Neuroscience. It was an honor working with you. Special thanks are also given to Dr. Alessandro Del Vecchio for his dedication and assistance during my stay at the Imperial College London (ICL). I hope we keep our fruitful collaboration. Thanks to all my colleagues at ICL that made my stay in London memorable.

I would also like to thank all the collaborators I had during this PhD. Firstly, thanks to Luciana S. Moreira for being a great coworker, and for all the time we spent in the lab discussing experimental protocols and performing experiments. Thank you, Dr. Francesco Negro, for all the stimulating discussions we had. Also, to all my friends from the Neural Engineering Research Lab. for ongoing discussions in our lab meetings.

Within the Department of Biomedical Engineering, I would like to express my gratitude to all professors for envisaging the importance of my work and providing me financial support to attend scientific conferences. I also thank Prof. Dr. Pedro Peres for fighting for the resources with CAPES (Coordination for the Improvement of Higher Education Personnel, Brazil) that allowed me to get the Visiting Student Grant. Thanks also to the technical personnel from the Center for Biomedical Engineering that provided support to the study: Mr. Mauro Martinazo, Mr. Renato Moura, Mr. Flavio Santos, and Mr. Carlos Silva.

A special thanks to CAPES for the PhD Scholarship and Visiting Student Grant (PDSE/CAPES, Ministry of Education, Brazil, proc. no. 88881.134842/2016-01). Thank is also given to agencies that provided funding to Prof. Dr. Leonardo A. Elias. These funding opportunities were fundamental for setting up the laboratory. Research Grants from Teaching, Research, and Extension Support Fund of the University of Campinas (FAEPEX/UNICAMP, procs. nos. 1483/14 and 3289/16), CNPq (Brazilian NSF, proc. no. 312442/2017-3), and FAPESP (The Sao Paulo Research Foundation, proc. no. 2017/22191-3).

Finally, I wish to acknowledge my family for all the love and support during this PhD. All my love and gratitude to my husband, parents, and brother. Without them, the lengthy process of completing a PhD would be much more difficult.

## ABSTRACT

---

Peripheral feedback is of paramount importance not only for sensory perception but also for the neural control of voluntary movements. Cutaneous afferents are responsible for a wide range of touch sensation and have a crucial role in modulating motor behavior. An exciting effect induced by the stimulation of mechanoreceptors at the skin is the improvement of sensorimotor performance. The beneficial effect of vibrotactile stimulation is attributed to the occurrence of stochastic resonance in the nervous system. The central hypothesis is that a specific intensity of vibrotactile stimulus would increase the afferent inflow, thereby improving the sensorimotor integration in the central nervous system. In this work, we aim at evaluating the effects of a sinusoidal vibrotactile stimulation on the neurophysiological control of muscle force. We first explored the effects of sinusoidal vibrotactile stimulation on force steadiness during isometric visuomotor tasks. We further evaluated the influence of contraction intensity and handedness on the motor improvement caused by vibrotactile stimulation. Finally, we evaluated the firing properties of a population of motor units recorded during a motor-enhanced task. At the end of this material, we will provide novel interpretations on the neurophysiological mechanisms behind the influence of cutaneous sensory inputs on muscle force control.

Keywords: motor control; sensorimotor system; motor units; cutaneous mechanoreceptors.

## RESUMO

---

A realimentação das vias sensoriais periféricas é de suma importância, não apenas para a percepção sensorial, mas também para o controle neural dos movimentos voluntários. As aferentes cutâneas são responsáveis por uma ampla gama de sensações de toque e têm um papel crucial na modulação do comportamento motor. Um interessante efeito induzido pela estimulação dos mecanorreceptores cutâneos é a melhora do desempenho sensório-motor. O efeito benéfico da estimulação vibrotátil é atribuído à ocorrência de ressonância estocástica no sistema nervoso. A hipótese principal é que uma intensidade específica do estímulo vibrotátil aumentaria o influxo das aferentes, melhorando assim a integração sensório-motora no sistema nervoso central. Neste trabalho, pretendemos avaliar os efeitos de uma estimulação vibrotátil senoidal no controle neurofisiológico da força muscular. Primeiramente, exploramos os efeitos da estimulação vibrotátil senoidal na variabilidade da força muscular durante tarefas visuomotoras isométricas. Ademais, avaliamos a influência da intensidade de contração e lateralidade na melhora motora causada pela estimulação vibrotátil. Por fim, avaliamos as propriedades de disparos de uma população de unidades motoras registradas durante uma tarefa motora aprimorada pela estimulação vibrotátil. No final deste material, forneceremos novas interpretações dos mecanismos neurofisiológicos por trás da influência das aferentes sensoriais cutâneas no controle da força muscular.

Palavras-chave: controle motor; sistema sensório-motor; unidades motoras; mecanorreceptores cutâneos.



# LIST OF FIGURES

---

Figure 1. Schematic diagram illustrating the putative connections between cutaneous afferents and neuronal circuits in the central nervous system (CNS). A $\beta$  cutaneous afferents from the index finger project to alpha motor neurons (MNs) innervating the first dorsal interosseous (FDI) muscle through oligosynaptic pathways encompassing spinal and supraspinal interneurons (INs), along with cortical motor neurons. Cutaneous inputs can also influence the activity of primary afferent depolarization (PAD) INs, which are responsible for the presynaptic inhibition of Ia afferents from muscle spindles. Adapted from Pierrot-Deseilligny and Burke (2012). 18

Figure 2. Schematic representation of the experimental setup and representative data. (a) Mechanical apparatus used to record index finger abduction forces. Isometric forces were measured at the distal interphalangeal joint (i) by a piezoresistive force transducer. The linear resonant actuator and accelerometer were placed at the radial surface of the metacarpophalangeal joint of the index finger (ii). All the fingers, but the index, and wrist were fixed to the apparatus with Velcro straps. (b) Example of a typical force signal recorded from a subject. Six vibrotactile stimuli were randomly applied to the finger skin during force-matching tasks. Vibrations with five different intensities (marked as V1 to V5) and a no-vibration control condition (CTR) were applied to the finger skin for 4s each block. The total duration of the trial was 30s (initial and final segments of the time series were discarded for the analysis). (c) Illustrative analysis of force coefficient of variation (CoV) for one subject. The effect of vibration intensities on force variability (relative to the control condition) was evaluated at 5% (light gray), 10% (dark gray) and 15% (black) of the maximal voluntary contraction (MVC). Black circles depict the optimal vibration, which was defined as the vibration amplitude that produced the lowest force CoV (relative to CTR) for each contraction intensity. 29

Figure 3. Representative force CoV in different vibration intensities relative to the condition without vibration (CTR). Values below one (dashed line) indicate a decrease in force CoV as compared to the CTR condition. Lines represent individual data (per subject) at 5%MVC (a), 10%MVC (b), and 15%MVC (c). The optimal vibration (OV) for each subject is marked with a black dot. 34

Figure 4. Data from the repetitions performed by each subject (columns) at 5%MVC (a), 10%MVC (b), and 15%MVC (c). Individual trials are depicted in gray light lines, while the average force CoV is represented by black tick lines with error bars (95% confidence interval). Missing data (see third and fourth columns in the middle panel and the last column in the bottom panel) represent subjects that did not present an OV. 34

Figure 5. Force CoV (a), standard deviation (SD) (b), and approximate entropy (ApEn) (c) at three contraction intensities (5%MVC, 10%MVC and 15%MVC) for CTR (black) and OV (gray) conditions. Asterisks represent the statistical significance for vibration conditions (OV vs CTR, \*\*  $0.001 < p < 0.010$ , \*\*\*  $p < 0.001$ ). 36

Figure 6. (a) Relation between force CoV and the mean force. (b) Relation between force SD and the mean force. In both panels, black and open circles represent CTR and OV conditions, respectively.

Dashed and dotted lines are fittings to the experimental data (see inset equations and  $R^2$  values). Black thick line in panel A is the difference between the fittings for CTR and OV data. 36

Figure 7. Frequency-domain properties of force signals. (a) Relative power in the low-frequency (0-4Hz) band. (b) Relative power in the intermediate-frequency band (4-8Hz) (c) Relative power in the 8-12Hz band (physiological tremor). Data are presented for the three contraction intensities (5%MVC, 10%MVC and 15%MVC) in both CTR and (black) OV (gray) conditions. Asterisks represent the statistical significance for vibration conditions (\*\*  $0.001 < p < 0.010$ , \*\*\*  $p < 0.001$ ). 38

Figure 8. Schematic representation of the experimental setup and representative data. (a) Mechanical apparatus used to record index finger abduction forces. Isometric forces were measured at the distal interphalangeal joint (i) by a piezoresistive force transducer. The linear resonant actuator and accelerometer were placed at the radial surface of the metacarpophalangeal joint of the index finger (ii). The wrist and all fingers, but the index, were fixed to the apparatus with Velcro straps. (b) Power spectrum for the acceleration measured on the surface of the linear resonant actuator for different vibration intensities (inset) (c) Average acceleration measured for each vibration intensity: control (CTR) condition, and five different vibration intensities (V1 to V5). (d) Example of a typical force signal recorded from a subject. Six vibrotactile stimuli (CTR and V1 to V5) were randomly applied to the finger skin during force-matching tasks in blocks of 4s each. The total duration of the trial was 30s. Experiments were carried out on dominant and non-dominant hands. Gray lines represent the segments used for data analysis. 52

Figure 9 - (a) Force coefficient of variation (CoV) for non-dominant (ND, in black) and dominant (D, in gray) hands in no-vibration condition (CTR) and in five intensities of vibrations (V1 to V5). (b) Vibration intensity selected as optimal vibration (OV) for each subject (columns) for ND (black diamond) and D (gray square). (c) Effect of OV (showed in (b)) on force CoV. (d) Effect of OV selected from either ND ( $OV_{ND}$ , demarked as black diamonds in (b)) or D ( $OV_D$ , demarked as gray squares in (b)) on force CoV. Light gray lines indicate average force CoV for CTR. † Different from CTR, \* Significant differences (\*\*  $0.001 < p < 0.010$ , \*\*\*  $p < 0.001$ ). 56

Figure 10. Force coefficient of variation (CoV) from the condition without vibration (CTR), and from the vibration condition selected using the three methods: i) the best performance when all vibration intensities were considered in the statistical model (V3); ii) the optimal vibration (OV) obtained from each hand separately; and the OV obtained from a single hand ( $OV_D$ ). † Different from CTR, \* Significant differences (\*\*  $0.001 < p < 0.010$ ). 58

Figure 11. (a) Approximate entropy (ApEn) of force signals in CTR and OV conditions. (b) Relative power of the force in the frequency band between zero and 5Hz. (c) The same as (b) but for the frequency band between 7Hz and 12Hz (physiological tremor). Black bars represent data from the non-dominant (ND) hand, while gray bars represent data from the dominant hand (D). Asterisks represent the statistical significance (\*\*  $0.001 < p < 0.010$ , \*\*\*  $p < 0.001$ ). 59

Figure 12 Experimental protocol and data analysis. (a) Mechanical apparatus used to record index finger abduction force. Isometric forces were measured at the distal interphalangeal joint and a linear resonant actuator was placed at the radial surface of the metacarpophalangeal joint of the index finger (i). A high-density (HD) surface EMG grid with 64 electrodes was placed on the first dorsal interosseous

(FDI) muscle (ii). (b) Representative recordings of force signals from a single participant in CTR (black) and OV (gray) conditions at 5%MVC. Data analysis was carried out on data confined between the dashed lines (i.e., between 23 s and 44 s) so as to avoid non-stationarities. (c) Representative analysis of the influence of vibrotactile stimulation on force steadiness (force CoV) for two participants. The effects of low-intensity (LV), intermediate-intensity (IV), and high-intensity (HV) vibration on force CoV were normalized to the non-vibration control condition (CTR). Black circles depict the optimal vibration (OV), which was defined as the vibration amplitude that produced the lowest force CoV (relative to CTR) for each participant at each contraction intensity. Note that the participant on the right panel did not have an OV at 2.50%MVC. (d) Data analysis performed on HD surface EMG signals. Leftmost signals represent the data from the 64 EMG channels (rows) recorded during CTR (black) and OV (gray) conditions. The EMG channels were decomposed into motor unit spike trains (middle), so that each row represents one motor unit and the vertical bars represent the discharge timings. The neural drive to the muscle (rightmost signals) was estimated as the smoothed cumulative spike train (sCST), which consists of a lowpass filtered (LPF) version (at 2.50Hz) of the cumulative spike trains (see Sec. 2.5.3 for details).

73

Figure 13. Schematic diagram of the motor neuron pool model for the two scenarios explored here: (a) with a single common input (corticomotor drive), and (b) with two common inputs (corticomotor and secondary drives). In addition, in both scenarios each motor neuron received independent commands (noise). Common presynaptic commands were represented by Gamma point processes with mean interspike intervals ( $\mu$ ) and order ( $k$ ) varying according to the values presented between the brackets.

79

Figure 14. Experimental results. (a) Force CoV as a function of force intensities (2.50% and 5%MVC) and vibration conditions (control, CTR, and optimal vibration, OV). (b-d) The same as (a), but for the interspike (ISI) coefficient of variation (CoV), smoothed cumulative spike train (sCST), and proportion of common input (PCI), respectively. Error bars represent the 95% confidence interval ( $n = 11$ ). Asterisks indicate significant differences ( $p < 0.017$ ).

84

Figure 15 Computer simulation results for the scenario where the variability of the corticomotor input (single common input) was reduced ( $kCM = 8$  and  $kCM = 10$ ) with respect to the control condition ( $kCM = 4$ ). Effects on (a) force CoV, (b) ISI CoV, (c) sCST CoV, and (d) PCI. Error bars represent the 95% confidence interval ( $n = 17$ ). Asterisks indicate significant differences ( $p < 0.05$ ).

86

Figure 16 Computer simulation results for the scenario where the secondary common input was added to the model. (a)-(d) Results achieved when  $kCM = kS = 4$ . (e)-(h) Results achieved when  $kCM = 4$  and  $kS = 10$  (more regular input). Effects are shown for: (a) and (e) force CoV; (b) and (f) ISI CoV; (c) and (g) sCST CoV; and (d) and (h) PCI. Error bars represent the 95% confidence interval ( $n = 17$ ). Asterisks indicate significant differences ( $p < 0.05$ ).

87

Figure 17. Theoretical analysis on the effects of order ( $k$ ) and mean intensity ( $\mu$ ) of the two common inputs (Gamma point processes) on the variance of the global common input ( $\sigma G2$ ). Panels (a)-(d) show analytical curves for different orders of the corticomotor input (i.e.,  $kCM = 1, 4, 6$ , and  $10$ , respectively).

89

Figure 18. Variance of the global common input. (a) Relationship between the common input variance ( $\sigma_{G2}$ ) and the order of the corticomotor input ( $k_{CM}$ ), which was the single input in the model for this scenario. (b)-(c) Input variance when two common inputs are considered in the model. Panel (b) shows the relationship between the input variance and the intensity of the corticomotor input ( $\mu_{CM}$ ) when  $k_{CM} = k_S = 4$ , while panel (c) shows the same relationship when  $k_S = 10$ . Error bars represent the 95% confidence interval ( $n = 17$ ). Asterisks indicate significant differences ( $p < 0.05$ ). 90

## LIST OF TABLES

---

**Table 1.** Outcomes from the two-way RM-ANOVA performed on the experimental data. Asterisks indicate the significant differences ( $p < 0.017$ ). Effect size is reported as the partial eta-squared ( $\eta p^2$ ).

85

**Table 2.** Outcomes from the multiple ANOVA performed on the computer simulation data. Asterisks indicate significant differences ( $p < 0.05$ ). Effect size is reported as the partial eta-squared ( $\eta p^2$ ).

87

## LIST OF ABBREVIATIONS

---

*ANOVA: Analysis of variance*

*ApEn: Approximate entropy*

*CNS: Central nervous system*

*CoV: Coefficient of variation*

*CST: Cumulative spike train*

*CTR: Control condition (no vibration)*

*D: Dominant hand*

*EMG: Electromyogram*

*FDI: First dorsal interosseous*

*HD: High-density (EMG)*

*HV: High vibration intensity*

*IN: Interneuron*

*ISI: Interspike interval*

*IV: Intermediate vibration intensity*

*LV: Low vibration intensity*

*MN: Motor neuron*

*MVC: Maximal voluntary contraction*

*ND: Non-dominant hand*

*OV: Optimal vibration*

*PCI: Proportion of common input*

*PWM: Pulse-width modulation*

*RM: Repeated measure (ANOVA)*

*sCST: Smoothed cumulative spike train*

*SD: Standard deviation*

# TABLE OF CONTENTS

---

Introduction .....	17
1 Objectives .....	23
Sinusoidal Vibrotactile Stimulation Differentially Improves Force Steadiness Depending on Contraction Intensity .....	24
Abstract.....	24
1 Introduction.....	25
2 Materials and Methods.....	27
3 Results .....	33
4 Discussion .....	38
5 Conclusions .....	45
6 Ethical Approval .....	45
Improvement of Force Control Induced by Vibrotactile Stimulation does not Depend on Handedness.....	46
Abstract.....	46
1 Introduction.....	47
2 Materials and Methods.....	50
3 Results .....	54
4 Discussion .....	59
5 Conclusion.....	66

Neurophysiological Correlates of Force Control Improvement Induced by Sinusoidal Vibrotactile Stimulation .....	67
Abstract.....	67
1 Introduction.....	68
2 Materials and Methods.....	71
3 Results .....	83
4 Discussion .....	90
Final Comments.....	100
List of Publications .....	105
References.....	107
Attachments.....	124



## INTRODUCTION

---

The central nervous system (CNS) is a complex network with billions of neurons interconnected through synapses. The key neural element of motor control is the alpha motor neuron (MN) that is located in the ventral horn of the spinal cord and the brainstem (HECKMAN; ENOKA, 2012). The MN pool (i.e., a collection of MNs innervating a given muscle) integrates not only information from the descending tracts from supraspinal structures (e.g., brain, brainstem) (LEMON, 2008), but also from sensory afferents, such as cutaneous mechanoreceptors and proprioceptive receptors from muscles and joints (PROSKE; ALLEN, 2019; PROSKE; GANDEVIA, 2012).

Stimulation applied to mechanoreceptors of the skin is transduced into spike trains traveling through the sensory axons to the CNS (see Figure 1 for a putative representation of the connections between cutaneous afferents and the neuronal circuits in the CNS) (BENSMAÏA et al., 2005; SATO, 1961). This afferent information ascends to supraspinal circuits (e.g., brainstem, thalamus, cerebellum, and sensorimotor cortex), which are responsible for sensory perception and motor control (KANDEL et al., 2013). Afferent inputs from cutaneous mechanoreceptors are also integrated into the spinal cord circuitry.

In the spinal cord, cutaneous afferents establish oligosynaptic connections with MNs through spinal interneurons (INs) (PIERROT-DESEILLIGNY; BURKE, 2012). However, there is a differential influence of cutaneous inputs depending on the type of MNs, so that high-threshold

(large) MNs are excited while low-threshold (small) MNs are inhibited by the activity of cutaneous afferents ( $A\beta$  sensory afferents) (DATTA; STEPHENS, 1981; GARNETT; STEPHENS, 1980, 1981). Cutaneous inputs can also decrease the presynaptic inhibition of primary afferents from muscle spindles, thereby influencing the excitability of MNs (AIMONETTI et al., 2000; NAKASHIMA et al., 1990). Moreover, there are shreds of evidence of both long-latency inhibition (CHANDRAN et al., 1988) and long-latency excitation (PIERROT-DESEILLIGNY; BURKE, 2012) of MNs through a transcortical feedback loop. Therefore, it is evident that the activation of cutaneous afferents can largely influence the MN activity and consequently, the motor behavior.

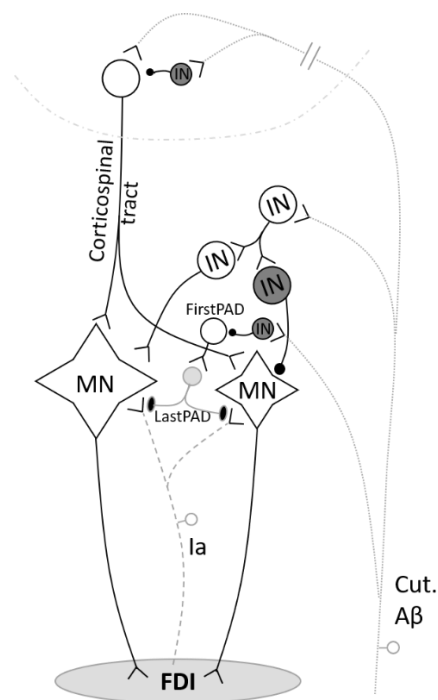


Figure 1. Schematic diagram illustrating the putative connections between cutaneous afferents and neuronal circuits in the central nervous system (CNS).  $A\beta$  cutaneous afferents from the index finger project to alpha motor neurons (MNs) innervating the first dorsal interosseus (FDI) muscle through oligosynaptic pathways encompassing spinal and supraspinal interneurons (INs), along with cortical motor neurons. Cutaneous inputs can also influence the activity of primary afferent depolarization (PAD) INs, which are responsible for the presynaptic inhibition of Ia afferents from muscle spindles. Adapted from Pierrot-Deseilligny and Burke (2012).

In the last decades, several studies have been exploring the exciting phenomenon of motor improvement caused by either electrical or mechanical stimulation of cutaneous mechanoreceptors of the glabrous skin. The experimental findings of some reported studies range from improvements in postural control (DE NUNZIO et al., 2018; MAGALHAES; KOHN, 2011; PRIPLATA et al., 2002, 2003) and force control (GERMER et al., 2019b; MENDEZ-BALBUENA et al., 2012; TRENADO et al., 2014a, 2014c) to the reduction of pathological tremor (TRENADO et al., 2014b). The studies mentioned above hypothesized the occurrence of stochastic resonance phenomenon in the sensorimotor system. They observed that a specific stimulation intensity improved sensorimotor performance by increasing the sensitivity of the mechanoreceptors or the sensorimotor integration within the CNS. Stochastic resonance is a counterintuitive phenomenon in which the addition of noise (with a specific intensity) to a nonlinear system may improve the transmission or detection of a weak input signal (MCDONNELL; WARD, 2011; MOSS, 2004). Roughly, one can characterize the integration of synaptic inputs by a MN pool as a nonlinear system that would improve the transmission of a common input signal by the addition of a “noisy” input (cutaneous afferents).

Albeit the motor improvement caused by cutaneous stimulation has been described in several experimental conditions (KURITA et al., 2013, 2016; MAGALHAES; KOHN, 2011; MANJARREZ et al., 2003; MENDEZ-BALBUENA et al., 2012; TRENADO et al., 2014b), few studies (KOUZAKI et al., 2012; MANJARREZ et al., 2002; TRENADO et al., 2014a, 2014c) devised methods to investigate the neurophysiological basis of this phenomenon in

the intact motor system. We believe that by using different paradigms to investigate the neural pathways that cutaneous afferents establish with the CNS (Figure 1), we could improve our knowledge about the mechanisms underlying the motor enhancement caused by sensory stimulation. For instance, Trenado et al. (2014c) observed that the beta-band corticomuscular coherence (a measure of coupling between cortical circuits and the MN pool) increased during the application of a Gaussian vibrotactile stimulation while the participants performed an index finger sensorimotor task. Also, they showed an increased beta-band power of the electroencephalogram measured over the sensorimotor area, which is similar to the findings of Manjarrez et al. (2002). In another study, Trenado et al. (2014a) applied Gaussian vibratory stimuli filtered in different frequency bands to infer on which mechanoreceptor mostly influenced the enhanced sensorimotor control. They observed that the steady-state fluctuations of finger position (while the participant applied a low-intensity force against a mechanical apparatus) were largely reduced when high-frequency vibration (both narrowband and broadband) was applied, suggesting that the Pacinian corpuscle is the major contributor to the motor enhancement. The Pacinian corpuscles are fast adapting receptors that respond to the intensity and frequency of the vibration stimulus applied to the skin (BOLANOWSKI; ZWISLOCKI, 1984), with a higher sensitivity to frequencies in the range of 80Hz to 300Hz (ABRAIRA; GINTY, 2013; SATO, 1961).

One possible question is whether the beneficial effect of vibrotactile stimulation in sensorimotor control would occur if a deterministic (sinusoidal) vibrotactile stimulation is applied instead of a stochastic vibration. In a

psychophysical experiment, Iliopoulos et al. (2014) showed that sensory perception could be improved by using either white Gaussian electrical noise or a sinusoidal electrical stimulation of sensory afferents. Therefore, we can hypothesize that deterministic stimulation might also be used to improve motor performance.

Other aspects were neglected or poorly explored in previous studies. For example, one can argue that the beneficial effect of vibrotactile stimulation in motor control can be influenced by the contraction intensity performed by the participant during the motor task. The increased volitional command from descending tracts recruits a large proportion of MNs of the pool (DE LUCA et al., 1982; DE LUCA; CONTESSA, 2012), and the interaction between the recruitment of higher threshold MNs and the cutaneous inputs would produce a differential effect in the motor enhancement caused by vibrotactile stimulation.

Another essential characteristic of the motor system is the differential excitability of motor neurons associated with the control of dominant limbs (TAN, 1989a, 1989b). Moreover, the neural circuits of the CNS controlling non-dominant limbs are thought to be more specialized in the integration of proprioceptive feedback than those responsible for the control of non-dominant limbs (ADAMO et al., 2012; FRIEDLI et al., 1987; HAN et al., 2013a, 2013b; NAITO et al., 2011). These findings might explain the differences observed in force control of the hand's muscles between dominant and non-dominant sides (ADAM et al., 1998; GOBLE; BROWN, 2008; YADAV; SAINBURG, 2014). Therefore, lateral dominance (or handedness) might be a

significant issue when considering the effect of vibrotactile stimulation on motor control.

Lastly, to the best of our knowledge, few studies investigated the discharge properties of motor units during a motor task enhanced by sensory stimulation. The study by Kouzaki et al. (2012) showed that the variability of interspike intervals (ISIs) of soleus motor units decreased during subthreshold electrical stimulation applied to the posterior tibial nerve in a low-intensity isometric contraction task. Additionally, the referred authors reported an unconvincing decrease of motor unit synchronization as estimated by the cross-correlogram between pairs of motor units. They argued that the decreased ISI variability and decreased motor unit synchronization are both responsible for the decreased force variability. However, the study by Kouzaki et al. (2012) is limited since they only recorded a small number of motor units (10), which is not representative of the whole population of motor units active during the task.

Modern technologies for the recording of high-density surface electromyogram (HD-EMG) have been used to estimate the activity of a large population of motor units (CASTRONOVO et al., 2015; DE LUCA; CONTESSA, 2012; DEL VECCHIO et al., 2018), which might be used to provide insights regarding the neural drive to the muscle, along with information about the common inputs impinging onto the MNs. Since the motor units (the MN and its innervating muscle fibers) are the final common pathway for motor control (Sherrington, 1925), it is invaluable to know how they behave during a motor task enhanced by vibrotactile stimulation. Therefore, this knowledge might

provide clues on the neurophysiological basis of the improvement in sensorimotor control induced by stimulation of cutaneous mechanoreceptors.

## 1 OBJECTIVES

The main objective of the present PhD thesis was to evaluate the effect of a sinusoidal vibrotactile stimulation on the neurophysiological control of muscle force produced by a hand muscle during isometric contractions. Specifically, in this work, we will address the following scientific questions:

- 1) Does a sinusoidal vibrotactile stimulation improve force steadiness?
- 2) Does the contraction intensity influence the improvement of force steadiness induced by sinusoidal vibrotactile stimulation?
- 3) Does the handedness of participants influence the improvement of force steadiness induced by sinusoidal vibrotactile stimulation?
- 4) How does sinusoidal vibrotactile stimulation influence the motor unit firing properties?

# Chapter 1

## SINUSOIDAL VIBROTACTILE STIMULATION DIFFERENTIALLY IMPROVES FORCE STEADINESS DEPENDING ON CONTRACTION INTENSITY<sup>1</sup>

---

### ABSTRACT

Studies have reported the benefits of sensory noise in motor performance, but it is not clear if this phenomenon is influenced by muscle contraction intensity. Additionally, most of the studies investigated the role of a stochastic noise on the improvement of motor control and there is no evidence that a sinusoidal vibrotactile stimulation could also enhance motor performance. Eleven participants performed a sensorimotor task while sinusoidal vibrations were applied to the finger skin. The effects of an optimal vibration (OV) on force steadiness were evaluated in different contraction intensities. We assessed the standard deviation (SD) and coefficient of variation (CoV) of force signals. OV significantly decreased force SD irrespective of contraction intensity, but the decrease in force CoV was significantly higher for low-intensity contraction. To the best of our knowledge, our findings are the first evidence that sinusoidal vibrotactile stimulation can enhance force steadiness in a motor task. Also, the significant improvement caused by OV during low-intensity contractions is probably due to the higher sensitivity of the motor system to the synaptic noise. These results add to the current knowledge on the effects of vibrotactile stimulation in motor control and have potential implications for the development of wearable haptic devices.

---

<sup>1</sup>This chapter is a copy of the manuscript published in the journal *Medical & Biological Engineering & Computing* (DOI: 10.1007/s11517-019-01999-8) with only aesthetical modifications.



## 1 INTRODUCTION

Voluntary control of human movement is influenced by the action of sensory feedback from muscular, cutaneous, and joint receptors. This proprioceptive feedback is integrated at different regions of the CNS (e.g., the sensorimotor cortex, brain stem, and the neuronal circuits within the spinal cord), which modulates the neural drive to skeletal muscles and the motor output (PROCHAZKA; ELLAWAY, 2012; PROSKE; GANDEVIA, 2012).

An intriguing phenomenon that involves the proprioceptive feedback system is the improvement of sensorimotor control due to the application of an optimal stimulus to sensory receptors. For instance, stochastic vestibular galvanic stimulation (MULAVARA et al., 2011; SAMOUDI et al., 2015) or stochastic vibrotactile stimulation applied to feet (DETTMER et al., 2015; PRIPLATA et al., 2002, 2003, 2006) or to the fingertip (MAGALHAES; KOHN, 2011) improved balance control in healthy and diseased subjects. Besides, the application of either stochastic vibrotactile or electrotactile stimuli enhanced tactile sensation (COLLINS et al., 1996; LAKSHMINARAYANAN et al., 2015) and sensorimotor performance (MANJARREZ et al., 2002, 2003; MENDEZ-BALBUENA et al., 2012; TOLEDO et al., 2017). More recently, Trenado et al. (2014b) showed that a stochastic vibrotactile stimulation could improve force control in patients with essential tremor. Additionally, in another study by Trenado et al. (2014a), the effects of broadband and narrowband stochastic vibration were evaluated during the performance of a force-matching task at low-intensity contractions (<10%MVC).

The results of the papers described above are attributed to the occurrence of stochastic resonance in the nervous system (MCDONNELL; WARD, 2011; MOSS, 2004). From a theoretical standpoint, the stochastic resonance phenomenon consists of an improvement in the transmission and/or detection capacity of a nonlinear system when a stochastic noise is applied to its input (MCDONNELL; ABBOTT, 2009). However, in the study by Durand et al. (2013), a computational neuron model was used to show that the detection of a stochastic signal can be improved by the application of a sinusoidal (deterministic) signal at the input of the system, in a phenomenon referred to as the reverse stochastic resonance. Recently, a psychophysical experiment by Iliopoulos et al. (2014) showed that sinusoidal electrotactile stimuli could also be used to enhance tactile sensation. The latter results raise the question of whether a sinusoidal vibrotactile stimulation would be used to improve motor performance similarly to stochastic vibration. Based on the results by Trenado et al. (2014a), that showed an improvement in force control when a narrowband (250-300Hz) stochastic noise was applied to the fingertip, we hypothesize that sinusoidal vibrotactile stimulation with a frequency within the sensitivity range of cutaneous mechanoreceptors (mostly the Pacinian corpuscles) would improve force control during isometric contractions of a hand's muscle.

Another factor that influences the motor performance is the contraction intensity (JONES et al., 2002; SLIFKIN; NEWELL, 2000; WATANABE et al., 2013). Most of the previous studies evaluated the effects of vibrotactile stimulation during motor tasks that required low-intensity muscle activation (MAGALHAES; KOHN, 2011; PRIPLATA et al., 2002, 2003,

2006; TRENADO et al., 2014a, 2014b). The results from these studies cannot be directly translated to motor tasks which require an increased level of contraction. To the best of our knowledge, no previous study systematically evaluated whether the contraction intensity would influence the improvement in the sensorimotor control caused by vibrotactile stimulation. One hypothesis is that the effect of vibrotactile stimulation would be high during low-intensity contractions due to the higher sensitivity of the motor system to presynaptic commands in these conditions (DIDERIKSEN et al., 2012).

In the present study, human experiments were conducted to investigate the two scientific problems described above: 1) does a sinusoidal vibration improve force steadiness? 2) does the contraction intensity influence the improvement of force steadiness caused by vibrotactile stimulation? The results of the present study will add to the current knowledge on the effects of vibrotactile stimulation in force control. Additionally, the results might be invaluable for the development of new technologies for the improvement of motor performance and rehabilitation (KURITA et al., 2013). Preliminary results were reported as an abstract (GERMER et al., 2017).

## 2 MATERIALS AND METHODS

### 2.1 Participants

Twelve healthy young adults (aged  $28 \pm 2$  years, six men) participated in the study. All subjects were right-handed (as assessed by the Edinburgh Handedness Inventory (OLDFIELD, 1971)), with normal or corrected-to-normal vision, and reported to have no known neurological, psychiatric or

motor impairments. The subjects gave their written informed consent before the experiments.

## 2.2 Force measurement and vibrotactile stimulation

Isometric muscle forces were measured with a piezoresistive transducer (FlexiForce A201, Tekscan) fixed at the surface of a rigid apparatus that will be described below (see Figure 2a). Force signals were amplified (FlexiForce Quickstart Board, Tekscan), digitized at 2kHz (USB-6002, National Instruments), and low-pass filtered (30Hz cutoff frequency).

Periodic vibratory stimuli (175Hz) were applied to the radial surface of the metacarpophalangeal joint of the index finger by a linear resonant actuator (C10-100, Precision Microdrives) (see Figure 2a). Stimulus frequency was chosen to activate the Pacinian corpuscles in the glabrous skin (ABRAIRA; GINTY, 2013; SATO, 1961). The linear actuator was driven by a pulse-width modulation (PWM) signal, whose duty cycle was adjusted to provide vibrations with different intensities (from zero to 1.50G peak-to-peak). Vibration amplitudes were measured by a 3-axis analog accelerometer (ADXL337, Analog Devices), whose signals were sampled at 2kHz.

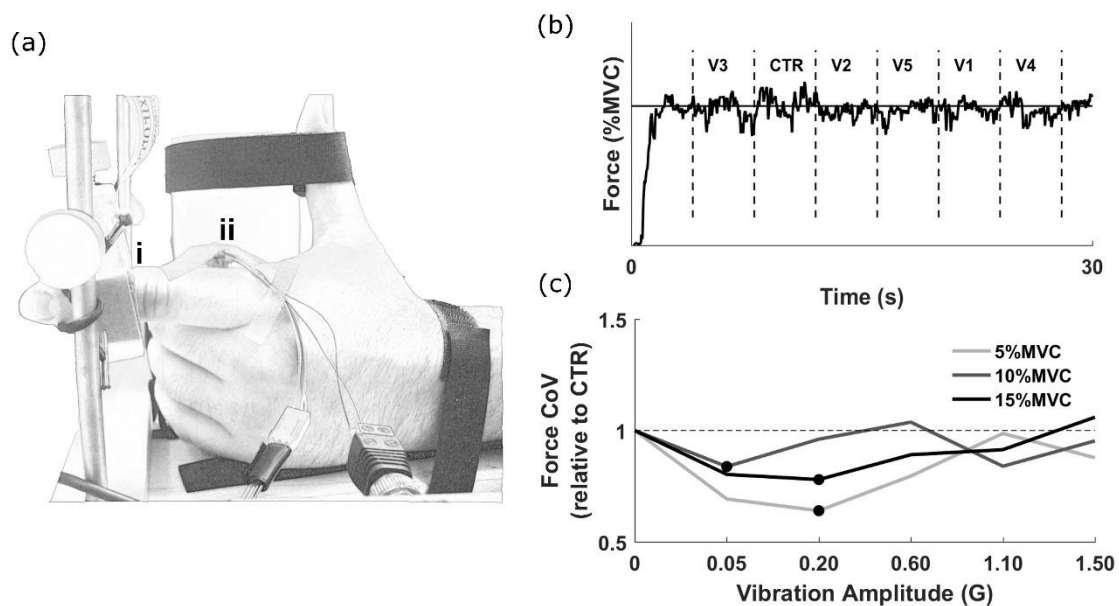


Figure 2. Schematic representation of the experimental setup and representative data. (a) Mechanical apparatus used to record index finger abduction forces. Isometric forces were measured at the distal interphalangeal joint (i) by a piezoresistive force transducer. The linear resonant actuator and accelerometer were placed at the radial surface of the metacarpophalangeal joint of the index finger (ii). All the fingers, but the index, and wrist were fixed to the apparatus with Velcro straps. (b) Example of a typical force signal recorded from a subject. Six vibrotactile stimuli were randomly applied to the finger skin during force-matching tasks. Vibrations with five different intensities (marked as V1 to V5) and a no-vibration control condition (CTR) were applied to the finger skin for 4s each block. The total duration of the trial was 30s (initial and final segments of the time series were discarded for the analysis). (c) Illustrative analysis of force coefficient of variation (CoV) for one subject. The effect of vibration intensities on force variability (relative to the control condition) was evaluated at 5% (light gray), 10% (dark gray) and 15% (black) of the maximal voluntary contraction (MVC). Black circles depict the optimal vibration, which was defined as the vibration amplitude that produced the lowest force CoV (relative to CTR) for each contraction intensity.

### 2.3 Experimental protocol

During the experiments, subjects were comfortably seated in a chair with both arms on a table. Shoulders were kept relaxed, and the elbow was flexed at 140deg. The left arm was positioned on a custom-made apparatus so that the forearm and wrist were immobilized with Velcro straps. A manipulandum was used to support the left (non-dominant) hand in a vertical position. The index finger was maintained perpendicular to the thumb in an extended position (Figure 2a). All the fingers, but the index, were fixed to the manipulandum during the tasks. An LCD monitor (Samsung SyncMaster

713N, 17", 1280x1024px) was placed 60cm in front of the subject at the eyes level to provide visual feedback of the force. The visual gain was equal to 8px/%MVC for all subjects. Participants wore a headphone during experiments driven by a white Gaussian noise sound to mask the ambient noise.

At the beginning of the experiment three trials were performed to estimate the maximal voluntary contraction (MVC) of each subject. Each MVC trial lasted 10s and the MVC value was defined as the maximum value from the 3 repetitions. Prior to the force-matching tasks, subjects were familiarized with the tasks and performed one test trial at each force level (5%, 10%, and 15%MVC).

The main experiment consisted of performing isometric contractions at three target intensities: 5%, 10%, and 15%MVC. Each contraction intensity was evaluated five times in randomized trials lasting 30s each. A sequence of five supra-sensory vibrotactile stimuli (amplitude from 0.05G to 1.50G) and a control condition without vibration (CTR) was applied for 24s (4s each intensity) (see Figure 2b). Vibration intensities were presented in a random order after 4s from the beginning of the trial.

## 2.4 Data analysis and statistics

Data presented in this paper is available for download in FigShare (GERMER et al., 2018a). Force signals were processed offline in MatLab (The MathWorks). Recorded data were low-pass filtered (fourth-order Butterworth digital filter, 15Hz cutoff frequency), detrended, and cut according to the six vibration intensities adopted in each trial (Figure 2b). The initial 0.60s of each

vibration block were discarded to avoid transient effects. Force variability was measured using the standard deviation (SD) and the coefficient of variation (CoV). Dependent variables were analyzed for each vibration intensity for the three levels of force.

The effect of vibrotactile stimulation on sensorimotor performance is subject dependent (MAGALHAES; KOHN, 2011; TRENADO et al., 2014c) due to differences in cutaneous sensitivity. Therefore, any evaluation based on the use of multiple vibration intensities to infer about population outcomes would reduce the chance of finding a significant effect (see TOLEDO et al., 2017) for a discussion on this issue). Similar to other studies previously reported in the literature (MENDEZ-BALBUENA et al., 2012; TRENADO et al., 2014a, 2014b), here we selected the vibration level at which the best motor performance was achieved (i.e., the lowest force CoV) so as to normalize the beneficial effect of vibrotactile stimulation to force control among the participants. The selected vibration for each subject was defined as the optimal vibration (OV) while the no-vibration condition was considered as the CTR (see Figure 2c for an illustrative example). Consistency of OV was measured as the percentage of trials (performed by each subject) that effectively decreased force CoV in relation to CTR. Additionally, the likelihood of having an improvement by a given vibration at each contraction level was measured as the proportion of vibrations that decreased the relative force CoV.

Time-domain and frequency-domain structures of force signals were assessed by the approximate entropy (ApEn (SLIFKIN; NEWELL, 1999)) and the power spectrum, respectively. ApEn is an estimate of time series

regularity (PINCUS, 1991), whose values range between 0 (for a regular time series) and 2 (for a completely random time series). The ApEn is calculated by Equation 1, where  $\varphi^m(r)$  is the conditional probability that  $m$  consecutive values are within a tolerance limit  $r$  for a time series of length  $N$ . In other words, ApEn is a similarity index of data vectors with length  $m$  along the time series. In the present study, ApEn parameters were set as  $m = 2$  and  $r = 0.20 SD$ .

$$ApEn(m, r, N) = \varphi^m(r) - \varphi^{m+1}(r) \quad (1)$$

Force power spectrum was estimated using Welch's method with a non-overlapping 3.40s Hanning window. Power spectrum analysis was performed in three frequency bands: 0-4Hz (related to the common drive (LODHA; CHRISTOU, 2017; NEGRO et al., 2009)), 4-8Hz, and 8-12Hz (related to the physiological tremor (NOVAK; NEWELL, 2017)). The relative power (with the total power as the reference) was calculated in the three frequency bands. The total power was estimated as the area of the force power spectra from zero to 15Hz.

Statistical analysis was performed using SPSS (IBM). A two-way analysis of variance with repeated measures (two-way RM-ANOVA) and Bonferroni's *post hoc* tests were used to compare data between vibration conditions (CTR and OV) and contraction intensities (5%, 10%, and 15%MVC). When an interaction was detected by the RM-ANOVA the simple main effects were evaluated with a one-way RM-ANOVA. Since the OV was selected out of five vibration intensities there is a probability that the reduction in force CoV was due to chance. Nonetheless, it is worth noting that



we tried to reduce this probability by repeating each task five times and presenting each vibration intensity in a random order across the trials (see Figure 2b and description above). Despite this experimental control, we decided to correct the significance level  $\alpha = 0.05$  using the Bonferroni's method in order to reduce the probability of type I errors in our analysis, and hence the corrected significant level used in the subsequent analysis was 0.01 ( $\alpha/5$ ). Additionally, we calculated the partial eta squared ( $\eta_p^2$ ) to estimate the effect size. The effects were considered large for  $\eta_p^2 > 0.25$  and low for  $\eta_p^2 < 0.01$  (COHEN, 1988). All data hereafter is presented as mean  $\pm$  95% confidence interval.

### 3 RESULTS

The average forces performed by the subjects were  $4.86 \pm 0.01\%MVC$ ,  $9.75 \pm 0.01\%MVC$ , and  $14.67 \pm 0.02\%MVC$  for the three contraction intensities evaluated. Therefore, all subjects were able to match the target force level. Mean force level did not change with the application of vibrotactile stimuli ( $p = 0.843$ ).

All subjects had an improvement in force steadiness for at least one vibration intensity at 5%MVC, and 83.33% of the vibration intensities applied were efficient in decreasing force CoV (Figure 3a). However, two subjects and one subject did not reduce force variability for any vibratory stimulus in 10%MVC and 15%MVC (Figure 3b and c), respectively. In total, 45% and 56.67% of vibration intensities decreased force CoV at 10%MVC and 15%MVC, respectively. Figure 4 illustrates force CoV during CTR and OV for individual trials. OV decreased force CoV in  $75 \pm 9.80\%$ ,  $66 \pm 14.37\%$  and

72.73  $\pm$  13.24% of repetitions at 5%MVC, 10%MVC and 15 %MVC, respectively.

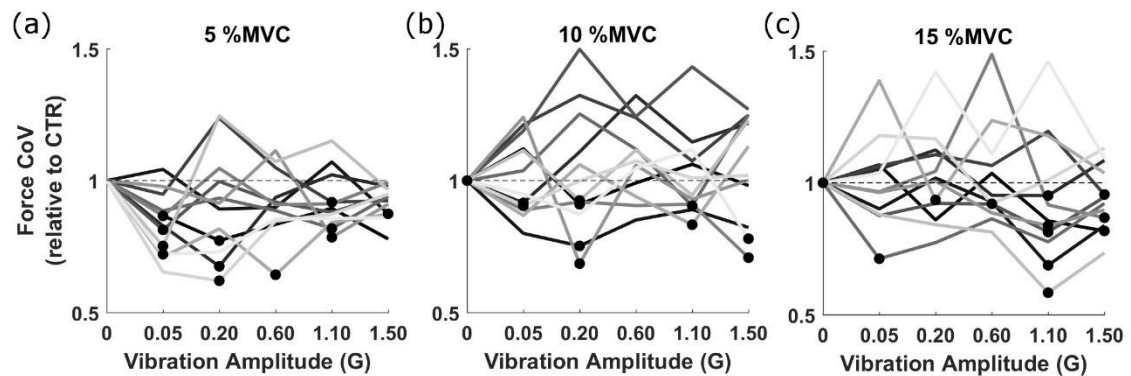


Figure 3. Representative force CoV in different vibration intensities relative to the condition without vibration (CTR). Values below one (dashed line) indicate a decrease in force CoV as compared to the CTR condition. Lines represent individual data (per subject) at 5%MVC (a), 10%MVC (b), and 15%MVC (c). The optimal vibration (OV) for each subject is marked with a black dot.

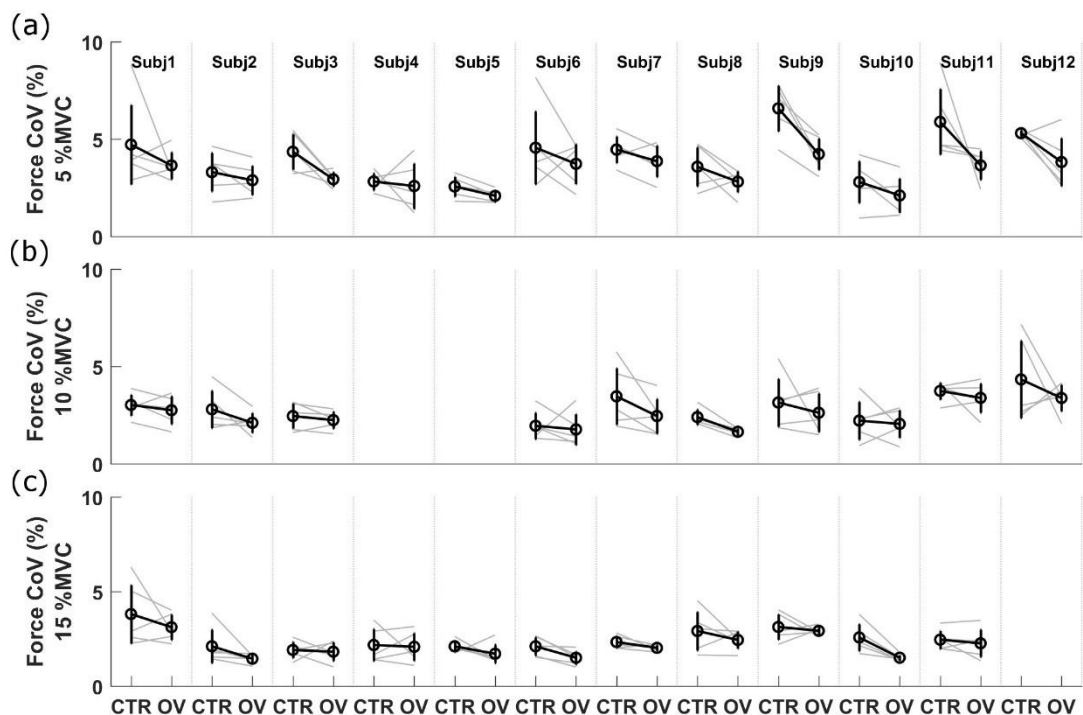


Figure 4. Data from the repetitions performed by each subject (columns) at 5%MVC (a), 10%MVC (b), and 15%MVC (c). Individual trials are depicted in gray light lines, while the average force CoV is represented by black tick lines with error bars (95% confidence interval). Missing data (see third and fourth columns in the middle panel and the last column in the bottom panel) represent subjects that did not present an OV.

Force CoV decreased with the application of an OV and the effect depended on the contraction intensity (Figure 5a). There was a significant and large interaction between the two factors (force levels and vibration conditions,  $F(2,22) = 6.235$ ,  $\eta_p^2 = 0.362$ ,  $p = 0.007$ ). Albeit vibration decreased force variability in all contraction intensities the effect of OV was higher at 5%MVC, with a relative reduction of 24.68% ( $F(1,11) = 22.472$ ,  $\eta_p^2 = 0.714$ ,  $p < 0.001$ ) as compared to 15.06% ( $F(1,11) = 17.495$ ,  $\eta_p^2 = 0.614$ ,  $p = 0.002$ ) and 15.85% ( $F(1,11) = 19.351$ ,  $\eta_p^2 = 0.638$ ,  $p = 0.001$ ) at 10%MVC and 15%MVC, respectively. Simple main effects of contraction intensity in force CoV was also found for CTR ( $F(2,22) = 13.357$ ,  $\eta_p^2 = 0.728$ ) and OV ( $F(2,22) = 17.288$ ,  $\eta_p^2 = 0.776$ ). Figure 5 shows that force CoV was statistically higher at 5%MVC than at 10%MVC ( $p = 0.001$  and  $p = 0.004$  for CTR and OV, respectively) and 15%MVC ( $p = 0.001$  and  $p < 0.001$  for CTR and OV, respectively). Nevertheless, no significant difference was found between the force CoV at 10%MVC and 15%MVC, neither in CTR ( $p = 0.557$ ) nor in OV ( $p = 0.267$ ). It is worth noting that the relations between force CoV and mean force were well fitted by power functions:  $CoV = \alpha + \beta \times Force^{-1}$  (see Figure 6A,  $R^2=0.972$  and  $R^2=0.978$  for CTR and OV, respectively).

No interaction was observed between force and vibration for the force SD ( $F(2,22) = 0.565$ ,  $\eta_p^2 = 0.490$ ,  $p = 0.576$ ). The RM-ANOVA detected a significant and large effect of vibration for the force SD ( $F(1,11) = 91.634$ ,  $\eta_p^2 = 0.893$ ,  $p < 0.001$ ) (Figure 5b). Also, Figure 6b shows that force SD linearly increased with the contraction intensity ( $F(2,22) = 38.157$ ,  $\eta_p^2 = 0.776$ ,  $p < 0.001$ ).

The regularity (time-domain structure) of force signals significantly decreased ( $F(1,11) = 25.533, \eta_p^2 = 0.699, p < 0.001$ ) with the OV since the value of ApEn was higher in this condition (Figure 5c). However, there was no significant interaction between force levels and vibration conditions ( $F(2,22) = 1.833, \eta_p^2 = 0.143, p = 0.184$ ), as well as no effect of force level ( $F(2,22) = 0.224, \eta_p^2 = 0.020, p = 0.801$ ).

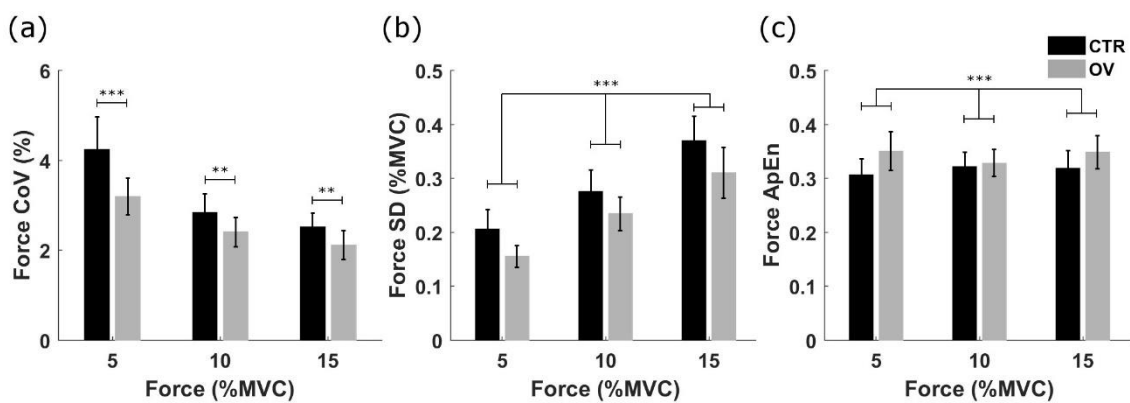


Figure 5. Force CoV (a), standard deviation (SD) (b), and approximate entropy (ApEn) (c) at three contraction intensities (5%MVC, 10%MVC and 15%MVC) for CTR (black) and OV (gray) conditions. Asterisks represent the statistical significance for vibration conditions (OV vs CTR, \*\*  $0.001 < p < 0.010$ , \*\*\*  $p < 0.001$ ).

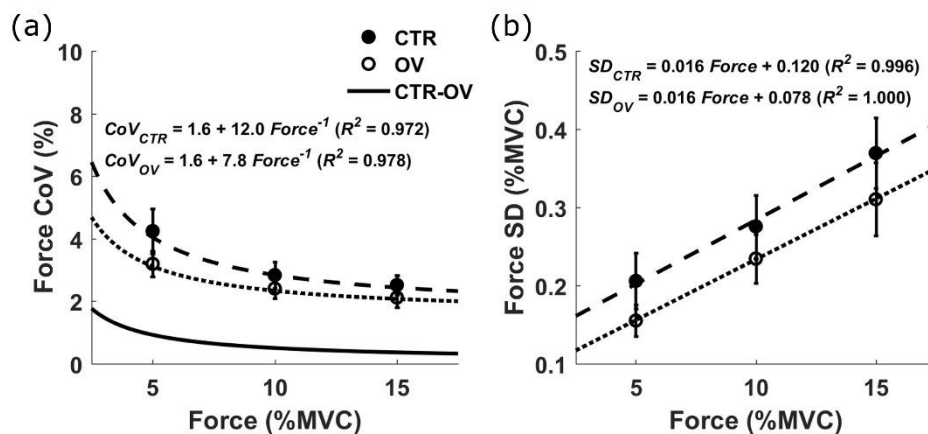


Figure 6. (a) Relation between force CoV and the mean force. (b) Relation between force SD and the mean force. In both panels, black and open circles represent CTR and OV conditions, respectively. Dashed and dotted lines are fittings to the experimental data (see inset equations and  $R^2$  values). Black thick line in panel A is the difference between the fittings for CTR and OV data.

Most of the power (>80%) of force signals was confined in the low-frequency (0-4Hz) band. For this band, no interaction was found between force levels and vibration conditions ( $F(2,22) = 2.440, \eta_p^2 = 0.182, p = 0.110$ ). In the low-frequency band, there was a significant and large decrease of relative power with OV (Figure 7a,  $F(1,11) = 26.271, \eta_p^2 = 0.705, p < 0.001$ ), but no significant effect of force level ( $F(2,22) = 2.334, \eta_p^2 = 0.175, p = 0.120$ ). In the intermediate (4-8Hz) frequency band, no effect was found ( $p = 0.048, p = 0.027$  and  $p = 0.115$ , for force, vibration, and interaction, respectively). In the frequency band associated to the physiological tremor (8-12Hz), no interaction was found between force levels and vibration conditions ( $F(2,22) = 1.094, \eta_p^2 = 0.090, p = 0.353$ ). OV increased the relative power of physiological tremor (Figure 7b,  $F(1,11) = 48.312, \eta_p^2 = 0.815, p < 0.001$ ), and although an effect of force level was found ( $F(2,22) = 5.745, \eta_p^2 = 0.343, p = 0.010$ ), no significant difference was detected in the *post hoc* analysis ( $p = 0.038, p = 0.034, p = 1.00$ , for 5% and 10%MVC, 5% and 15%MVC and 10% and 15%MVC). It is worth noting that in the analysis of the 4-8Hz band one subject was considered outlier and was excluded from the analysis.

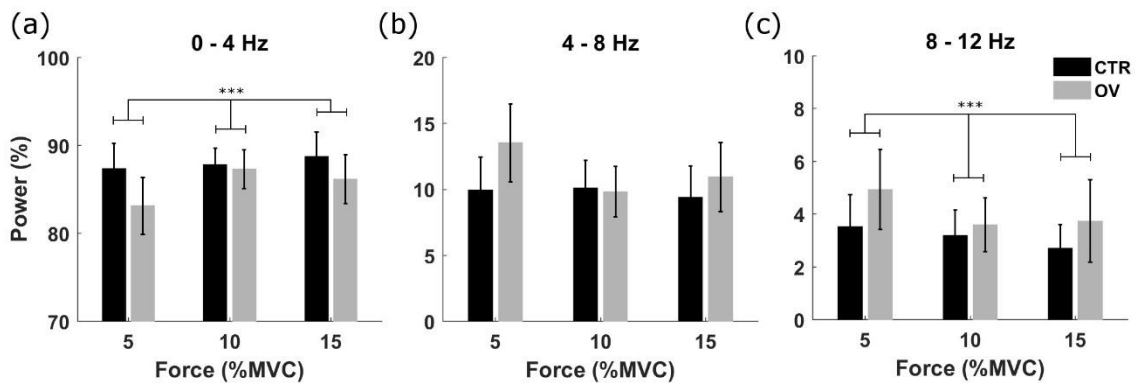


Figure 7. Frequency-domain properties of force signals. (a) Relative power in the low-frequency (0-4Hz) band. (b) Relative power in the intermediate-frequency band (4-8Hz) (c) Relative power in the 8-12Hz band (physiological tremor). Data are presented for the three contraction intensities (5%MVC, 10%MVC and 15%MVC) in both CTR and (black) OV (gray) conditions. Asterisks represent the statistical significance for vibration conditions (\*\*  $0.010 < p < 0.010$ , \*\*\*  $p < 0.001$ ).

## 4 DISCUSSION

In the present study, we show that an optimal level of sinusoidal vibrotactile stimulation (applied to the skin of the index finger) significantly improved force steadiness during an isometric index finger sensorimotor task. The relevant (and, to the best of our knowledge, novel) finding was the differential effect of OV depending on the contraction intensity. As observed in Figure 5A, the reduction in force CoV due to OV was more pronounced when the subjects performed contractions at 5%MVC as compared to 10%MVC and 15%MVC. Additionally, OV significantly changed force structure, both in time and frequency domains (see Figure 5c and Figure 7, respectively). In the following subsections we shall present a detailed discussion of the possible mechanisms behind these findings.

## 4.1 On the use of periodic vibrotactile stimulation

Previous studies evaluated the effects of vibrotactile stimulation on the improvement of motor control in different motor tasks (KURITA et al., 2013; MAGALHAES; KOHN, 2011; MENDEZ-BALBUENA et al., 2012; PRIPLATA et al., 2002, 2006; SEO et al., 2014; TRENADO et al., 2014a). Most of these studies adopted stochastic vibrotactile stimuli to enhance sensorimotor control and, consequently, motor performance. The putative mechanism behind these experimental findings is the stochastic resonance phenomena occurring in the motor system (MCDONNELL; WARD, 2011; MOSS, 2004). Here, we showed that motor performance (quantified by the force CoV) could also be improved by high-frequency (175Hz) sinusoidal (i.e., deterministic) vibration.

The motor task performed in the current study is similar to that adopted in the study by Trenado et al. (2014a). In the referred study, the authors showed that the mean absolute deviation of index finger position (while the subject performed a steady force at 8%MVC) was significantly reduced when the vibratory stimulus was either a broadband noise (0-300Hz) or a narrowband noise (0-15Hz or 250-300Hz), but the effect was more significant when the vibration had a high-frequency content. Additionally, they did not observe a statistical difference between the broadband vibrotactile stimuli and the vibrotactile stimuli confined to frequencies in the range 250-300Hz (see their Figure 4). The high-frequency stimulation is thought to activate the Pacinian corpuscles in the glabrous skin preferentially (ABRAIRA; GINTY, 2013; SATO, 1961). Therefore, our findings suggest that irrespective of the nature of vibrotactile stimulation (stochastic or

deterministic) the high-frequency content increases the excitability of Pacinian corpuscles and, consequently, the afferent inflow through cutaneous afferents.

Freeman and Johnson (1982) showed that cutaneous afferents from Pacinian corpuscles phase locked their discharge to high-frequency vibratory stimuli. Also, the discharge rate of cutaneous afferents became more regular (almost periodic) when high-frequency sinusoidal vibration was applied to mechanoreceptors. A recent computer simulation study (DURAND et al., 2013) showed that periodic stimuli improved the detection of stochastic signals in a CA1 neuron model, in a phenomenon referred to as the reverse stochastic resonance. Moreover, Iliopoulos et al. (2014) showed that a subthreshold periodic electrotactile stimulation could enhance sensory perception. In this vein, the outcomes of the present study might be an example of the occurrence of the reverse stochastic resonance phenomenon in the optimization of the motor system.

## 4.2 Effects of vibrotactile stimulation on force variability

A relevant finding of the present study was that the effect of OV on force CoV depended on the contraction intensity (Figure 5a). We will first provide a mathematical argument for this finding. The curve fittings reported in Figure 6b show that force SD and the mean force are linearly related ( $SD = \alpha \times Force + \beta$ ) irrespective of vibration condition. Therefore, it is evident that the relation between force CoV and the mean force follows a decreasing power function (Figure 6a), with an asymptotically constant value ( $\alpha$ ) for larger forces. The OV reduced force SD irrespective of force level (Figure 5b),



thereby reducing the parameter  $\beta$  (intercept) of the linear fitting without changing the slope ( $\alpha$ ). In the relation between force CoV and mean force, the parameter  $\beta$  is responsible for the scaling of the power function, particularly for low force values (since there was no change in  $\alpha$ ), and this explains the significant difference between CTR and OV (thick black line in Figure 6A) in low-intensity contractions.

The linear scaling between force SD and the mean force observed here (Figure 6b) is compatible with other studies in the literature that evaluated isometric contractions of a hand's muscle (BAWEJA et al., 2009; SLIFKIN; NEWELL, 2000). From a physiological standpoint, this linear scaling (frequently referred to as the signal-dependent noise (HARRIS; WOLPERT, 1998)) is attributed to intrinsic properties of the neuromuscular system (e.g., the recruitment order and recruitment thresholds of the motor units, and the range of twitch amplitudes of muscle units) (JONES et al., 2002; KEENAN; VALERO-CUEVAS, 2007). Other studies, however, argued that the variability in the discharge rate of motor units (which is primarily influenced by the synaptic noise (CALVIN; STEVENS, 1967)) is also determinant for the scaling of force SD with the contraction intensity (MORITZ et al., 2005; WATANABE et al., 2013). Nonetheless, Dideriksen et al. (2012) showed that the influence of synaptic noise (or discharge rate variability) is limited to low-intensity contractions (<10%MVC) due to the filtering effect of the intrinsic properties of the neuromuscular system. The difference observed between CTR and OV for the parameter  $\beta$  (intercept of the linear fittings) can, therefore, be physiologically explained by a reduction in the synaptic noise during vibrotactile stimulation. The reduced synaptic noise scales the force SD down

(Figure 5b and Figure 6b), but the influence of this reduction is prominent in contraction intensities where the sensitivity of the motor system to random fluctuations is high.

Hitherto, the reduction of the synaptic noise caused by the OV has no plausible explanation. We can only hypothesize that a more periodic cutaneous afferent inflow (see Discussion above) would reduce the fluctuations of the synaptic current on the motor neurons, thereby reducing their discharge rate variability. However, future studies should be carried out with similar experimental procedures and the recording of a population of motor units to provide further evidence of whether vibrotactile stimulation is capable of reducing the synaptic noise at the motor neuron pool.

### 4.3 Effects of vibrotactile stimulation on force structure

The improvement observed in force steadiness was followed by an increase in the ApEn of the force (Figure 5c). ApEn is frequently associated to the regularity of a given time series (PINCUS, 1991). Therefore, albeit less variable the forces produced by the subjects while receiving OV were less regular. In the context of isometric force control, Slifkin and Newell (SLIFKIN; NEWELL, 1999) showed that an increase in ApEn is followed by an increase in the signal-to-noise ratio ( $1/\text{CoV}$ ) of the system. The referred authors discussed that a decreased regularity (increased ApEn) is associated to an optimized performance of the neuromuscular system, where the information transmission is maximized in order to improve the adaptiveness of the system (SLIFKIN; NEWELL, 1999). Here, similar conclusions can be drawn. OV might be used to enhance the information transmission of the neuromuscular

system (by improving the sensorimotor integration (MENDEZ-BALBUENA et al., 2012)) so that the relative variability of the motor output is lower. However, differently from other studies, ApEn did not depend on contraction intensity (OFORI et al., 2012; SLIFKIN; NEWELL, 1999). The latter would suggest that force regularity is minimally influenced by contractions in the range (5-15%MVC) explored here (SOSNOFF; NEWELL, 2005).

As to the force power spectra, we observed an increase of the high-frequency (8-12Hz) content in parallel to a decrease of low-frequency (0-4Hz) content when an OV was applied (see Figure 7). This shift of power to higher frequencies is compatible with a less regular force time series (SLIFKIN; NEWELL, 1999). Lodha and Christou (2017) argued, based on several experimental results, that a reduction in force variability is associated to a decrease in low-frequency fluctuations, which are associated to the common synaptic drive to the motor pool (LODHA; CHRISTOU, 2017; MOON et al., 2014; NEGRO et al., 2009). Therefore, our findings reinforce this view. The physiological mechanism, again, is of difficult explanation without a broader investigation of the neural signals (e.g., the activity of motor units) involved in the motor task. However, a recent computer simulation study showed that Ia afferent activity has a significant influence on force variability and power spectrum (NAGAMORI et al., 2018). The authors of the referred study showed that a simulated decrease in presynaptic inhibition of Ia afferents reduces force CoV, reduces force power in the low-frequency range (<5Hz), and increases the power in the frequency range associated to the physiological tremor (5-12Hz in that study). These simulation data are similar to our experimental outcomes when an optimal level of vibrotactile

stimulation is applied. In fact, other experimental data suggest that activation of cutaneous mechanoreceptors decreases presynaptic inhibition of Ia afferent terminals (AIMONETTI et al., 2000; NAKASHIMA et al., 1990). Therefore, an explanation for the present results is that OV would reduce presynaptic inhibition and, consequently, increase the feedback gain from Ia afferents.

#### 4.4 Potential implications for the development of wearable enhancer devices

The improvement of motor performance induced by vibrotactile stimulation has been arousing keen interest not only for those involved in motor control research, but also for those interested in developing the so called wearable enhancer devices (KURITA et al., 2013, 2016; PRIPLATA et al., 2003). The data provided in the present paper might be of paramount importance since the generation of sinusoidal vibration is less challenging when compared to the generation of stochastic signals and band-limiting filters. If high-frequency sinusoidal vibration (within the sensitivity range of Pacinian corpuscles) is employed in a wearable device, there is a single parameter (vibration amplitude) to adjust during the tuning of the system. The fine tuning of stimulus intensity is required since the effect of vibration depends on the contraction intensity required to perform the motor task (as we showed in the Results). Nonetheless, we did not find a pattern for the relation between vibration intensity for optimal performance and the contraction intensity performed by a given subject (data not shown). The latter result might be due to the highly nonlinear effect of vibrotactile stimulation on the motor system (for instance, see the results from

(TRENADO et al., 2014a)), which is also highly nonlinear (i.e., the contraction intensity changes the number and the discharge rate of recruited motor units, the degree of synchronization between the motor units, the variability of the synaptic noise, and the activity of sensory feedback from proprioceptors). Additionally, our data suggest that albeit motor performance is consistently improved (in approximately 80% of the cases) for forces up to 15%MVC, these wearable enhancer devices would produce better results during motor tasks which require low-intensity contractions, such as dexterous manual manipulation (e.g., gripping, grasping, and pinching) of lightweight objects.

## 5 CONCLUSIONS

An optimal level of sinusoidal vibrotactile stimulation improved force control in an index finger sensorimotor task, but this effect depended on the contraction intensity performed by the subjects. The highest improvement caused by the optimal vibrotactile stimulation was observed during low-intensity contractions, which might be explained by a higher sensitivity of the motor system to changes in the synaptic noise in this condition.

## 6 ETHICAL APPROVAL

All procedures performed in studies involving human participants were in accordance with the ethical standards of the institutional and/or national research committee and with the 1964 Helsinki declaration and its later amendments or comparable ethical standards. The procedures were approved by the Research Ethics Committee of the University of Campinas (CAAE #59961616.8.0000.5404).

## *Chapter 2*

### IMPROVEMENT OF FORCE CONTROL INDUCED BY VIBROTACTILE STIMULATION DOES NOT DEPEND ON HANDEDNESS

---

#### ABSTRACT

Humans have keen interest in improving their motor capabilities, and hence the possibility of having wearable devices for motor enhancement is attracting great attention. It is thought that the increased activity of cutaneous mechanoreceptors by vibrotactile stimulation would improve sensorimotor integration in the central nervous system, thereby enhancing motor performance in several conditions, for instance, during force control of hand muscles. Nevertheless, the neural circuits controlling hand muscles have lateral asymmetries and differences in the reliability to process sensory information from ipsilateral and contralateral limbs. In the present study, we will investigate whether the sensory asymmetry due to lateral dominance would influence the enhancement of force control induced by vibrotactile stimulation. Ten participants performed a visually guided force-matching task while different intensities of vibrations were applied to the finger skin. Tasks consisted of abductions of the index fingers of non-dominant (ND) and dominant (D) hands (in independent trials). Participants performed steady forces at 5% of their maximal voluntary contractions estimated from each hand. Force variability (measured as the coefficient of variation, CoV) in the condition without vibration was used as the reference (control) for later comparison with five vibration intensities. Also, force CoV in control condition was compared to those obtained from an OV selected from both hands or from a single hand (D or ND). Despite the sensory asymmetries in cortical and spinal circuits, the improvement on motor performance induced by vibrotactile stimulation did not depend on lateral dominance. Irrespective of the criterion for selection of OV, a single intensity of vibrotactile stimulation was capable of reducing force variability in both hands without significant difference. These findings have implications to the development of wearable motor-enhancer devices.

## 1 INTRODUCTION

The seek of humans for improvements of body capabilities in either normal or pathological conditions leads to the development of tools, gadgets, treatments, and methods of training. Some of the known treatments are whole-body vibration (KAUT et al., 2016), nerve or muscle stimulation (JITKRITSADAKUL et al., 2015), and neuromodulation (BOGGIO et al., 2006). These treatments, however, can be time-consuming, might not have long-lasting effects, and can depend on technological support to deliver the stimulation. An emerging alternative for the improvement of motor capabilities are the so-called wearable motor-enhancer devices. For instance, Kurita and collaborators developed an instrumented glove (KURITA et al., 2013) and a surgical grasping forceps (KURITA et al., 2016) that improved sensorimotor performance of users. It is believed that these devices improve sensorimotor performance by means of the stochastic resonance phenomenon, which is known to improve the sensitivity and/or transmission capacity of a nonlinear system in the presence of an optimal level of noise applied to its input (MCDONNELL; ABBOTT, 2009). Although the concept of stochastic resonance is based on the existence of an optimal level of stimulation noise (a given metric of the system output follows an U-like shape relation with the input noise (MCDONNELL; ABBOTT, 2009)), Kurita's works suggested that a rigorous optimization is not necessary for a significant effect on sensorimotor improvement.

Previous studies have explored the beneficial effect of vibrotactile stimulation in different conditions of the sensorimotor system. For instance, during a standing position, a light vibrotactile stimulation to the feet

(DETTMER et al., 2015; PRIPLATA et al., 2002) or to the fingertip (MAGALHAES; KOHN, 2011) improved balance control. Also, vibrotactile stimulation was shown to improve tactile sensation (COLLINS et al., 1996; LAKSHMINARAYANAN et al., 2015) and sensorimotor performance (MANJARREZ et al., 2002, 2003; MENDEZ-BALBUENA et al., 2012). Recently, we showed that an improvement in force steadiness induced by the application of vibrotactile stimulation depended on the contraction level of the muscle (GERMER et al., 2019b). Not only the reduction in force variability was greater during low-intensity contractions but also most of vibration intensities applied to the participants improved force steadiness. On the other hand, increasing contraction intensity decreased the observed amount of improvement, as well as decreased the chances of inducing motor improvement.

Dexterous manipulation of objects requires a complex control of hand muscles. To the best of our knowledge, no previous study evaluated whether the effectiveness of the motor-enhancer devices would depend on the lateral dominance of the user. Asymmetries in the motor lateralization reflect asymmetries in the neuronal circuitries involved in a voluntary movement. Theories behind handedness are based on the effective role of each limb during motor tasks (dynamic-dominance model) (SAINBURG, 2002), and on the asymmetry of sensory feedback control of movement (FLOWERS, 1975). The former concept suggests that while the dominant (D) limb is specialized in skilled dynamic movements the non-dominant (ND) limb has a fundamental role for the stabilization of static posture (GOBLE; BROWN, 2008). Also, the D limb executes automatic movements with a greater



involvement of spinal circuits (AIMONETTI et al., 1999; GOBLE; BROWN, 2008; TAN, 1989a), while the ND limb is highly controlled by supraspinal commands (MARCHAND-PAUVERT et al., 1999; PRIORI et al., 1999; SEMMLER; NORDSTROM, 1995). Conversely, the latter concept suggests an asymmetry in the use of sensory feedback during movement control. Specifically, the preferred arm of a given subject relies on visual feedback (TASK; HONDA, 1982), whereas the ND arm is mostly influenced by proprioceptive feedback (ADAMO et al., 2012; FRIEDLI et al., 1987; HAN et al., 2013a, 2013b; NAITO et al., 2011).

In this study, we aim at investigating the beneficial effect of vibrotactile stimulation on motor performance taking into consideration the existence of lateral asymmetries in upper limbs. Our previous study already showed that the force produced by the muscle of ND limb is improved by an optimal vibration (GERMER et al., 2019b). The question here is whether this improvement is maintained if the task is performed with the D limb. We hypothesize that lateral asymmetries will influence the effects of vibrotactile stimulation on the improvement of force control, due to a greater specialization of the ND limb in integrating sensory information, along with a lower motor neuron excitability as compared to the D limb (AIMONETTI et al., 1999; MARCHAND-PAUVERT et al., 1999; TAN, 1989a). Preliminary results were reported as an abstract (GERMER et al., 2019a).

## 2 MATERIALS AND METHODS

### 2.1 Participants

Ten healthy young adults (aged  $29 \pm 2$  years, six men) participated in the study. One subject was left handed and the others right handed (as assessed by the Edinburgh Handedness Inventory (OLDFIELD, 1971)), with normal or corrected-to-normal vision, and reported to have no known neurological, psychiatric or motor impairments. The subjects gave their written informed consent before the experiments.

### 2.2 Force measurement and vibrotactile stimulation

A piezoresistive transducer (FlexiForce A201, Tekscan) was used to measure isometric muscle forces (Figure 8a). Force signals were amplified (FlexiForce Quickstart Board, Tekscan), digitized at 2kHz (USB-6002, National Instruments), and low-pass filtered (30Hz cutoff frequency).

Vibratory stimuli were induced by a linear resonant actuator (C10-100, Precision Microdrives). This actuator is relatively small (10mm of diameter) and can be easily employed in haptic devices, such as gloves. It provides a periodic vibratory stimulus (175Hz, Figure 8b) for the activation of Pacinian corpuscles (ABRAIRA; GINTY, 2013; SATO, 1961). In the experiments, the actuator was placed in the radial surface of the metacarpophalangeal joint of the index finger (Figure 8a). Vibration intensity was controlled by adjusting the duty cycle of a PWM signal and ranged from zero to 1.47G peak-to-peak (Figure 8c). A three-axis analog accelerometer (ADXL337, Analog Devices) measured the vibration intensity (sampled at 2kHz).

## 2.3 Experimental protocol

During the experiments, subjects were comfortably seated in a chair with both arms on a table. A custom-made apparatus was used to keep the elbow flexed at 140deg and Velcro straps immobilized the forearm and wrist of the testing hand. A manipulandum was used to support the hand in a vertical position, maintaining the index finger perpendicular to the thumb in an extended position (Figure 8a). All fingers, but the index, were fixed to the manipulandum during the tasks. An LCD monitor (Samsung SyncMaster 713N, 17", 1280x1024px) was placed 60cm in front of the subject at eye level to provide visual feedback of the force. The visual gain was equal to 8px/%MVC for all subjects. Participants wore a headphone driven by a white Gaussian noise to mask the ambient noise.

The experiment consisted of two blocks of trials, each performed with one hand. The hand to start the task was selected randomly for each subject prior to the experiment. At the beginning of each block, three trials were performed to estimate the MVC of each subject. Each MVC trial lasted 10s and the MVC value was defined as the maximum value from the three repetitions. After a familiarization section, participants performed isometric contractions at 5%MVC. The selection of the contraction level was based on our previous study that showed a higher effect of vibration for this contraction intensity (GERMER et al., 2019b). Five trials (30s each) were performed with each hand independently. A sequence of five suprasensory vibrotactile stimuli (amplitude from 0.03G to 1.47G, Figure 8c) and a control condition without vibration (CTR) was applied for 24s (4s each intensity) (Figure 8d). Vibration intensities were presented in a random order after 4s of task onset.

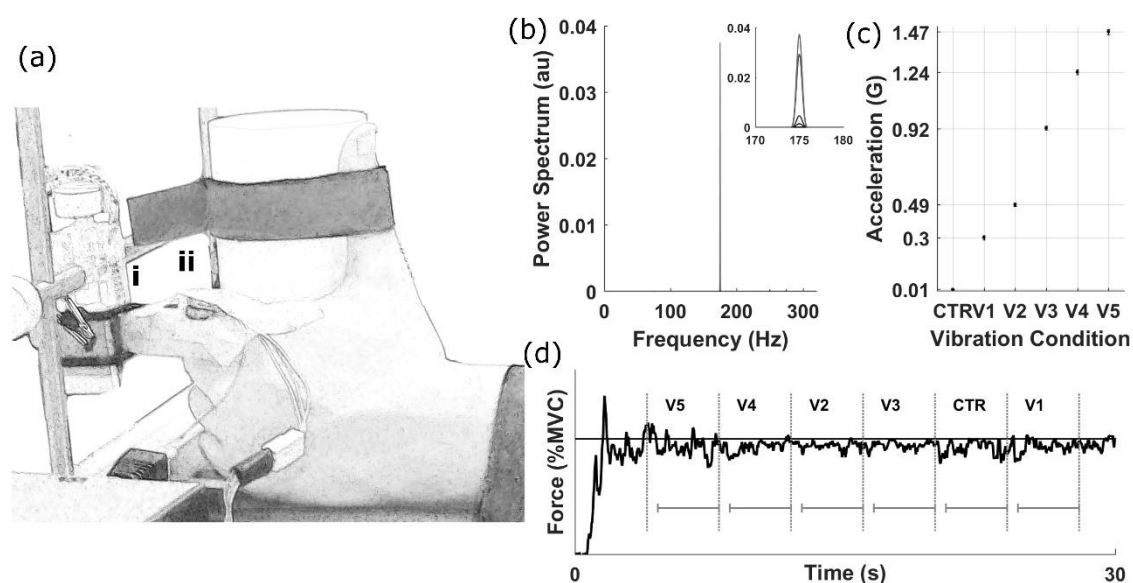


Figure 8. Schematic representation of the experimental setup and representative data. (a) Mechanical apparatus used to record index finger abduction forces. Isometric forces were measured at the distal interphalangeal joint (i) by a piezoresistive force transducer. The linear resonant actuator and accelerometer were placed at the radial surface of the metacarpophalangeal joint of the index finger (ii). The wrist and all fingers, but the index, were fixed to the apparatus with Velcro straps. (b) Power spectrum for the acceleration measured on the surface of the linear resonant actuator for different vibration intensities (inset) (c) Average acceleration measured for each vibration intensity: control (CTR) condition, and five different vibration intensities (V1 to V5). (d) Example of a typical force signal recorded from a subject. Six vibrotactile stimuli (CTR and V1 to V5) were randomly applied to the finger skin during force-matching tasks in blocks of 4s each. The total duration of the trial was 30s. Experiments were carried out on dominant and non-dominant hands. Gray lines represent the segments used for data analysis.

## 2.4 Data analysis and statistics

Force signals were processed offline in MatLab (The MathWorks). Signals were lowpass filtered (fourth-order Butterworth digital filter, 15-Hz cutoff frequency), detrended, and cut according to the six vibration intensities adopted in each trial. The initial 0.60s of each vibration block were discarded to avoid transient effects (Figure 8d). Force variability was estimated using the CoV. Time-domain and frequency-domain structures of force signals were assessed by the ApEn (SLIFKIN; NEWELL, 1999) and the power spectrum, respectively. In the present study, ApEn parameters were set as  $m = 2$  and  $r = 0.20 \cdot SD$ . Force power spectrum was estimated using Welch's method with

a non-overlapping 3.40-s Hanning window. Power spectrum analysis was performed in two frequency bands: 0-5Hz (related to the common drive (LODHA; CHRISTOU, 2017; NEGRO et al., 2009)) and 7-12Hz (related to the physiological tremor (NOVAK; NEWELL, 2017)). The relative power (with the total power as the reference) was calculated in the two frequency bands. The total power was estimated as the area of the force power spectra from zero to 15Hz.

The effects of vibrotactile stimulation on force measures were compared with the no-vibration condition (CTR) using three methods: (1) without selecting an optimal vibration (i.e., all vibration intensities were considered in the statistical model); (2) OV selected from the trials performed with D and ND hands separately (OV was considered the vibration intensity that produced the lowest force CoV in each limb); and (3) the vibration intensity associated to the OV estimated from one hand (ND or D) was used to estimate the effect on the performance in both hands. The effect of vibrotactile stimulation on force CoV was evaluated using the three methods described above. However, the effects of vibrotactile stimulation on ApEn and relative power of force were assessed only in method (2). Consistency of OV was measured as the percentage of trials that effectively decreased force CoV in relation to CTR (from five trials). Additionally, the likelihood of having an improvement in a given vibration intensity at each hand was measured as the proportion of vibrations that decreased the relative force CoV.

Statistical analysis was performed using SPSS (IBM). Assumptions for normality and sphericity were accessed by Shapiro-Wilk test and Mauchly's test of sphericity, respectively. For method (1) described above, a two-way

analysis of variance with repeated measures (two-way RM-ANOVA) was used to evaluate the effects of vibration intensities (CTR, V1 to V5) and hand (ND and D, respectively). Differences between each vibration intensity (V1 to V5) with CTR was performed using a paired t-test that were then compared with Dunnett's table (DUNNETT, 1964). The Dunnett's critical value for a model with 45 degrees of freedom and five intensities of vibrations to compare with CTR condition is 2.62. Therefore, paired t-tests with t values greater than the critical value were considered significant. For method (2), a two-way RM-ANOVA was used to evaluate the effects of vibration condition (CTR and OV) and hand (ND and D). *Post hoc* test was corrected with Bonferroni method. Finally, for method (3), CTR was compared to OV selected from ND ( $OV_{ND}$ ) or D ( $OV_D$ ). Therefore, a two-way RM-ANOVA with Bonferroni's test for multiple comparisons was used to evaluate the effect of hand (ND and D) and vibration condition (CTR,  $OV_{ND}$  and  $OV_D$ ). The results for each method were compared with Bonferroni's test. The significance level adopted in this study was 0.05. All data hereafter is presented as mean  $\pm$  95% confidence interval.

### 3 RESULTS

Participants were able to maintain the contractions at the target force level irrespective of the hand ( $F[1,9] = 0.008$ ,  $p = 0.929$ ) and vibration intensity ( $F[5,45] = 1.544$ ,  $p = 0.195$ ). The average forces performed were  $4.74 \pm 0.07\%MVC$  and  $4.74 \pm 0.06\%MVC$  for the ND and D, respectively.

### 3.1 Vibration intensities

In total, 70% and 66% of vibration intensities applied to the finger skin decreased force CoV as compared to the CTR condition for ND and D, respectively. There was no significant interaction between the hand used in the force task and vibration intensity ( $F[5,45] = 1.146$ ,  $p = 0.348$ ). Also, no significant main effect of hand was observed ( $F[1,9] = 2.293$ ,  $p = 0.164$ ). However, a significant main effect of vibration intensity was found ( $F[5,45] = 2.568$ ,  $p = 0.040$ ). Multiple comparisons showed that vibrations V2 ( $t = 3.137$ ,  $p = 0.005$ ), V3 ( $t = 3.229$ ,  $p = 0.004$ ), and V4 ( $t = 3.310$ ,  $p = 0.004$ ) significantly decreased force CoV as compared to CTR condition (Figure 9a). Vibration that most decreased force CoV was V3, with a mean absolute difference of 0.55% relative to CTR, which corresponds to 13.70% of improvement.

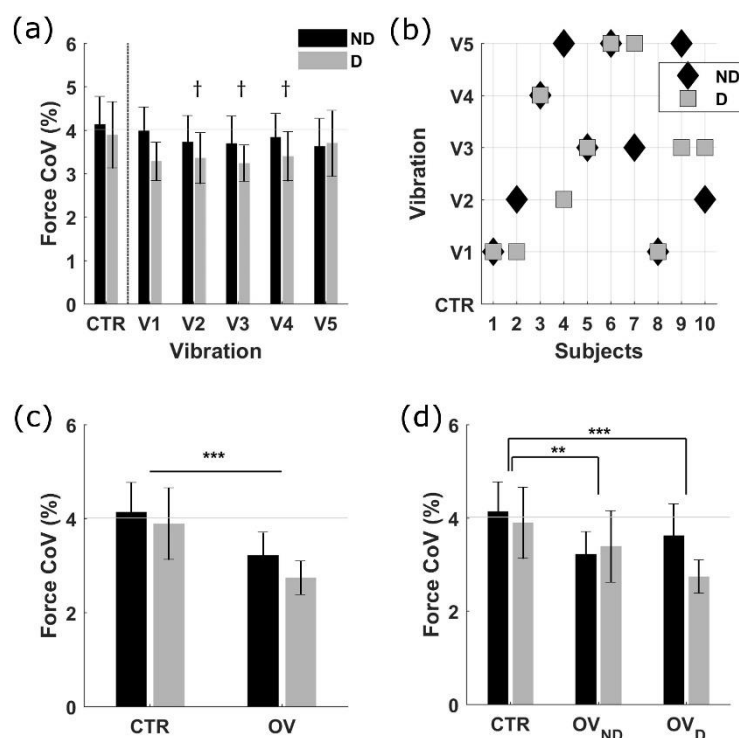


Figure 9 - (a) Force coefficient of variation (CoV) for non-dominant (ND, in black) and dominant (D, in gray) hands in no-vibration condition (CTR) and in five intensities of vibrations (V1 to V5). (b) Vibration intensity selected as optimal vibration (OV) for each subject (columns) for ND (black diamond) and D (gray square). (c) Effect of OV (showed in (b)) on force CoV. (d) Effect of OV selected from either ND (OV<sub>ND</sub>, demarked as black diamonds in (b)) or D (OV<sub>D</sub>, demarked as gray squares in (b)) on force CoV. Light gray lines indicate average force CoV for CTR. † Different from CTR, \* Significant differences (\*\* 0.001 < p < 0.010, \*\*\* p < 0.001).

### 3.2 Optimal vibration

All participants had their force steadiness (force CoV) improved by at least one vibration intensity for both ND and D. For half of subjects, OV was the same for ND and D (Figure 9b). Consistency of improvement by OV was  $70 \pm 14.61\%$  and  $84 \pm 9.78\%$  of repetitions for ND and D, respectively. Force CoV decreased with the application of OV ( $F[1,9] = 35.395$ ,  $p < 0.001$ ) but there was no significant interaction between factors (vibration condition and hand,  $F[1,9] = 0.724$ ,  $p = 0.417$ ). Additionally, no difference between hands was detected ( $F(1,9) = 1.579$ ,  $p = 0.241$ ) (Figure 9c). Force CoV decreased



from  $4.01 \pm 0.61\%$  in CTR to  $2.98 \pm 0.32\%$  in OV, which corresponded to an average improvement of 25.50%.

When the OV was selected from one hand and applied to classify the performance of both hands, a significant decrease of force CoV was still observed (effect of vibration condition,  $F[2,18] = 32.244$ ,  $p < 0.001$ ). There was no significant interaction ( $F[2,18] = 2.969$ ,  $p = 0.077$ ) and no effect of hand ( $F[1,9] = 1.461$ ,  $p = 0.258$ ) (Figure 9d). On average, force CoV decreased from  $4.01 \pm 0.61\%$  in CTR to  $3.30 \pm 0.53\%$  for  $OV_{ND}$  (i.e., the OV selected from the performance of the non-dominant hand) and  $3.18 \pm 0.43\%$  for  $OV_D$  (i.e., the OV selected from the performance of the D hand). The largest decrease in force CoV was for  $OV_D$ , with a mean absolute difference of 0.83%, which corresponds to 20.70% of improvement.

Figure 10 summarizes the results from the three methods used for the selection of the vibration intensity that most improved force steadiness. Since there was no effect of hand in the three methods, data (for ND and D) were pooled. As mentioned before, all methods significantly decreased force CoV as compared to CTR. Nevertheless, the selection of OV for each hand had a greater effect when compared to the V3 ( $p = 0.001$ ), which was the best vibration when all the vibration intensities were considered (see Figure 9a).

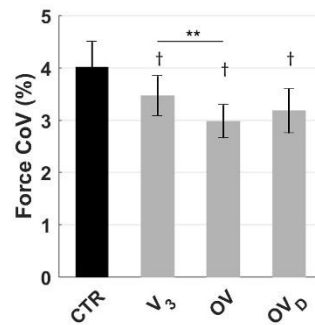


Figure 10. Force coefficient of variation (CoV) from the condition without vibration (CTR), and from the vibration condition selected using the three methods: i) the best performance when all vibration intensities were considered in the statistical model (V3); ii) the optimal vibration (OV) obtained from each hand separately; and iii) the OV obtained from a single hand (OV<sub>0</sub>). † Different from CTR, \* Significant differences (\*\* 0.001 < p < 0.010).

### 3.3 Force structure

The regularity (time-domain structure) of force signals significantly decreased ( $F[1,9] = 68.417$ ,  $p < 0.001$ ) with the OV since the value of ApEn was higher in this condition (Figure 11a). However, there was no significant interaction between hand and vibration conditions ( $F[1,9] = 0.345$ ,  $p = 0.571$ ), as well as no effect of the hand used to perform the force task ( $F[1,9] = 0.247$ ,  $p = 0.631$ ).

Most of the power (>85%) of force signals was confined to the low-frequency (0-5Hz) band (Figure 11b). For this band, no interaction was found between hand and vibration conditions ( $F[1,9] = 0.223$ ,  $p = 0.648$ ). Also, no effect of the hand used to perform the force task was detected in the analysis ( $F[1,9] = 2.774$ ,  $p = 0.130$ ). In the low-frequency band, there was a significant decrease of the relative power with OV ( $F[1,9] = 19.955$ ,  $p = 0.002$ ). Similarly, the frequency band associated to physiological tremor (7-12Hz) showed no significant interaction ( $F[1,9] = 0.001$ ,  $p = 0.970$ ). The hand used to perform the force task had no effect on the performance ( $F[1,9]$

= 1.548,  $p = 0.245$ ), but a significant effect of vibration was observed ( $F[1,9] = 21.942$ ,  $p = 0.001$ ). Therefore, OV significantly increased relative power of physiological tremor (Figure 11c).

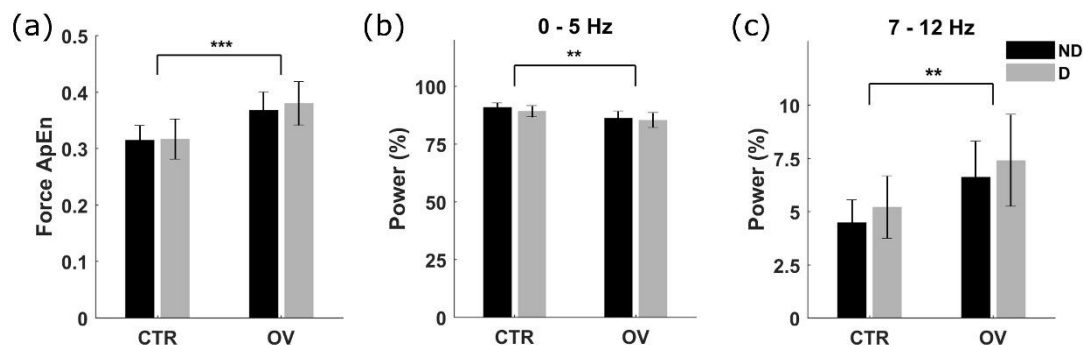


Figure 11. (a) Approximate entropy (ApEn) of force signals in CTR and OV conditions. (b) Relative power of the force in the frequency band between zero and 5Hz. (c) The same as (b) but for the frequency band between 7Hz and 12Hz (physiological tremor). Black bars represent data from the non-dominant (ND) hand, while gray bars represent data from the dominant hand (D). Asterisks represent the statistical significance (\*\*  $0.001 < p < 0.010$ , \*\*\*  $p < 0.001$ ).

## 4 DISCUSSION

In the present study, we showed that vibrotactile stimulation applied to the skin of the index finger significantly improved force steadiness. The effect was observed by either considering the whole set of vibration intensities adopted in the study or selecting an optimal vibrotactile intensity (defined for each hand independently of from the performance of one specific hand). Additionally, we observed that irrespective of the known lateral asymmetries in sensory processing by cortical and spinal circuits, the improvement on motor performance induced by vibrotactile stimuli did not depend on handedness.

## 4.1 Implications for the development of wearable motor-enhancer devices

Our results showed significant reduction in force variability for three out of five vibration intensities applied. Moreover, approximately 68% of vibration intensities applied significantly decreased force CoV. To our point of view, these findings have potential implications to the development of haptic enhancer devices. In stochastic resonance phenomenon, the transmission capability of a non-linear system is enhanced by the application of an external noise (in an optimal range), following a U-like shape (MCDONNELL; ABBOTT, 2009) so that there is a specific noise intensity that optimizes the system performance. Since the effect of improvement on motor performance induced by the application of an electrical or mechanical stimulus can be relatively small (up to 20% of improvement), it is usually preferable or necessary to find the optimal noise (GERMER et al., 2019b; TOLEDO et al., 2017; TRENADO et al., 2014c). However, the finding of the optimal stimulus intensity is challenging. Different stimulation intensities should be tested in a preliminary step to find the subject-specific optimal intensity (TRENADO et al., 2014c), and it is necessary to tune the stimulus for each condition of the sensorimotor system (e.g., for each contraction intensity (GERMER et al., 2019b)). Furthermore, the choice of the optimal intensity is not trivial. For instance, OV did not follow a linear pattern with the intensity of contraction (GERMER et al., 2019b). As to the development of a wearable device, it is difficult and undesirable to predetermine the optimal stimulation intensity. An interesting finding of the present study is that it is not necessary to tune the vibration intensity to observe a significant improvement in the force steadiness during

low-intensity (5%MVC) steady contractions (see Figure 9a). Similar conclusions were found in studies by Kurita (2013, 2016) with respect to touch sensitivity. Our result is probably due to the success of decreasing force CoV with most of vibrations tested. Nevertheless, for a greater enhancement, we would suggest finding the optimal vibration for each subject. The vibration intensity that most decreased force CoV showed an improvement of 13.70% (Figure 9), whereas the improvement was 25.50% when the optimal vibration intensity was tuned for both hands. Finally, we showed that the optimal stimulus intensity was relatively similar between hands, in a way that good results of enhancement (20.70%) could also be accomplished by finding and applying OV from only one hand.

#### 4.2 Effects of vibrotactile stimulation on force variability and force structure

The beneficial effect of vibrotactile stimulation on the motor control has been observed in different sensorimotor tasks, specifically the vibration has been shown to reduce force and position variability during steady contractions (GERMER et al., 2019b; MENDEZ-BALBUENA et al., 2012; TRENADO et al., 2014a, 2014c). Our findings support these studies and provide further evidences that a sinusoidal vibrotactile stimulus might also induce a motor enhancement. Moreover, we showed that the improvement was followed by an increase in the ApEn and in the force power spectra at higher frequencies band. A reduction in the regularity of the force time series (increase in ApEn) and a small shift of the force power spectrum to higher frequencies reflect an increase in the complexity of the system output (PINCUS, 1991). Moreover, the decreased regularity in the force time series

has been associated to an improved adaptiveness of the neuromuscular system (SLIFKIN; NEWELL, 1999). The outcomes regarding force regularity is in the same direction of our previous findings (GERMER et al., 2019b), and support the indirect hypothesis that OV might have improved sensorimotor integration in the nervous system (MENDEZ-BALBUENA et al., 2012; TRENADO et al., 2014a). Also, a recent computer simulation study has shown that the increased participation of Ia afferents in force control leads to a decrease in force CoV associated with a shift in the power spectrum to higher frequencies (7-12Hz) (NAGAMORI et al., 2018), which is similar to our experimental results. It is well known that cutaneous afferents can reduce presynaptic inhibition of Ia afferents (AIMONETTI et al., 2000; NAKASHIMA et al., 1990), thereby increasing the influence of this afferent input to the motor neuron pool. Therefore, we cannot rule out the involvement of Ia afferents in our results.

### 4.3 Lateral dominance

We did not observe any difference between D and ND hand for force CoV, ApEn, and force power spectrum. These findings support other results in the literature where the motor performance during steady contractions was equal for both hands. For instance, tremor amplitude during the contraction of first dorsal interosseous (FDI) muscle (index finger abduction) was similar between hands for right-handed participants (BEUTER, 2000; NOVAK; NEWELL, 2017; SEMMLER; NORDSTROM, 1995). Different attributes of the neuromuscular system yield force variability (and tremor), from intrinsic properties of motor units (e.g., the recruitment order and recruitment

thresholds of motor neurons, and the range of twitch amplitudes of muscle units) (JONES et al., 2002; KEENAN; VALERO-CUEVAS, 2007) to motor unit discharge properties (e.g., motor unit discharge variability and synchronization) (MORITZ et al., 2005; WATANABE et al., 2013). As to the discharge properties of FDI motor units, results reported in the literature did not show significant differences between D and ND hands for the mean discharge rate and discharge variability during low-intensity contractions (0.50N) (SEMMLER; NORDSTROM, 1995, 1998). However, differences were observed during higher-intensity contractions (30%MVC) (ADAM et al., 1998). Therefore, since in our study the subjects performed low-intensity contractions, the similar motor output variability (i.e., force CoV) could be attributed to similar discharge properties of individual FDI motor units. On the other hand, reports on motor unit synchronization have shown contrasting results. There was evidence of higher level of synchronization between the motor units of ND hand (KAMEN et al., 1992; SEMMLER; NORDSTROM, 1995, 1998), but also for the motor units from D hand (SCHMIED et al., 1994). The influence of motor unit synchronization on force variability has been a topic of contentious debate in the literature (FARINA; NEGRO, 2015). The current view is that the motor unit synchronization has little influence on force variability. Therefore, handedness can account on lateral asymmetries observed in motor unit synchronization, but these differences would not impact the force variability.

Other contrasting results in the literature concern on the regularity of the force signal (entropy) and the relative power in the physiological tremor band (7-12Hz). Some studies reported the ApEn and relative power in the

tremor band are both similar between D and ND sides (NOVAK; NEWELL, 2017), or higher in the D side (BEUTER, 2000). However, it is worth noting that the statistical effect observed in the latter study was borderline for both ApEn ( $p = 0.046$ ) and relative power ( $p = 0.046$ ), and hence they should be interpreted cautiously. Since ApEn is associated to the adaptiveness of a given system (PINCUS, 1991; SLIFKIN; NEWELL, 1999), our results suggest that the motor control strategy and motor adaptability are similar to both hands (SLIFKIN; NEWELL, 1999).

#### 4.4 Independence of handedness on the effect of vibrotactile stimulation

In the present study, we showed that OV significantly decreased force CoV, but the hypothesis of a higher effect on the ND hand was rejected. Force variability has been shown to largely reflect low-frequency fluctuations of the discharge rate of motor neurons (LODHA; CHRISTOU, 2017; NEGRO et al., 2009). The low-frequency fluctuations of the common inputs to the motor neuron pool depend on the oscillations from voluntary descending commands and sensory afferent feedback. Since we did not observe differences between hands on the effect of OV on force steadiness (no significant interaction between vibration condition and hand) we would suggest that any potential effect of OV should be similar among the neuronal circuits controlling D and ND hands. In fact, short-latency cutaneous reflex from wrist extensors (thought to involve only spinal circuitry) did not exhibit any asymmetry between the D and ND sides (BARSS et al., 2014; MARCHAND-PAUVERT et al., 1999). In contrast, the voluntary descending command is thought to contribute to lateral asymmetries. It has been shown that the excitability of



motor neurons innervating the muscles from the ND hand are more influenced by corticospinal activity (PRIORI et al., 1999; SEMMLER; NORDSTROM, 1995). Since the fluctuations of motor output are strongly influenced by the statistics of pre-motoneuronal commands (WATANABE et al., 2013), we would also suggest that the similar effect of OV on force CoV between hands was governed by the contribution of cutaneous afferent activity on spinal circuits rather than supraspinal ones. Otherwise, whether the OV influenced the statistics of descending commands a differential effect between hands would be expected. Yet, a deeper understanding on the motor unit discharge properties is necessary to evaluate these hypotheses.

The hypothesis of a greater effect of vibrotactile stimulation on the ND hand was based on the advantages of the ND side to integrate sensory afferent feedback. Psychophysical experiments show a greater accuracy of the ND limb during active movement proprioception, thereby supporting the latter hypothesis (HAN et al., 2013b, 2013a). Additional support to the specialization of the ND side for sensory perception and integration comes from a neuroimaging study, where the right hemisphere of right-handed participants was significantly more activated than the left hemisphere during kinesthetic illusory flexion of the wrist (NAITO et al., 2011). Finally, the threshold for sensory perception has been shown to be lower for the ND hand (FRIEDLI et al., 1987). Despite having evidence of an advantage of the ND side for the integration of sensory feedback, this ability is highly influenced by visual feedback (LI et al., 2015). In fact, most of the studies prevent participants to rely on visual feedback during the trials (ADAMO et al., 2012; HAN et al., 2013b, 2013a; NAITO et al., 2011). Therefore, we hypothesize

that the proprioceptive asymmetry was occluded by visuomotor feedback of the force we provided during our experiment, which can explain the lack of differences between hands on both force variability and the effect of OV.

## 5 CONCLUSION

An optimal level of vibration improved motor performance by enhancing adaptiveness of the system and sensorimotor integration. Irrespective of the lateral asymmetries in cortical and spinal levels, improvement on motor performance induced by vibrotactile stimuli did not depend on handedness. We suggest that either vibrotactile stimulation would not activate pathways that project asymmetrically to the central nervous system, or the presumed advantage of the ND side on the integration of sensory feedback was occluded by the visual feedback provided to the subjects in this study.

## Chapter 3

# NEUROPHYSIOLOGICAL CORRELATES OF FORCE CONTROL IMPROVEMENT INDUCED BY SINUSOIDAL VIBROTACTILE STIMULATION

---

### ABSTRACT

*Objective.* An optimal level of vibrotactile stimulation has been shown to improve sensorimotor control in healthy and diseased individuals. However, the underlying neurophysiological mechanisms behind the enhanced motor performance caused by vibrotactile stimulation is yet to be fully understood. Here we aim to partially overcome this gap by evaluating the effect of a cutaneous vibration on the firing behavior of a population of motor units in a condition of improved force steadiness.

*Approach.* Participants performed a visuomotor task, which consisted of low-intensity isometric contractions of the FDI muscle, while sinusoidal (175Hz) vibrotactile stimuli with different intensities were applied to the index finger. High-density surface electromyogram (HD EMG) was recorded from the FDI muscle, and a decomposition algorithm was used to extract the motor unit spike trains. Also, computer simulations were performed using a multiscale neuromuscular model to provide a potential explanation for the experimental findings. *Main results.* Experimental outcomes show that an optimal level of vibration significantly decreased force variability (estimated as the coefficient of variation), the variability of the neural drive to the FDI muscle, and the proportion of common inputs to the FDI motor nucleus. However, the interspike interval (ISI) variability did not change with the vibration. A mathematical approach, together with computer simulation results suggest that vibrotactile stimulation would activate a more regular pathway to the motor neuron pool, thereby decreasing the variance of the common synaptic input to the motor neuron pool. *Significance.* Therefore, the decreased variability of the common input accounts for the enhancement in force control induced by vibrotactile stimulation.

## 1 INTRODUCTION

Since the study by Collins and coworkers (1996) vibrotactile stimulation has been shown to improve both sensory perception and sensorimotor control in humans. For instance, Priplata et al. (2002, 2003) reported an improved balance control when a bandlimited Gaussian vibratory noise stimulated the foot soles of young and elderly participants. Similarly, Magalhaes and Kohn (2011) showed that vibrotactile noise applied to the fingertip of participants during a postural task could reduce the body sway. Mendez-Balbuena et al. (2012) and Trenado et al. (2014b) used an index finger sensorimotor task to show that stochastic vibrotactile stimulation could decrease the mean variation of index finger position in healthy participants and patients with essential tremor, respectively. More recently, Germer et al. (2019b) reported that a sinusoidal vibrotactile stimulation applied to the index finger could also improve force steadiness during isometric contractions of the FDI muscle, but the improvement was more significant for low-intensity contractions. On top of the behavioral findings described above, neurophysiological studies have reported that vibrotactile stimulation could increase the power of the electroencephalogram (EEG) recorded in the somatosensory area (MANJARREZ et al., 2002), and the beta-band corticomuscular coherence (an estimate of the coupling between cortical and spinal circuits) (TRENADO et al., 2014c).

The studies mentioned above allude to the occurrence of stochastic resonance phenomenon in the sensorimotor system. Stochastic resonance is a counterintuitive phenomenon in which the capacity of a nonlinear system to detect/transmit a weak input signal can be improved by the addition of

noise with appropriate intensity into the system (MCDONNELL; ABBOTT, 2009; MCDONNELL; WARD, 2011; MOSS, 2004). Although the occurrence of stochastic resonance in an individual neural element is evident (CORDO et al., 1996), the neural basis for this phenomenon is somewhat challenging to grasp when a more complex system (e.g., the neuromuscular system) is taken into consideration. Notwithstanding, the studies reported in the literature suggest that vibrotactile stimulation would increase the sensitivity of cutaneous mechanoreceptors, thereby improving sensorimotor integration in both spinal and supraspinal neural circuits (MAGALHAES; KOHN, 2011; MENDEZ-BALBUENA et al., 2012; PRIPLATA et al., 2002; TRENADO et al., 2014a, 2014b, 2014c). However, these explanations add little to the neurophysiological knowledge since no activity of neural elements are directly recorded during the motor-enhanced tasks.

A key element of motor control is the MN and the muscle fibers they innervate (i.e., the motor unit (HECKMAN; ENOKA, 2012; SHERRINGTON, 1925)). Modern technologies for electromyogram (EMG) signal recording and processing warrant accurate monitoring of the activity of a population of motor units during isometric or *quasi*-isometric contractions (FARINA et al., 2016; FARINA; HOLOBAR, 2016; HOLOBAR et al., 2014; MARTINEZ-VALDES et al., 2016). Therefore, the analysis of motor unit spike trains yields a more precise interpretation regarding the neural control of muscle force. Some studies found a relation between the discharge rate variability of motor units (primarily estimated as the CoV of the motor unit interspike intervals, ISI) and force steadiness (KOUZAKI et al., 2012; LAIDLAW et al., 2000; MORITZ et al., 2005). It is well known that the discharge rate variability of motor units

is mostly influenced by the synaptic noise (CALVIN; STEVENS, 1967, 1968), which is comprised of both common and independent commands impinging onto the MNs. More recent findings, however, have shown that force variability are more related to the fluctuations of the common synaptic inputs received by a population of MNs (FARINA et al., 2014; FEENEY et al., 2018; NEGRO et al., 2009), and that the averaging process performed by the MN pool filters out the contribution of independent synaptic inputs (FARINA et al., 2014, 2016; FARINA; NEGRO, 2015).

To the best of our knowledge, no previous study evaluated the activity of a population of motor units during a motor task enhanced by vibrotactile stimulation. The study by Kouzaki et al. (2012) recorded few motor units (ten) using intramuscular EMG electrodes during a motor task enhanced by subthreshold electrical stimulation delivered percutaneously to the peripheral nerve of ankle extensor muscles. They found a decreased ISI CoV and motor unit synchronization both associated with an increased force steadiness. However, the findings of a motor task enhanced by electrical stimulation cannot be directly translated to vibration-induced enhanced motor performance. Moreover, the recording of a small sample of neural elements precludes a broader overview of the neurophysiological mechanisms behind the improved sensorimotor control.

An improved sensorimotor control would be a result of (1) a reduced fluctuation of the common synaptic input, and/or (2) a reduction in the synaptic noise. If the latter is the determinant factor, one would expect a reduced discharge rate variability of motor units (lower ISI CoV), which is similar to the findings of (KOUZAKI et al., 2012). However, if the former

mechanism yields the improved sensorimotor control, we will observe a reduced variability of the neural drive to the muscle (FARINA et al., 2010, 2014; NEGRO et al., 2009), along with a decreased proportion of common inputs (PCI) to the recruited motor units (NEGRO et al., 2016). Based on recent experimental results (presented above) that were able to record a large population of motor units, we hypothesize that vibrotactile stimulation would influence the fluctuations of the common synaptic input instead of changing the independent component of the synaptic inputs to the motor neurons.

In the present study, we aim at providing a neural basis for the improved motor performance caused by vibrotactile stimulation. As an experimental model, we adopted low-intensity isometric contractions of the FDI muscle (index finger abduction) with and without stimulation of cutaneous mechanoreceptors by high-frequency sinusoidal vibration (GERMER et al., 2019b). Additionally, computer simulations were carried out on a multiscale model of the neuromuscular system (CISI; KOHN, 2008; WATANABE et al., 2013) as an aid to better understanding the potential mechanisms underlying the experimental findings. Partial results were presented as an abstract (GERMER et al., 2018b).

## 2 MATERIALS AND METHODS

### 2.1 Participants

Eleven subjects ( $25 \pm 6$  years,  $65.45 \pm 7.12$  kg, 7 men) participated in the study. All subjects were right-handed, had normal or corrected-to-normal vision, and reported no previous history of neuromuscular diseases.

Participants gave their written informed consent before the experiments. The procedures were in accordance with the Declaration of Helsinki and were approved by the Imperial College Research Ethics Committee.

## 2.2 Force measurement and vibrotactile stimulation

Abduction force of the index finger was measured with a three-axis force transducer (Nano25, ATI Industrial Automation) attached to a mechanical apparatus (Figure 12a). The force signal was digitized at 2048Hz (USB-6225, National Instruments) and lowpass filtered (15-Hz cutoff frequency) with a fourth-order Butterworth filter.

Vibrotactile stimulation was performed by a linear resonant actuator (resonant frequency of 175Hz, C10-100, Precision Microdrives) placed on the radial surface of the metacarpophalangeal joint (Figure 12a). A previous study demonstrated the efficiency of this vibration protocol in improving force control (GERMER et al., 2019b). Three intensities of vibration were applied: (1) nearly imperceptible low-intensity vibration (0.01G); (2) intermediate-intensity vibration (0.45G); and (3) high-intensity vibration (1.50G).



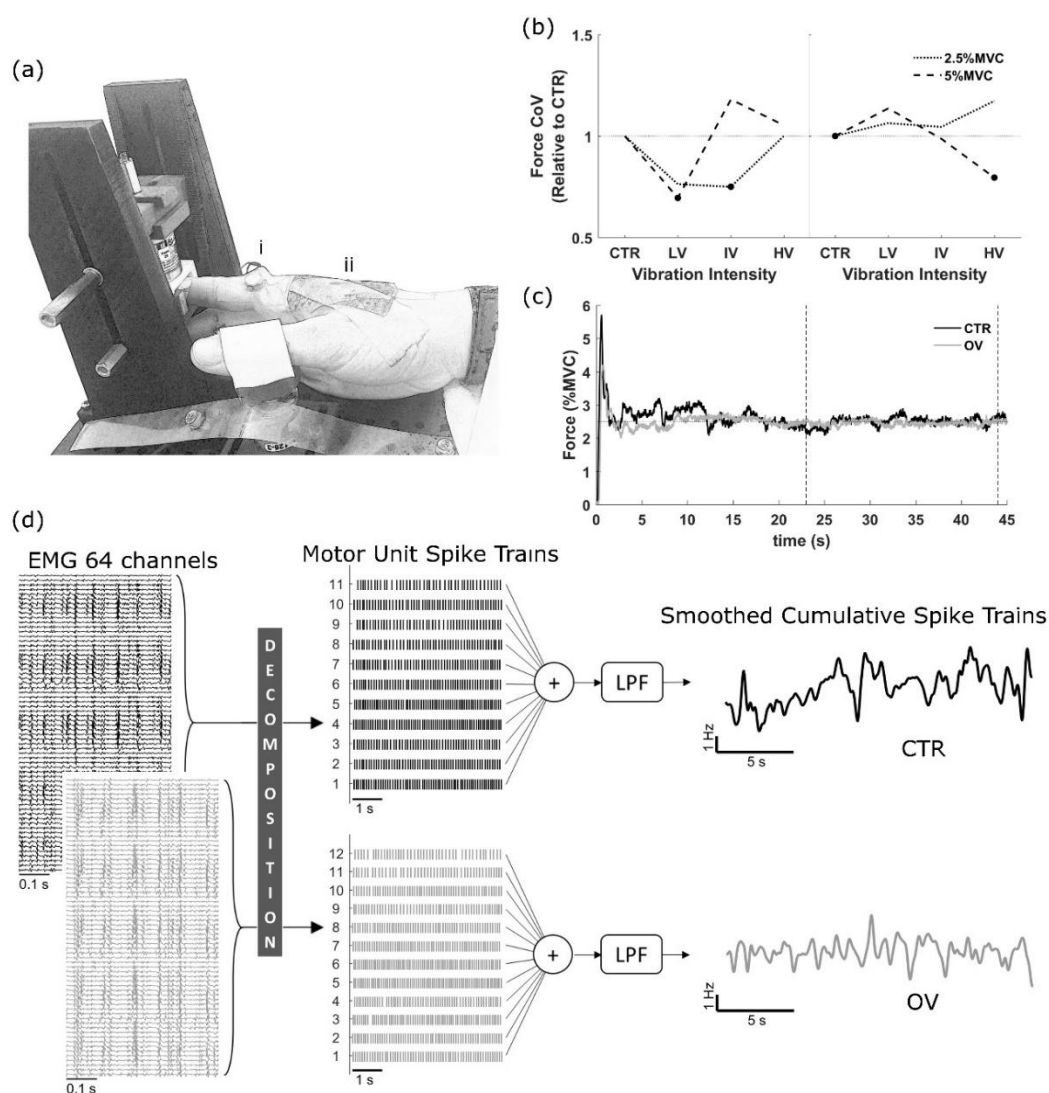


Figure 12 Experimental protocol and data analysis. (a) Mechanical apparatus used to record index finger abduction force. Isometric forces were measured at the distal interphalangeal joint and a linear resonant actuator was placed at the radial surface of the metacarpophalangeal joint of the index finger (i). A high-density (HD) surface EMG grid with 64 electrodes was placed on the first dorsal interosseus (FDI) muscle (ii). (b) Representative recordings of force signals from a single participant in CTR (black) and OV (gray) conditions at 5%MVC. Data analysis was carried out on data confined between the dashed lines (i.e., between 23 s and 44 s) so as to avoid non-stationarities. (c) Representative analysis of the influence of vibrotactile stimulation on force steadiness (force CoV) for two participants. The effects of low-intensity (LV), intermediate-intensity (IV), and high-intensity (HV) vibration on force CoV were normalized to the non-vibration control condition (CTR). Black circles depict the optimal vibration (OV), which was defined as the vibration amplitude that produced the lowest force CoV (relative to CTR) for each participant at each contraction intensity. Note that the participant on the right panel did not have an OV at 2.50%MVC. (d) Data analysis performed on HD surface EMG signals. Leftmost signals represent the data from the 64 EMG channels (rows) recorded during CTR (black) and OV (gray) conditions. The EMG channels were decomposed into motor unit spike trains (middle), so that each row represents one motor unit and the vertical bars represent the discharge timings. The neural drive to the muscle (rightmost signals) was estimated as the smoothed cumulative spike train (sCST), which consists of a lowpass filtered (LPF) version (at 2.50Hz) of the cumulative spike trains (see Sec. 2.5.3 for details).

### 2.3 Recording of high-density surface electromyogram

A 13x5 flexible grid of electrodes (4-mm interelectrode distance, ELSCH064NM4, OT Bioelettronica) was placed on the FDI muscle (Figure 12a). Skin preparation was performed before placement of the electrode grid. HD-EMG signals were recorded with a multichannel amplifier (Quattrocento, OT Bioelettronica) in monopolar mode. Signals were bandpass filtered (10-500Hz) and digitized with 16-bit resolution at 2048Hz.

### 2.4 Experimental protocol

Participants were comfortably seated on a chair with both arms resting on a table. A custom-made apparatus supported the right hand in vertical position (Figure 12a). Velcro® straps were used to immobilize the forearm and wrist. The index finger was aligned with the forearm and the thumb was kept in a resting position at the same height as the index finger. An LCD monitor was placed ~60cm in front of the subject at the eyes level to provide a visual feedback of the force. The target force was showed as a red line at the center of the monitor screen, and the force feedback signal was provided as a moving yellow line in which the y-axis position corresponded to the force component normal to the sensor surface. Participants wore a headphone driven by a white Gaussian noise sound to mask the ambient noise.

Experiments started with participants performing their MVC in trials that lasted 10s. The MVC was defined as the maximum value of three attempts. The experiment consisted of steady isometric abductions of the index finger in two contraction intensities (2.50% and 5%MVC). Trials were

performed without vibration (control condition, CTR) and with the three vibration intensities defined above (low, intermediate, and high). In vibration trials, vibratory stimulus started at the beginning of the trial up to its end. Prior to the main trials, participants performed eight familiarization tests (all combinations of target forces and vibration intensities) that consisted of steady isometric contractions with 15s duration. After acquaintance, the participants performed the tasks that lasted 45s, and each task was repeated three times. The order of presentation of each combination of target force and vibration intensity was randomized, and a 30-s resting interval was adopted between trials.

## 2.5 Data analysis

### 2.5.1 Force signals

Force signals were processed offline in MATLAB (The MathWorks Inc.). The force signal was lowpass filtered (fourth-order Butterworth digital filter, 15-Hz cutoff frequency) and detrended. The initial 23s and last 1s of each recording were discarded to avoid non-stationarities of force signals (Figure 12b). Force variability was measured as the CoV of the force signal.

For each contraction intensity (i.e., 2.50%MVC and 5%MVC), the average force CoVs calculated from the three attempts were compared between the vibration intensities. In order to normalize the subject-dependent effect of vibrotactile stimulation on sensorimotor performance (MENDEZ-BALBUENA et al., 2012; TRENADO et al., 2014a, 2014b, 2014c), we selected an OV for each participant. OV was defined as the vibration intensity that provided the lowest force CoV (Figure 12c) and was determined

for each force intensity (GERMER et al., 2019b). Henceforth, all analyses were carried out on dependent variables measured in the two contraction intensities (2.50% and 5%MVC) and two vibration conditions (CTR and OV).

### *2.5.2 HD surface EMG signals*

HD surface EMG signals were decomposed into motor unit spike trains using a blind source separation algorithm (Figure 12d) (HOLOBAR et al., 2014; HOLOBAR; ZAZULA, 2007). The pulse to noise ratio that estimated the accuracy in discharge identification was set to 30 dB (HOLOBAR et al., 2014; HOLOBAR; ZAZULA, 2007). After the automatic decomposition, the motor unit spike trains were visually inspected by an experienced researcher to correct for misclassified spikes. Motor units that exhibited intermittent firing were discarded from the analysis.

### *2.5.3 Motor unit spike trains*

We assessed the mean ISI, as well as the SD and CoV of ISIs. The neural drive to the FDI muscle was estimated as the smoothed cumulative spike train (sCST, Figure 12d). The CST of each trial was estimated as the sum of all motor unit spike trains and normalized by the number of motor units. The CST was smoothed using a non-overlapping 400-ms duration Hanning window. The mean and CoV of the sCST was calculated for each condition.

The PCI to the motoneuron pool was estimated from the coherence function (NEGRO et al., 2016) in the frequency band between 0.20Hz and 2Hz (Eq. 2). Briefly, for each trial, coherence functions between two groups with  $m$  motor units were computed, where  $m$  ranged from one to half the number of decomposed motor unit spike trains.

$$\bar{C}_{f_1, f_2} = \frac{|m^2 A|^2}{(mB + m^2 A)^2} \quad (2)$$

where,  $\bar{C}_{f_1, f_2}$  is the average coherence in the frequency band  $[f_1, f_2]$ ,  $A$  and  $B$  are parameters to be optimized.

The parameters  $A$  and  $B$  in Eq. 2 are related to the power of the common synaptic input, and the squared root of the ratio  $A/B$  is an estimate of the PCI (NEGRO et al., 2016). We solved the nonlinear least-squares optimization method with the function 'lsqcurvefit' available in MATLAB. The values of  $\bar{C}_{f_1, f_2}$  were estimated using the pooled coherence between two long time series (AMJAD et al., 1997), which comprised the concatenation of all possible permutations of groups of  $m$  motor units or up to a maximum of 1,000 permutations. Coherence was estimated using the Welch's averaged periodogram with non-overlapping Hanning window of 5-s duration (resolution of 0.20Hz). Only trials with at least six motor units were used for the PCI analysis.

## 2.6 Computer simulations

### 2.6.1 Model description

Computer simulations were carried out using a multiscale neuromuscular model extensively described elsewhere (CISI; KOHN, 2008; ELIAS et al., 2012; ELIAS; KOHN, 2013; WATANABE; KOHN, 2017, 2015; WATANABE et al., 2013). Here we will provide only a brief description of the model. The original model was parameterized to represent the leg muscles, but in the present study we adapted the model to represent the MN pool innervating the FDI muscle. The MN pool consisted of 120 type-identified MNs

(101 S-type, 17 FR-type, and 2 FF-type) (ENOKA; FUGLEVAND, 2001). Each MN was represented by a two-compartment model (soma-dendrite). The soma encompassed the passive properties of the membrane (resistance and capacitance), and active ionic currents yielding action potential (fast sodium and potassium currents) and afterhyperpolarization (slow potassium) time courses. To speed up the simulations, state variables associated to the dynamics of ionic currents were simplified using the approach by Destexhe (1997). The dendrite was a passive compartment, since we have no clear evidence of the involvement of active dendritic currents (e.g., persistent inward currents) during low-intensity isometric contractions. Morphological and electrophysiological parameters were adopted equal to those reported in (CISI; KOHN, 2008; WATANABE et al., 2013), with a piecewise linear interpolation of the reference values (see Table 2 in (CISI; KOHN, 2008) and Table 1 in (WATANABE et al., 2013)) to represent the population of MNs.

The MN pool was commanded by a combination of common and independent presynaptic inputs (all located at the dendritic compartment). Two scenarios were explored: (1) a single common input that represented the corticomotor drive (Figure 13a); and (2) two common inputs, where one input represented the corticomotor drive and the secondary input was adopted to represent the activity from cutaneous afferents (Figure 13b). It is worth noting that the cutaneous pathway to MNs is oligosynaptic (PIERROT-DESEILLIGNY; BURKE, 2012), but for simplicity we assumed that the whole circuit would result in a single common input to the MNs.

Synaptic inputs were represented by a first-order kinetic model (DESTEXHE et al., 1994), whose parameters followed those reported in Cisi

and Kohn (2008) for excitatory synapses (i.e., reversal potential equal to 70mV, and time constant equal to 0.11ms). Each synapse from common inputs had a maximum conductance of 600nS, while the synapses from independent inputs had a maximum conductance of 6,000nS. The latter was larger than the former since each MN had a single independent input, while common inputs were many (100 for corticomotor drive and 100 for the secondary common input). The common inputs were activated by Gamma stochastic point processes, while the independent inputs were activated by Poisson point processes (mean ISI equal to 50ms).

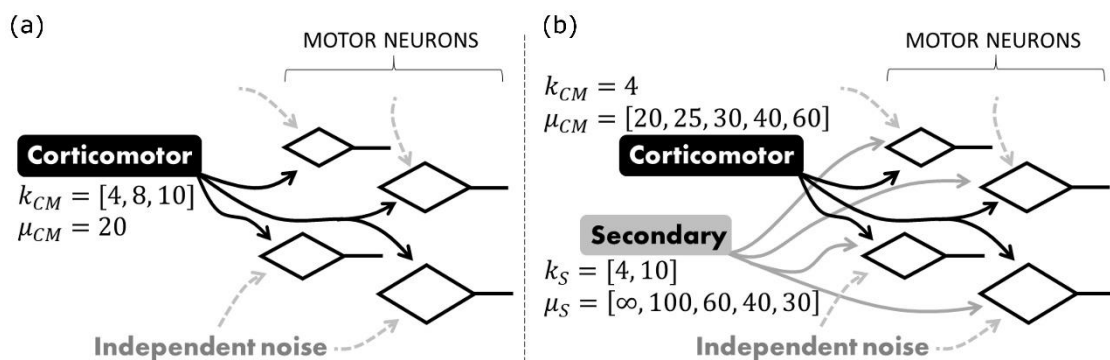


Figure 13. Schematic diagram of the motor neuron pool model for the two scenarios explored here: (a) with a single common input (corticomotor drive), and (b) with two common inputs (corticomotor and secondary drives). In addition, in both scenarios each motor neuron received independent commands (noise). Common presynaptic commands were represented by Gamma point processes with mean interspike intervals ( $\mu$ ) and order ( $k$ ) varying according to the values presented between the brackets.

Muscle unit force was produced by the impulse response of a second-order critically damped system (MILNER-BROWN et al., 1973). Twitch amplitudes and contraction times ranged from 1mN to 140mN and 30ms to 100ms, respectively (FUGLEVAND et al., 1993; MILNER-BROWN et al., 1973). The FDI muscle force was computed as the sum of the forces produced by each active muscle unit.

The model was implemented in Java programming language (Oracle), and the differential equations were solved using a fourth order Runge-Kutta method with a fixed step ( $50\mu\text{s}$ ).

### 2.6.2 Simulation protocols

Each simulation had 10-s duration and 17 simulations were performed to evaluate the variability between each simulation run. First, the maximum muscle force was estimated as the average contraction yielded by a neural drive of 30Hz (ENOKA; FUGLEVAND, 2001). Subsequent simulations were performed to achieve submaximal muscle force. The commands to the MN pool were adjusted so that the mean ISI and ISI CoV from the model were both similar to the experimental counterparts.

In the first scenario (see description above and Figure 13a), we tested the hypothesis that the OV would directly influence the variability of a single common input (corticomotor drive). Therefore, the order ( $k_{CM}$ ) of the Gamma point process was systematically changed from 4 (control) to 8 and 10 (more regular), while the mean ISI ( $\mu_{CM}$ ) was set to 20ms. In the second scenario (Figure 13b), we added a secondary common input to evaluate the hypothesis that the pathway from cutaneous afferents is independent from the corticomotor drive and would differentially influence the variance of the global common input to the MN pool. We evaluated the effect of the secondary common input with the same distribution of the control case (i.e.,  $k_S = k_{CM} = 4$ ) and for a more regular Gamma point process ( $k_S = 10$ ). The reciprocal of the mean ISI (i.e., the mean rate) of the global common input ( $\mu_G$ ) followed Eq. 3, and we evaluated five different combinations  $[\mu_{CM}; \mu_S]$ : [20;0]ms, [25;100]ms, [30;60]ms, [40;40]ms, and [60;30]ms. Please, note that in all



combinations the mean rate (mean ISI) of the global common input was maintained at 50Hz (20ms).

$$\frac{1}{\mu_G} = \frac{1}{\mu_{CM}} + \frac{1}{\mu_S} \quad (3)$$

### 2.6.3 Simulation data analysis

Simulation data were analyzed in the same way as the experimental data (see Sec. 2.5). The dependent variables measured from the simulations were: mean force; force CoV; mean ISI from the MNs; MN ISI CoV; mean sCST; sCST CoV; PCI; and the resultant variance of the common input (estimated from the Gamma point processes).

## 2.7 Theoretical calculation of common input variance

From the theory of stochastic point processes, the variance of ISI of a Gamma point process (renewal process) is given by  $\sigma_{ISI}^2 = \mu/k$ , where  $\mu$  is the mean ISI (in milliseconds) and  $k$  is the order of the Gamma point process. Similarly, the asymptotic variance of the firing rate ( $\sigma_{FR}^2$ ) is given by Eq. 4 (COX, 1962).

$$\sigma_{FR}^2 = \frac{\sigma_{ISI}^2 \cdot 1,000}{\mu^3} + \frac{1}{6} + \frac{(\sigma_{ISI}^2)^2}{2\mu^4} - \frac{\mu_3}{3\mu^3} \quad (4)$$

where,  $\mu_3$  is the skewness of the ISI distribution.

In the present study, we would like to calculate the firing rate variance of the global common input to the MN pool. Since the corticomotor input is assumed to be independent on the secondary (cutaneous afferent) input, the firing rate variance is given by Eq. 5.

$$\sigma_G^2 = \sigma_{CM}^2 + \sigma_S^2 \quad (5)$$

Substituting the asymptotic variance of each independent input (Eq. 4 for CM and S) in Eq. 5, and, for simplicity, ignoring the influence of skewness (i.e., the last term of Eq. 4), we can calculate the theoretical variance of the global input using the parameters described in Sec. 2.6.2.

$$\sigma_G^2 = \left( \frac{1,000}{k_{CM} \cdot \mu_{CM}^2} + \frac{1}{6} + \frac{1}{2k_{CM}^2 \cdot \mu_{CM}^2} \right) + \left( \frac{1,000}{k_S \cdot \mu_S^2} + \frac{1}{6} + \frac{1}{2k_S^2 \cdot \mu_S^2} \right) \quad (6)$$

## 2.8 Statistical analysis

Statistical analysis was performed using SPSS (IBM). The significance level adopted in the study was 0.05. Data are represented as mean  $\pm$  95% confidence interval. Prior to the regression analysis, a normality test was performed using the Shapiro-Wilk method. The effect size was calculated as the partial eta-squared ( $\eta_p^2$ ). Large effects were considered when  $\eta_p^2 > 0.25$ , while small effects were considered when  $\eta_p^2 < 0.01$  (COHEN, 1988).

For the experimental data, a two-way RM-ANOVA and Bonferroni's *post hoc* tests were used to compare the dependent variables between contraction intensities (2.50% and 5%MVC) and vibration conditions (CTR and OV). In order to minimize type I error in our analysis due to the selection of an OV out of three vibration intensities, we corrected the significance level to 0.017 (0.05/3).

Computer simulation data were analyzed using a multiple ANOVA and Dunnet's tests to compare the dependent variables measured in different input conditions with those in the control condition ( $k_{CM} = 4$  and  $\mu_{CM} = 20$ ms).

In the scenario with a single common input (Figure 13a), the control condition was compared with two conditions where the order of the corticomotor input was changed ( $k_{CM} = 8$  and  $10$ ). Similarly, in the scenario with two common inputs (Figure 13b) the control condition was compared with different conditions where the intensities of the two inputs were systematically varied ( $\mu_{CM}/\mu_S$  equal to  $25/100$ ,  $30/60$ ,  $40/40$ , and  $60/30$ ).

## 3 RESULTS

### 3.1 Human experiments

All the participants were able to maintain the muscle force at the target levels regardless of the vibration intensity ( $p = 0.758$ ). When the target force was 5%MVC at least one vibration intensity was able to decrease the force CoV (steadiness) for all participants. However, at 2.50%MVC no OV was observed for two participants of the study. Figure 14a and Table 1 show that force CoV was significantly decreased (large effect) in OV as compared to the CTR condition, irrespective of the force intensity. Also, force CoV was significantly larger when the target force was 2.50%MVC.

In total, 295 (305) and 357 (350) motor units were decomposed in CTR (OV) at 2.50% and 5%MVC, respectively. The following analyses were performed with the spike trains from these motor units. No interaction between force intensities (2.50% and 5%MVC) and vibration conditions (CTR and OV) was observed for the dependent variables measured from the motor unit spike trains (i.e., ISI CoV, sCST CoV, and PCI; see Table 1). Mean ISI and mean sCST were significantly influenced by contraction intensity (mean

ISI decreased and mean sCST increased when the force was 5%MVC), but they had no significant effect of OV. Conversely, sCST CoV and PCI were both significantly decreased by OV (Figure 14c and Figure 14d) but had no effect of force intensity. ISI CoV did not change with either force or vibration (Figure 14b).

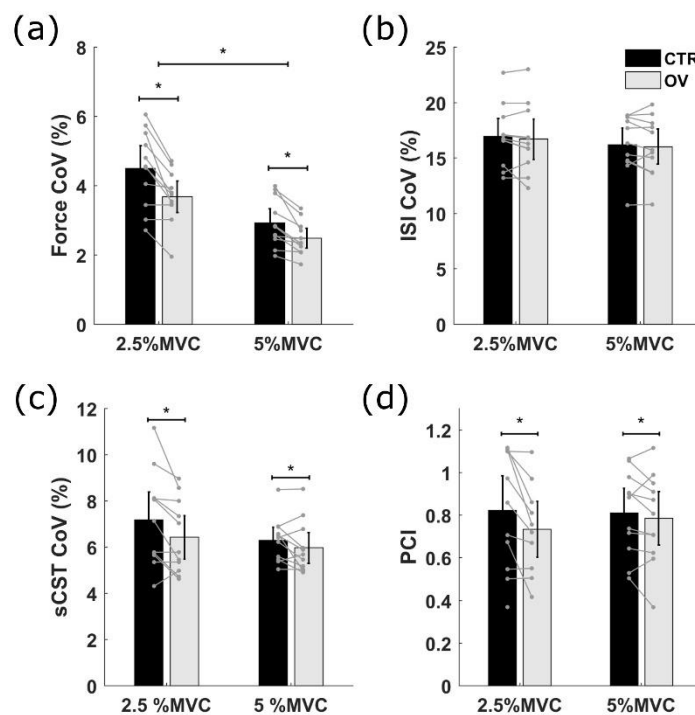


Figure 14. Experimental results. (a) Force CoV as a function of force intensities (2.50% and 5%MVC) and vibration conditions (control, CTR, and optimal vibration, OV). (b-d) The same as (a), but for the interspike (ISI) coefficient of variation (CoV), smoothed cumulative spike train (sCST), and proportion of common input (PCI), respectively. Error bars represent the 95% confidence interval ( $n = 11$ ). Gray lines indicate individual data (per subject). Asterisks indicate significant differences ( $p < 0.017$ ).

**Table 1.** Outcomes from the two-way RM-ANOVA performed on the experimental data. Asterisks indicate the significant differences ( $p < 0.017$ ). Effect size is reported as the partial eta-squared ( $\eta_p^2$ ).

		<b>Mean Force</b>	<b>Force CoV</b>	<b>Mean ISI</b>	<b>ISI CoV</b>	<b>Mean sCST</b>	<b>sCST CoV</b>	<b>PCI</b>
<b>Force</b>	<i>P</i>	<0.001*	<0.001*	0.003*	0.312	0.004*	0.087	0.743
	<i>F</i> (1,10)	37944.746	75.691	14.967	1.133	13.616	3.603	0.115
	$\eta_p^2$	1	0.883	0.599	0.102	0.577	0.265	0.013
<b>Vibration</b>	<i>P</i>	0.964	<0.001*	0.354	0.148	0.465	0.012*	0.004*
	<i>F</i> (1,10)	0.002	28.345	0.945	2.465	0.577	9.508	14.225
	$\eta_p^2$	0.000	0.739	0.086	0.198	0.055	0.487	0.612
<b>Force vs Vibration</b>	<i>P</i>	0.591	0.070	0.271	0.985	0.199	0.216	0.069
	<i>F</i> (1,10)	0.308	4.115	1.358	0.000	2.909	1.741	4.279
	$\eta_p^2$	0.030	0.292	0.120	0.000	0.225	0.148	0.322

### 3.2 Computer simulations

In the first scenario simulated in this study (see Sec. 2.6.2 for details), a more regular corticomotor input (the only common input impinging onto the MNs) significantly decreased all dependent variables as compared to the control condition ( $k_{CM} = 4$ ) (Figure 15), but did not decrease the mean force (Table 2). These results are in contrast with the experimental outcomes since in the experiments we did not observe significant changes in the ISI CoV (see Figure 14b).

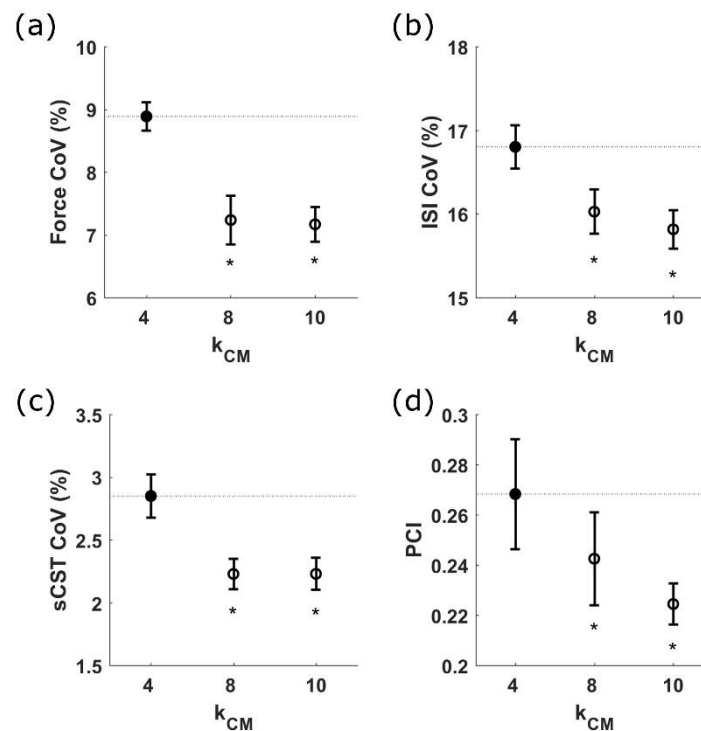


Figure 15 Computer simulation results for the scenario where the variability of the corticomotor input (single common input) was reduced ( $k_{CM} = 8$  and  $k_{CM} = 10$ ) with respect to the control condition ( $k_{CM} = 4$ ). Effects on (a) force CoV, (b) ISI CoV, (c) sCST CoV, and (d) PCI. Error bars represent the 95% confidence interval ( $n = 17$ ). Asterisks indicate significant differences ( $p < 0.05$ ).

The addition of a secondary input (second scenario described in Sec. 2.6.2) with  $k_S = 4$  did not significantly change any dependent variable evaluated in the study (see Figure 16a-d). Conversely, Figure 16e-h shows that when  $k_S = 10$  (more regular input) there was a significant decrease in force CoV, sCST CoV, and PCI when the intensity of the secondary input increased ( $\mu_{CM}/\mu_S = 40/40$  and  $\mu_{CM}/\mu_S = 60/30$ ). Also, in the latter condition, no difference was observed for the mean force, mean ISI, ISI CoV, and mean sCST among the different combinations of common input intensities, which is compatible with the experimental results presented in Sec. 3.1). Table 2 shows a complete description of the statistics from the computer simulation data.

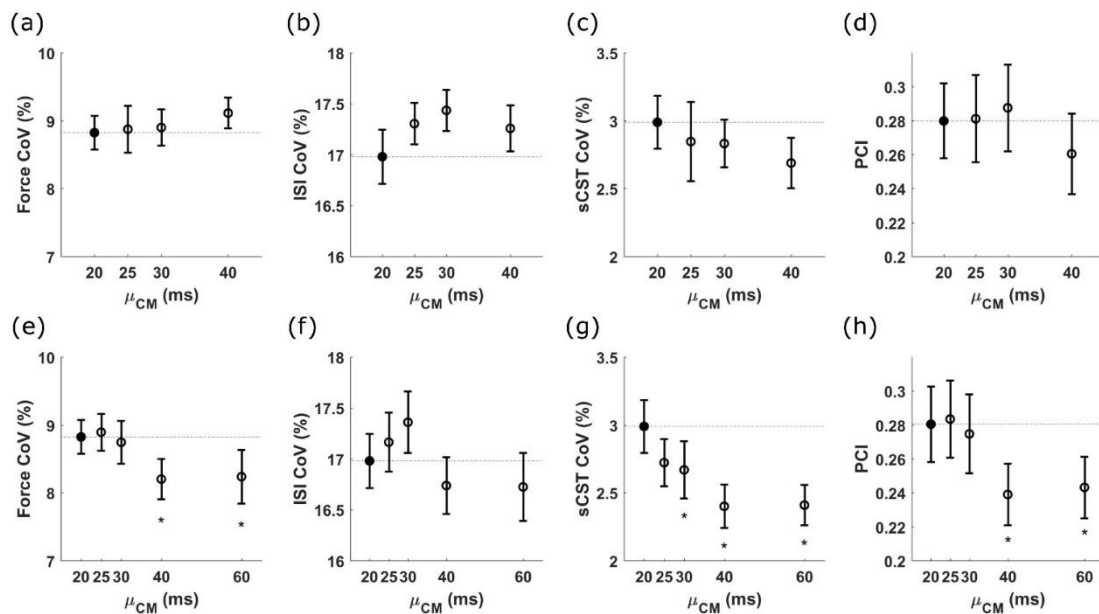


Figure 16 Computer simulation results for the scenario where the secondary common input was added to the model. (a)-(d) Results achieved when  $k_{CM} = k_S = 4$ . (e)-(h) Results achieved when  $k_{CM} = 4$  and  $k_S = 10$  (more regular input). Effects are shown for: (a) and (e) force CoV; (b) and (f) ISI CoV; (c) and (g) sCST CoV; and (d) and (h) PCI. Error bars represent the 95% confidence interval ( $n = 17$ ). Asterisks indicate significant differences ( $p < 0.05$ ).

**Table 2.** Outcomes from the multiple ANOVA performed on the computer simulation data. Asterisks indicate significant differences ( $p < 0.05$ ). Effect size is reported as the partial eta-squared ( $\eta_p^2$ ).

			Mean Force	Force CoV	Mean ISI	ISI CoV	Mean sCST	sCST CoV	PCI	Variance
$\mu_{CM} = 20ms$	Order ( $k_{CM}$ )	$P$	0.517	<0.001*	0.240	<0.001*	0.115	<0.001*	0.001*	<0.001*
		$F(2,62)$	0.666	60.566	1.462	25.946	2.239	33.045	7.765	28.522
		$\eta_p^2$	0.21	0.661	0.0445	0.456	0.067	0.516	0.200	0.479
	Multiple comparisons	4 vs. 8	0.225	<0.001*	0.745	<0.001*	0.807	<0.001*	0.033*	<0.001*
		4 vs. 10	0.615	<0.001*	0.115	<0.001*	0.998	<0.001*	<0.001*	<0.001*
$k_S: 4$	Condition	$P$	0.097	0.490	0.651	0.049*	0.268	0.307	0.453	0.897
		$F(3,64)$	2.199	0.815	0.548	2.765	1.343	1.227	0.887	0.199
		$\eta_p^2$	0.093	0.037	0.025	0.115	0.059	0.054	0.040	0.009
	Multiple comparisons ( $\mu_{CM} = 20ms$ )	vs. 25ms	0.726	0.832	0.956	0.998	0.145	0.361	0.777	0.480
		vs. 30ms	0.997	0.867	0.966	1.000	0.098	0.325	0.881	0.596
vs. 40ms		0.996	0.990	0.977	0.995	0.142	0.073	0.285	0.754	
vs. 60ms	-	-	-	-	-	-	-	-	-	
$k_S: 10$	Condition	$P$	0.237	0.003*	0.955	0.014*	0.907	<0.001*	0.006*	<0.001*
		$F(4,80)$	1.414	4.439	0.167	3.331	0.253	7.217	3.942	9.203
		$\eta_p^2$	0.660	0.182	0.008	0.143	0.013	0.265	0.165	0.315
	Multiple comparisons ( $\mu_{CM} = 20ms$ )	vs. 25ms	0.988	0.885	0.901	0.968	0.469	0.066	0.858	0.055
		vs. 30ms	0.999	0.666	0.934	0.998	0.473	0.026*	0.657	<0.001*
vs. 40ms		0.968	0.012*	0.798	0.316	0.699	<0.001*	0.014*	<0.001*	
vs. 60ms	0.794	0.018*	0.772	0.292	0.722	<0.001*	0.028*	<0.001*		

### 3.3 Variance of the common input

Figure 17 illustrates the effect of a secondary input on the resultant variance of the global common input. These results are based on the theoretical approach described in Sec. 2.7. If the corticomotor input was represented as a Poisson point process (Gamma point process with order  $k_{CM} = 1$ ), the addition of a secondary input of any order ( $k_S$ ) decreased the resultant input variance (Figure 17a). Conversely, when the regularity of the corticomotor input increased (i.e., higher  $k_{CM}$ ) the input variance depended on the regularity ( $k_S$ ) and intensity ( $\mu_S$ ) of the secondary input. When  $k_{CM} = 4$  the common input variance decreased only when  $k_S \geq 5$ , irrespective of the  $\mu_S$  (Figure 18b). However, when  $k_S = 4$  and  $k_S = 4$ , there were optimal regions where the balance between the intensities of the corticomotor and secondary inputs produced a minimum input variance. For  $k_{CM} = 6$  (Figure 17c) a decrease in the global common input variance was observed only when  $k_S \geq 7$ , but the observed decrease was almost negligible. Finally, when  $k_{CM} = 10$  the resultant global common input variance increased for any intensity and order of the secondary input (Figure 17d).



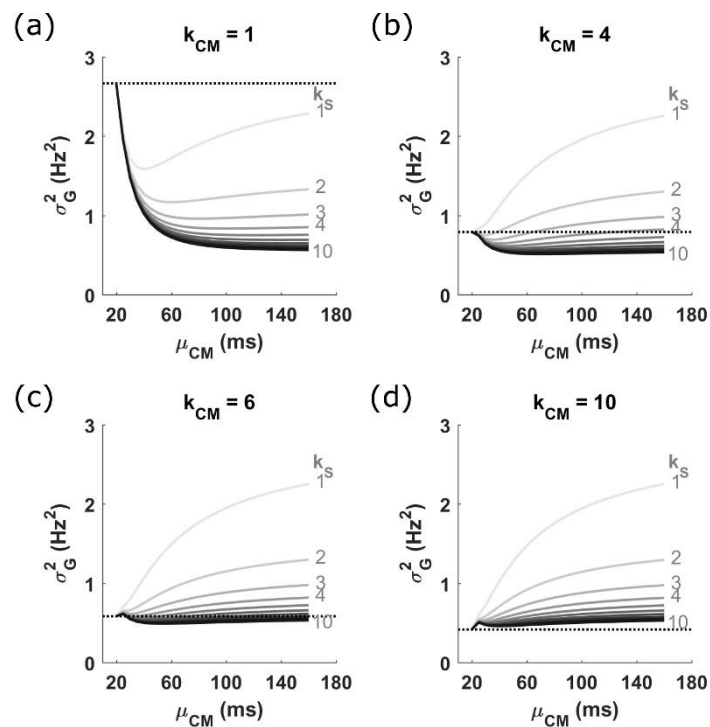


Figure 17. Theoretical analysis on the effects of order ( $k$ ) and mean intensity ( $\mu$ ) of the two common inputs (Gamma point processes) on the variance of the global common input ( $\sigma_G^2$ ). Panels (a)-(d) show analytical curves for different orders of the corticomotor input (i.e.,  $k_{\text{CM}} = 1, 4, 6, \text{ and } 10$ , respectively).

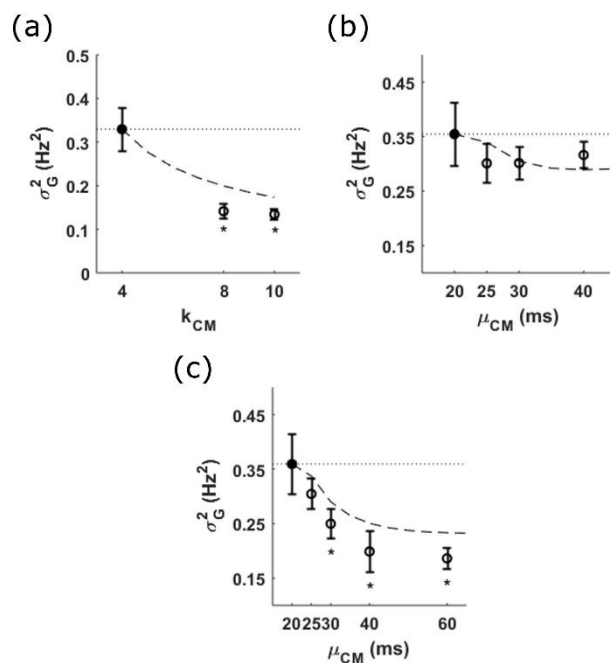


Figure 18 shows a comparison between computer simulation data and the theoretical analysis of the global common input variance. Figure 18a shows that when the common input is represented by a single corticomotor

input the input variance significantly decreased (as expected from the theoretical curve; see dashed line) when  $k_{CM}$  increased (more regular). When the two common inputs are considered in the model, there is no significant difference in the input variance when  $k_{CM} = k_S = 4$  (Figure 18b), whereas significant differences were observed when  $k_S = 10$  and  $\mu_S < 60\text{ms}$  (Figure 18c). These differences in the common input variance are related to the changes observed in force CoV, sCST CoV, and PCI from computer simulation data.

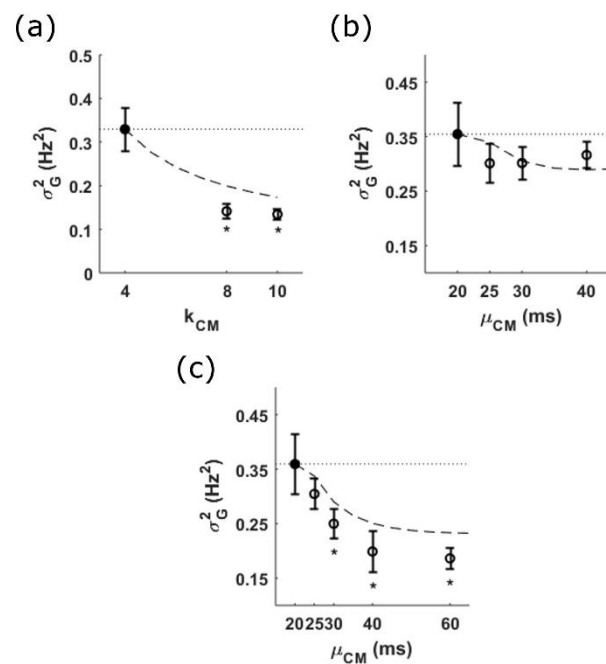


Figure 18. Variance of the global common input. (a) Relationship between the common input variance ( $\sigma_G^2$ ) and the order of the corticomotor input ( $k_{CM}$ ), which was the single input in the model for this scenario. (b)-(c) Input variance when two common inputs are considered in the model. Panel (b) shows the relationship between the input variance and the intensity of the corticomotor input ( $\mu_{CM}$ ) when  $k_{CM} = k_S = 4$ , while panel (c) shows the same relationship when  $k_S = 10$ . Error bars represent the 95% confidence interval ( $n = 17$ ). Asterisks indicate significant differences ( $p < 0.05$ ).

## 4 DISCUSSION

In the present study, we combined human experiments and computer simulations to provide clues on the neurophysiological mechanisms behind

the improved force control induced by sinusoidal vibrotactile stimulation. In the experiments, we observed that an optimal level of vibrotactile stimulation (OV) could reduce force variability (CoV) accompanied by a decrease in the variability of the neural drive to the FDI muscle (reduced sCST CoV) and a reduction in the proportion of common inputs (PCI) to the recruited motor units. However, OV did not change ISI variability as compared to the control (no vibration) condition. Computer simulations could resemble the experimental findings only when a combination of two independent common inputs were used in the model, and the secondary input had a lower variability. Additionally, from the theory of stochastic point processes, we showed that the variance of the global common input could be reduced by an appropriate balance between intensity and variability of the two independent inputs impinging on the motor pool. Therefore, the experimental findings can be explained by a reduction in the variance of the global common input due to the activation of a secondary input, which we hypothesize to be the neural activity induced by the vibrotactile stimulation. In the following subsections, we shall present a detailed discussion on each of these findings.

#### 4.1 Effects of an optimal vibrotactile stimulation on a population of motor units

A relevant experimental finding was that OV did not reduce either ISI CoV or the relationship between ISI SD and the mean ISI (data not shown), but was able to reduce the fluctuations of the neural drive to the muscle (estimated as the smoothed CST (FARINA et al., 2014)), as well as the proportion of common input (Figure 14 and Table 1).

Despite the evidence of correlation between ISI CoV and force CoV (KOUZAKI et al., 2012; MORITZ et al., 2005), the current opinion is that the low-frequency fluctuations of the common inputs to the MN pool account for the motor output variability (LODHA; CHRISTOU, 2017; MOON et al., 2014; NEGRO et al., 2009). Although the MN activity is intrinsically nonlinear, the population of recruited motor units acts as a lowpass linear system (DIDERIKSEN et al., 2012; NEGRO et al., 2009; NEGRO; FARINA, 2011a). In other words, the population of motor units linearly transmits the slowly varying components of the common input to the motor output and filters out the independent synaptic inputs received by each MN (FARINA et al., 2014). Our findings support this idea since the reduction in force CoV caused by OV was not followed by a reduction in the ISI CoV but by a reduction in sCST CoV, which roughly represents the variability of low-frequency components (up to 2.50Hz) of the common input.

The reduction of force CoV in OV was followed by a decrease in PCI. PCI is an estimate of the relative proportion between the common inputs impinging onto the MNs and the total synaptic inputs (NEGRO et al., 2016). This index may also be viewed as the proportion between the common fluctuations on MN membrane potential and the total membrane potential fluctuations (sum of common and independent inputs). Therefore, a decreased PCI could be a consequence of a reduced fluctuation of the common inputs and/or an increased fluctuation of the independent inputs. An increased synaptic noise (here considered only the independent part of the presynaptic commands to the MNs) would produce motor unit spike trains with higher variability (CALVIN; STEVENS, 1968). However, as we mentioned

above, OV did not change ISI CoV, thereby suggesting that the vibrotactile stimulation does not significantly influence the synaptic noise. As a consequence, the reduction in PCI likely reflects a decreased fluctuation of the common input to the motor pool.

Another possible explanation for the decreased PCI is a decorrelation between the activities of the motor units caused by activation of cutaneous afferents. Kouzaki et al. (2012) showed that motor unit synchronization was reduced when a subthreshold stochastic electrical stimulation was applied to the tibial nerve. Despite the expected difference between the experimental protocol of the referred study and ours (i.e., their protocol preferably excited muscle afferents), the reduced motor unit synchronization is in the same direction of our finding of reduced PCI (although we did not find any difference in motor unit synchronization – data not shown). Since PCI is a measure derived from the coherence between two motor unit CSTs, it also reflects the degree of correlation imposed by common inputs to the MN pool (NEGRO et al., 2016). Therefore, the activation of cutaneous afferents by vibrotactile stimulation would reduce the corticomotor drive (but the net excitatory input is maintained, since we did not observe changes in the mean excitability of the motor units in OV as compared to CTR), thereby decreasing the correlated discharge of motor units (KOUZAKI et al., 2012; NEGRO; FARINA, 2011b).

#### 4.2 On the influence of common input statistics

A theoretical analysis and computer simulations showed that the statistical properties of common inputs could largely influence the motor output variability, which was similar to the findings of Watanabe et al. (2013).

When a single common input was considered in the model (to represent the corticomotor drive), the reduced variability of the presynaptic command reduced force CoV, ISI CoV, sCST CoV, and PCI (see Figure 15). The latter results contrast with the experimental findings and, therefore, suggest that vibrotactile stimulation would not directly influence the variance of the corticomotor drive, which is compatible with experimental data from monkeys (BAKER et al., 2006). When the intensity of the global input was adjusted to produce simulated motor unit discharges at the same mean rate of the experimental data, the best scenario to reproduce the experimental outcomes was with a reduced variability of the second input as compared to the variability of the corticomotor drive. In this scenario, the activity of the secondary input (along with the corticomotor drive) reduced the force CoV, sCST CoV, and PCI, but did not change the ISI CoV (Figure 16 and Table 2).

The addition of a secondary input would influence the activity of motor units in two different (but complementary) ways. First, the analytical approach (Figure 17 and Figure 18) demonstrated that the variance of the global common input (a combination of corticomotor and secondary inputs) is mostly influenced by both the intensity and variability of each input (see Eq. 6). With a more regular secondary input, the global common input will have a lower variability that implies a more regular neural drive to the muscle (sCST with lower variability), and consequently a steadier force (DEL VECCHIO et al., 2018; DIDERIKSEN et al., 2012; FARINA; NEGRO, 2015; THOMPSON et al., 2018). Second, the activation of the secondary input would decorrelate the corticomotor input and MN pool output, similar to the findings

by Negro and Farina (2011b). Both factors (i.e., reduced global input variance and decorrelation of corticomotor drive) lead to a reduction of the PCI.

Nonetheless, so far, we explained the reduction of force variability caused by vibrotactile stimulation based on analyses that consider a population of motor units. When individual motor units were evaluated, we did not find modifications in ISI variability between CTR and OV conditions (Figure 14). A simple decrease in the common input variance will lead to a decrease in ISI CoV, as observed in the simulations with a single common input (Figure 15). The addition of a second input is not expected to change this property, but a reduction in the ISI CoV did not accompany the lower variance of the global input when the second input was added. It is well known that MN ISI variability depends on both afterhyperpolarization time course and the high-frequency fluctuations of the membrane potential (CALVIN; STEVENS, 1967; MATTHEWS, 1996). The former is an intrinsic property that is implausible to be influenced by OV. Therefore, a possible explanation for the unchanged ISI CoV is that the addition of a secondary input changed the low-frequency power spectrum of the global synaptic input but did not significantly alter its high-frequency content. Alternatively, Negro and Farina (NEGRO; FARINA, 2011b) showed that the nonlinearity in the spiking generation process produces constructive and destructive interferences when two common inputs concurrently activate the MN. This interference induced by the two inputs limits the transmission capacity of any common input to the output of a single MN, and hence the independent synaptic noise will play a significant role in shaping the variability of the MN

ISIs. Since we did not change the independent noise across simulated conditions, the ISI CoV did not change accordingly.

Another insight provided by the theoretical analysis and computer simulations is on the existence of conditions with increased common input variance depending on the combination of regularity and intensity of the two common inputs. In our study and several others published elsewhere (GERMER et al., 2019b; MENDEZ-BALBUENA et al., 2012; TRENADO et al., 2014a, 2014c), the beneficial effect of vibrotactile stimulation was not observed for some intensity of a vibratory stimulus. For a single subject, some intensities worsen force control (i.e., increase force CoV, see Figure 12c for an example). Also, the vibration intensity for optimal performance is frequently different across the subjects (TRENADO et al., 2014c). A possible explanation is that the global common input variance depends on a balance between the regularities and intensities of the two inputs (Figure 17). Small modifications in both variability and/or intensity of the corticomotor drive or cutaneous afferent drive would produce an input variance that is higher (or equal) than (to) a control condition, thereby decreasing (or unchanging) the motor performance.

### 4.3 On the role of cutaneous afferents on motor unit activity and force enhancement

Hitherto, our focus was on the influence of optimal vibrotactile stimulation on the activity of motor units. However, other experimental studies using different protocols have shown that stimulation (either electrical or mechanical) of cutaneous afferents can (i) reduce the presynaptic



inhibition of Ia muscle spindle afferents (AIMONETTI et al., 2000; ILES, 1996; NAKASHIMA et al., 1990), (ii) induce differential excitatory and inhibitory effects on high-threshold and low-threshold motor units, respectively (DATTA; STEPHENS, 1981), and (iii) influence the recruitment pattern of motor units by changing their recruitment thresholds (GARNETT; STEPHENS, 1981). Since we evaluated the activity of a population of motor units rather than tracking individual motor units between vibration and no-vibration conditions, we cannot rule out the possibility that cutaneous afferents would induce differential excitatory/inhibitory effects on the motor units. However, a different experimental protocol is necessary to explore these aspects of our vibrotactile stimulation protocol.

Changes in presynaptic inhibition can also be a putative neurophysiological mechanism underlying the findings of the present study. Aimonetti et al. (2000) reported that cutaneous vibration could reduce presynaptic inhibition of Ia terminals without changing the mean discharge rate of the motor units. A recent computer simulation study showed that force CoV, common drive index, and motor unit coherence decreased with an increased gain of the monosynaptic Ia pathway (NAGAMORI et al., 2018). In this vein, the Ia afferent activity would also comprise the hypothetical secondary input of our model, and its effects would be quite similar to those described in the previous sections. Nonetheless, the relative contribution of Ia and cutaneous to the finding should be evaluated in another protocol mixing vibrotactile and electrotactile stimulations.

Additionally, even in our protocol, we cannot rule out a direct activation of Ia afferents due to the proximity between the vibrotactile

actuator and the metacarpophalangeal joint. However, there is an extensive literature showing that tendon vibration would influence the activity of motor units differently from the findings reported here (BARRERA CURIEL et al., 2019; KIEHN; EKEN, 1997; MOSIER et al., 2017; TENAN et al., 2019). For instance, tendon vibration increases motor unit firing rate (KIEHN; EKEN, 1997), decreases discharge variability (HARWOOD et al., 2014), and changes the recruitment strategy of motor units (XU et al., 2018). Since we did not observe most of these effects in our data (notably, the increase in firing rate and ISI variability), we suggest that the direct activation of Ia afferents by our vibrotactile stimulation is minimal, and another neurophysiological mechanism is behind the findings reported elsewhere (e.g., tonic vibration reflex).

Our computer simulation results suggest that vibrotactile stimulation would activate a more regular (less variable) pathway during an OV condition. This hypothesis is plausible since the Pacinian corpuscles (thought to be activated by our stimulation protocol (ABRAIRA; GINTY, 2013)) have a preferred firing range, which depends on the vibration intensity and frequency (BOLANOWSKI; ZWISLOCKI, 1984). Spike train histograms from the Pacinian afferent activities exhibited a marked periodicity with small deviations from the preferred firing frequency. This feature is still present even when a bandlimited (100Hz to 300Hz) stochastic input is applied to the mechanoreceptor (BOLANOWSKI; ZWISLOCKI, 1984). Therefore, our results and interpretations can also be useful to explain the experimental outcomes from studies that used a stochastic vibrotactile stimulation to improve force control (MENDEZ-BALBUENA et al., 2012; TRENADO et al., 2014a, 2014c).



## *Chapter 4*

### FINAL COMMENTS

---

**A**s final comments, it is of paramount importance to discuss the results presented in the previous chapters in an integrative manner. Here we will provide the putative mechanisms (based on our previous results) behind the beneficial effect of vibrotactile stimulation to motor performance.

In Chapter 3, we provided evidences that force variability is highly influenced by low-frequency fluctuations of the common input to the motor neuron pool, which is translated to the neural drive to the muscle. We explored (using a neuromuscular model) a representative scenario in which the motor neuron pool received a common input (from descending drive and proprioceptive feedback), a secondary common input (from cutaneous afferents), and independent synaptic noise. In another scenario, we represented the inputs to the motor neuron pool as a single common input and independent noise. We showed that the fluctuations of the global common input, which influenced the force variability, could be modulated by the statistics of the two common inputs. In other words, specific conditions of the neural system, given by the combination of the voluntary drive, proprioceptive feedback and cutaneous (exteroceptive) commands, would lead to either a reduction or an increase in force variability. We suggest that an optimal level of vibrotactile stimulation would induce a neural condition in which a more regular discharge of cutaneous afferents impinging to spinal

and supraspinal neurons would reduce the low-frequency fluctuations of the common input, and consequently the neural drive to the muscle and the motor output (force).

With the previous results in mind, we can reinterpret the results from Chapter 1, where we showed that the application of a sinusoidal (deterministic) vibration can be used to improve force control in an isometric condition. Other studies have shown that stochastic vibrotactile stimulation was also effective in improving motor performance. The similarity between our protocol and those based on stochastic inputs (MENDEZ-BALBUENA et al., 2012; TRENADO et al., 2014a, 2014c) would be attributed to the transduction property of Pacinian corpuscles in the glabrous skin, which discharges regularly regardless of the stimulus nature (stochastic or deterministic). Therefore, the application of either deterministic or stochastic vibrotactile stimuli in the sensitivity range of Pacinian corpuscles would induce a motor improvement due to the low variability of cutaneous afferent discharges. However, future studies using stochastic and deterministic vibrotactile stimulations in the same protocol are necessary to support this idea.

Another key finding described in Chapter 1, was the differential effect of OV depending on the contraction intensity. A more prominent effect of OV was observed during low-intensity contractions. In the discussion of that Chapter (which was already published in a journal (GERMER et al., 2019b)), the analysis of the signal-dependent noise of muscle force (i.e., the relation between force SD and mean force level (JONES et al., 2002)) lead to the conclusion that OV would reduce the synaptic noise in the motor neuron pool. Taking the results of Chapter 3 into consideration, the latter conclusion turns

out to be partially true. The synaptic noise has two sources of randomness: (1) the randomness of common inputs; and (2) the randomness of independent inputs. Computer simulations combined with analysis of motor unit spike trains showed that the independent term would not change with the OV (CALVIN; STEVENS, 1968). However, the variance of the global common input is reduced due to the activity of cutaneous afferents. Therefore, the synaptic noise would be only partially reduced by OV, and the influence of higher frequency components of the synaptic inputs to the motor neuron pool seemed to be of little relevance (since the ISI CoV did not change) for the reduction of fluctuations of muscle force caused by vibrotactile stimulation.

Following a decrease in the force CoV, we reported a shift of the force power spectrum to higher frequency components, along with an increased ApEn (decreased regularity) (Chapters 1 and 2). The decrease in the proportion of low-frequency fluctuations in the force time series is in line with a reduced low-frequency fluctuation of the neural drive (Chapter 3). Moreover, we suggested that these results would reflect an increased activity of Ia afferents due to the reduction of presynaptic inhibition of Ia terminals caused by increased cutaneous activity (see the discussion of Chapters 1 and 2). The role of Ia afferents is out of the scope of this work, but an increased Ia inflow would also be represented as a second common input to the motor neurons, and hence all the interpretations based on cutaneous activity could be valid in this condition. Nonetheless, further studies are necessary to elucidate the role of presynaptic inhibition on the observed motor behavior.

An increase of ApEn with OV reflects a decreased regularity of the force time series. Similarly, it may also represent an increased complexity of the system output, which might be related to the number of components or processes contributing to the force control (SLIFKIN; NEWELL, 1999). We suggest that the increased afferent inflow would contribute to the neural control strategies during the stabilization of force in a target level, and hence OV would maximize the adaptiveness of the system. It is not clear, however, the correlation between complexity of the force structure (ApEn) and the fluctuations in the common input. Further investigations are needed for a better understanding of the neural mechanisms behind modifications of ApEn.

Finally, in Chapter 2, we showed that irrespective of lateral asymmetries in the sensory processing at cortical and spinal levels, the improvement of motor performance induced by vibrotactile stimulation did not depend on handedness. Our hypothesis was that the presumed advantage of the non-dominant hand in integrating sensory inputs was somehow occluded by the visual feedback provided to the subjects in our experimental protocols (LI et al., 2015). In this condition, it is possible that the common input to motoneurons in the dominant and non-dominant sides were similar, and hence any influence of OV in reducing the equivalent common input would occur in both sides.

In sum, with this study we were able to provide additional data to the literature regarding the improvement of force control caused by vibrotactile stimulation. The neurophysiological interpretations are novel and based on experimental data from a population of human motor units, which were recorded for the first time in a motor-enhancement protocol with vibrotactile

stimulation. Additionally, the possibility of using sinusoidal vibrotactile stimulation to improve force control is quite relevant to the development of haptic devices for motor rehabilitation and motor performance.



## LIST OF PUBLICATIONS

---

GERMER, C. M.; ELIAS, L. A. Influência da realimentação visual no controle da força isométrica de um músculo da mão. In: **XXV Congresso Brasileiro de Engenharia Biomédica**. Foz do Iguaçu – PR, Brazil: 2016.

GERMER, C. M.; ELIAS, L. A. Enhancement of force steadiness induced by sinusoidal vibrotactile stimulation depends on contraction intensity. In: **In Meeting of the Society for Neuroscience**. Washington – DC, USA: 2017.

GERMER, C. M. et al. Effects of vibrotactile stimulation on force steadiness on the behavior of motor units of the first dorsal interosseous muscle. In: **XXII International Society of Electrophysiology and Kinesiology**. Dublin, Ireland: 2018.

GERMER, C. M. et al. Improvement of force control induced by vibrotactile stimulation does not depend on the motor lateralization. In: **6th BRAINN Congress**. Campinas – SP, Brazil: 2019.

GERMER, C. M. et al. Sinusoidal vibrotactile stimulation differentially improves force steadiness depending on contraction intensity. **Medical & Biological Engineering & Computing**, p. 10, 2019. DOI:10.1007/s11517-019-01999-8.

### In Collaboration

S. MOREIRA, L. et al. Variabilidade de força e relação força/EMG de músculos mastigatórios na tarefa de mordida incisiva. In: **Anais do V Congresso Brasileiro de Eletromiografia e Cinesiologia e X Simpósio de**

**Engenharia Biomédica.** Uberlândia-MG, Brazil: Even3, 2017. p.891–894. DOI:10.29327/cobecseb.78892.

MOREIRA, L. S. et al. Estudo do controle motor de músculos mastigatórios na tarefa de mordida incisiva no bruxismo. In: **XXVI Brazilian Congress on Biomedical Engineering.** Búzios - RJ, Brazil: 2018. p.2.

MATOSO, D. E. C. et al. Signal-dependent noise in premotoneuronal commands is necessary to explain the interspike interval variability of spinal motor neurons XXVI Brazilian Congress on Biomedical Engineering. In: **XXVI Brazilian Congress on Biomedical Engineering.** Búzios - RJ, Brazil: 2018. p.2.

GERMER, C. M. et al. Shared common input to hand muscles during a two-degrees of freedom force task reveals muscle synergies. In: **XXII International Society of Electrophysiology and Kinesiology.** Dublin, Ireland: 2018.

CORREIA, M. F. C. et al. A study on the influence of contraction intensity on the H-reflex of a hand muscle. In: **XXCI Congresso de Iniciação Científica Unicamp.** Campinas - SP, Brazil: 2018. DOI:10.20396/revpibic.v0i0.id.

DEL-VECCHIO, A. et al. The human central nervous system transmits common synaptic inputs to distinct motor neuron pools during non-synergistic digit actions. **The Journal of Physiology,** p. JP278623, 2019. DOI:10.1113/JP278623.

## REFERENCES

---

ABRAIRA, V. E.; GINTY, D. D. The Sensory Neurons of Touch. **Neuron**, v. 79, n. 4, p. 618–639, 2013. DOI:10.1016/j.neuron.2013.07.051.

ADAM, A. et al. Hand Dominance and Motor Unit Firing Behavior. **Journal of Neurophysiology**, v. 80, p. 1373–1382, 1998. DOI:0022-3077/98.

ADAMO, D. E. et al. Upper limb kinesthetic asymmetries: Gender and handedness effects. **Neuroscience Letters**, v. 516, n. 2, p. 188–192, 2012. DOI:10.1016/j.neulet.2012.03.077.

AIMONETTI, J. M. et al. Proprioceptive control of wrist extensor motor units in humans: Dependence on handedness. **Somatosensory and Motor Research**, v. 16, n. 1, p. 11–29, 1999. DOI:10.1080/08990229970618.

AIMONETTI, J. M. et al. Mechanical cutaneous stimulation alters Ia presynaptic inhibition in human wrist extensor muscles: A single motor unit study. **Journal of Physiology**, v. 522, n. 1, p. 137–145, 2000. DOI:10.1111/j.1469-7793.2000.0137m.x.

AMJAD, A. M. et al. An extended difference of coherence test for comparing and combining several independent coherence estimates: Theory and application to the study of motor units and physiological tremor. **Journal of Neuroscience Methods**, v. 73, n. 1, p. 69–79, 1997. DOI:10.1016/S0165-0270(96)02214-5.

BAKER, S. N. et al. Afferent encoding of central oscillations in the monkey arm. **Journal of Neurophysiology**, v. 95, n. 6, p. 3904–3910, 2006. DOI:10.1152/jn.01106.2005.

BARRERA CURIEL, A. et al. The effects of vibration-induced altered stretch reflex sensitivity on maximal motor unit firing properties. **Journal of Neurophysiology**, n. 405, p. jn.00326.2018, 2019. DOI:10.1152/jn.00326.2018.

BARSS, T. S. et al. Equivalent bilateral early latency cutaneous reflex amplitudes during

graded contractions in right handers. **Biosystems and Biorobotics**, v. 7, p. 279–287, 2014. DOI:10.1007/978-3-319-08072-7\_47.

BAWEJA, H. S. et al. Removal of visual feedback alters muscle activity and reduces force variability during constant isometric contractions. **Experimental Brain Research**, v. 197, n. 1, p. 35–47, 2009. DOI:10.1007/s00221-009-1883-5.

BENSMAÏA, S. et al. Vibrotactile intensity and frequency information in the pacinian system: a psychophysical model. **Perception & psychophysics**, v. 67, n. 5, p. 828–841, 2005. DOI:10.3758/BF03193536.

BEUTER, A. Physiological tremor: Does handedness make a difference? **International Journal of Neuroscience**, v. 101, n. 1–4, p. 9–19, 2000. DOI:10.3109/00207450008986489.

BOGGIO, P. S. et al. Enhancement of non-dominant hand motor function by anodal transcranial direct current stimulation. **Neuroscience Letters**, v. 404, n. 1–2, p. 232–236, 2006. DOI:10.1016/j.neulet.2006.05.051.

BOLANOWSKI, S. J.; ZWISLOCKI, J. J. Intensity and frequency characteristics of pacinian corpuscles. I. Action potentials. **Journal of neurophysiology**, v. 51, n. 4, p. 793–811, 1984.

CALVIN, W. H.; STEVENS, C. F. Synaptic Noise as a Source of Variability in the Interval between Action Potentials. **Science**, v. 155, n. 3764, p. 842–844, 1967. DOI:10.1126/science.155.3764.842.

CALVIN, W. H.; STEVENS, C. F. Synaptic noise and other sources of randomness in motoneuron interspike intervals. **Journal of Neurophysiology**, v. 31, n. 4, p. 574–587, 1968. DOI:10.1152/jn.1968.31.4.574.

CASTRONOVO, A. M. et al. The proportion of common synaptic input to motor neurons

increases with an increase in net excitatory input. **Journal of Applied Physiology**, v. 119, n. 11, p. 1337–1346, 2015. DOI:10.1152/jappphysiol.00255.2015.

CHANDRAN, A. P. et al. Long latency inhibition of h-reflex recovery by cutaneous tactile stimulation in man: A cutaneous transcortical reflex. **Neuroscience**, v. 27, n. 3, p. 1037–1048, 1988. DOI:10.1016/0306-4522(88)90208-4.

CISI, R. R. L.; KOHN, A. F. Simulation system of spinal cord motor nuclei and associated nerves and muscles, in a Web-based architecture. **Journal of Computational Neuroscience**, v. 25, n. 3, p. 520–542, 2008. DOI:10.1007/s10827-008-0092-8.

COHEN, J. **Statistical power analysis for the behavioral sciences**. 2nd. ed. [s.l.] Lawrence Erlbaum, 1988.

COLLINS, J. J. et al. Noise-enhanced tactile sensation. **Nature**, v. 383, n. 6603, p. 770–770, 1996. DOI:10.1038/383770a0.

CORDO, P. et al. Noise in human muscle spindles. . 1996, p. 769–770. DOI:10.1038/383769a0.

COX, D. R. **Renewal Theory**. London: Butle & Tanner, 1962.

DATTA, A.; STEPHENS, J. A. The effects of digital nerve stimulation on the firing of motor units in human first dorsal interosseous muscle. **Journal of Physiology**, v. 318, p. 501–510, 1981. DOI:10.1113/jphysiol.1981.sp013880.

DE LUCA, C. J. et al. Behaviour of human motor units in different muscles during linearly varying contractions. **The Journal of physiology**, v. 329, n. 1982, p. 113–28, 1982.

DE LUCA, C. J.; CONTESSA, P. Hierarchical control of motor units in voluntary contractions. **Journal of neurophysiology**, v. 107, n. 1, p. 178–95, 2012. DOI:10.1152/jn.00961.2010.

DE NUNZIO, A. M. et al. Electro-tactile stimulation of the posterior neck induces body anteropulsion during upright stance. **Experimental Brain Research**, v. 236, n. 5, p. 1471–1478, 2018. DOI:10.1007/s00221-018-5229-z.

DEL VECCHIO, A. et al. The Central Nervous System Modulates the Neuromechanical Delay in a Broad Range for the Control of Muscle Force. **Journal of Applied Physiology**, p. japplphysiol.00135.2018, 2018. DOI:10.1152/japplphysiol.00135.2018.

DESTEXHE, A. et al. An efficient method for computing synaptic conductances based on a kinetic-model of receptor-binding. **Neural Computation**, v. 6, n. 1, p. 14–18, 1994.

DESTEXHE, A. Conductance-based integrate-and-fire models. **Neural Computation**, v. 9, n. 3, p. 503–514, 1997.

DETTMER, M. et al. Effects of aging and tactile stochastic resonance on postural performance and postural control in a sensory conflict task. **Somatosensory and Motor research**, v. 32, n. November, p. 1–8, 2015. DOI:10.3109/08990220.2015.1004045.

DIDERIKSEN, J. L. et al. Motor unit recruitment strategies and muscle properties determine the influence of synaptic noise on force steadiness. **Journal of Neurophysiology**, v. 107, n. 12, p. 3357–3369, 2012. DOI:jn.00938.2011 [pii]\n10.1152/jn.00938.2011.

DUNNETT, C. W. New Tables for Multiple Comparisons with a Control. **Biometrics**, v. 20, n. 3, p. 482–491, 1964. DOI:10.2307/2528490.

DURAND, D. M. et al. Reverse stochastic resonance in a hippocampal CA1 neuron model. In: **2013 35th Annual International Conference of the IEEE Engineering in Medicine and Biology Society (EMBC)**. IEEE, 2013. p.5242–5245. DOI:10.1109/EMBC.2013.6610731.

ELIAS, L. A. et al. Models of passive and active dendrite motoneuron pools and their

differences in muscle force control. **Journal of Computational Neuroscience**, v. 33, n. 3, p. 515–531, 2012. DOI:10.1007/s10827-012-0398-4.

ELIAS, L. A.; KOHN, A. F. Individual and collective properties of computationally efficient motoneuron models of types S and F with active dendrites. **Neurocomputing**, v. 99, p. 521–533, 2013. DOI:http://dx.doi.org/10.1016/j.neucom.2012.06.038.

ENOKA, R. M.; FUGLEVAND, A. J. Motor unit physiology: Some unresolved issues. **Muscle & Nerve**, v. 4598, n. February 2001, p. 3–17, 2001. DOI:10.1002/1097-4598(200101)24.

FARINA, D. et al. Decoding the neural drive to muscles from the surface electromyogram. **Clinical Neurophysiology**, v. 121, n. 10, p. 1616–1623, 2010. DOI:10.1016/j.clinph.2009.10.040.

FARINA, D. et al. The effective neural drive to muscles is the common synaptic input to motor neurons. **The Journal of Physiology**, v. 592, n. 16, p. 3427–3441, 2014. DOI:10.1113/jphysiol.2014.273581.

FARINA, D. et al. Principles of Motor Unit Physiology Evolve With Advances in Technology. **Physiology**, v. 31, n. 2, p. 83–94, 2016. DOI:10.1152/physiol.00040.2015.

FARINA, D.; HOLOBAR, A. Characterization of Human Motor Units From Surface EMG Decomposition. **Proceedings of the IEEE**, v. 104, n. 2, p. 353–373, 2016. DOI:10.1109/JPROC.2015.2498665.

FARINA, D.; NEGRO, F. Common synaptic input to motor neurons, motor unit synchronization, and force control. **Exercise and Sport Sciences Reviews**, v. 43, n. 1, p. 23–33, 2015. DOI:10.1249/JES.0000000000000032.

FEENEY, D. F. et al. Variability in common synaptic input to motor neurons modulates both force steadiness and pegboard time in young and older adults. **Journal of**

**Physiology**, v. 16, p. 3793–3806, 2018. DOI:10.1113/JP275658.

FLOWERS, K. Handedness and Controlled Movement. **British Journal of Psychology**, v. 66, n. 1, p. 39–52, 1975. DOI:10.1111/j.2044-8295.1975.tb01438.x.

FREEMAN, A. W.; JOHNSON, K. O. Cutaneous mechanoreceptors in macaque monkey: temporal discharge patterns evoked by vibration, and a receptor model. **The Journal of Physiology**, v. 323, n. 1, p. 21–41, 1982. DOI:10.1113/jphysiol.1982.sp014059.

FRIEDLI, W. G. et al. Detection threshold for percutaneous electrical stimuli: Asymmetry with respect to handedness. **Journal of Neurology, Neurosurgery and Psychiatry**, v. 50, n. 7, p. 870–876, 1987. DOI:10.1136/jnnp.50.7.870.

FUGLEVAND, A. J. et al. Models of recruitment and rate coding organization in motor-unit pools. **Journal of Neurophysiology**, v. 70, n. 6, p. 2470–2488, 1993.

GARNETT, B. Y. R.; STEPHENS, J. A. The reflex responses of single motor units in human first dorsal interosseus muscle following cutaneous afferent stimulation. **Journal of Physiology**, v. 303, p. 351–364, 1980. DOI:10.1113/jphysiol.1980.sp013290.

GARNETT, R.; STEPHENS, J. A. Changes in the recruitment threshold of motor units produced by cutaneous stimulation in man. **The Journal of physiology**, v. 311, p. 463–73, 1981. DOI:10.1113/jphysiol.1981.sp013598.

GERMER, C. et al. Force control with vibrotactile stimulation, 2018a. DOI:10.6084/m9.figshare.7447907.v1.

GERMER, C. M. et al. Enhancement of force steadiness induced by sinusoidal vibrotactile stimulation depends on contraction intensity. **47th Annual Meeting of the Society for Neuroscience**, 2017.

GERMER, C. M. et al. Effects of vibrotactile stimulation on force steadiness on the behavior of motor units of the first dorsal interosseous muscle. In: **XXII International**



**Society of Electrophysiology and Kinesiology**. Dublin, Ireland: 2018b.

GERMER, C. M. et al. Improvement of force control induced by vibrotactile stimulation does not depend on the motor lateralization. In: **6th BRAINN Congress**. Campinas - SP, Brazil: 2019a.

GERMER, C. M. et al. Sinusoidal vibrotactile stimulation differentially improves force steadiness depending on contraction intensity. **Medical and Biological Engineering and Computing**, v. 57, n. 8, p. 1813–1822, 2019b. DOI:10.1007/s11517-019-01999-8.

GOBLE, D. J.; BROWN, S. H. The biological and behavioral basis of upper limb asymmetries in sensorimotor performance. **Neuroscience and Biobehavioral Reviews**, v. 32, n. 3, p. 598–610, 2008. DOI:10.1016/j.neubiorev.2007.10.006.

HAN, J. et al. Bimanual proprioceptive performance differs for right- and left-handed individuals. **Neuroscience Letters**, v. 542, p. 37–41, 2013a. DOI:10.1016/j.neulet.2013.03.020.

HAN, J. et al. Proprioceptive performance of bilateral upper and lower limb joints: Side-general and site-specific effects. **Experimental Brain Research**, v. 226, n. 3, p. 313–323, 2013b. DOI:10.1007/s00221-013-3437-0.

HARRIS, C. M.; WOLPERT, D. M. Signal-dependent noise determines motor planning. **Nature**, v. 394, n. 6695, p. 780–784, 1998. DOI:10.1038/29528.

HARWOOD, B. et al. The effect of tendon vibration on motor unit activity, intermuscular coherence and force steadiness in the elbow flexors of males and females. **Acta Physiologica**, v. 211, n. 4, p. 597–608, 2014. DOI:10.1111/apha.12319.

HECKMAN, C. J.; ENOKA, R. M. Motor unit. **Comprehensive Physiology**, v. 2, n. 4, p. 2629–2682, 2012. DOI:10.1002/cphy.c100087.

HOLOBAR, A. et al. Accurate identification of motor unit discharge patterns from high-

density surface EMG and validation with a novel signal-based performance metric. **Journal of Neural Engineering**, v. 11, n. 1, 2014. DOI:10.1088/1741-2560/11/1/016008.

HOLOBAR, A.; ZAZULA, D. Multichannel blind source separation using convolution Kernel compensation. **IEEE Transactions on Signal Processing**, v. 55, n. 9, p. 4487–4496, 2007. DOI:10.1109/TSP.2007.896108.

ILES, J. F. Evidence for cutaneous and corticospinal modulation of presynaptic inhibition of Ia afferents from the human lower limb. **Journal of Physiology**, v. 491, n. 1, p. 197–207, 1996. DOI:10.1113/jphysiol.1996.sp021207.

ILIOPOULOS, F. et al. Electrical noise modulates perception of electrical pulses in humans: sensation enhancement via stochastic resonance. **Journal of Neurophysiology**, v. 111, n. 6, p. 1238–1248, 2014. DOI:10.1152/jn.00392.2013.

JITKRITSADAKUL, O. et al. Exploring the effect of electrical muscle stimulation as a novel treatment of intractable tremor in Parkinson's disease. **Journal of the Neurological Sciences**, v. 358, n. 1–2, p. 146–152, 2015. DOI:10.1016/j.jns.2015.08.1527.

JONES, K. E. et al. Sources of signal-dependent noise during isometric force production. **Journal of Neurophysiology**, v. 88, n. 3, p. 1533–1544, 2002.

KAMEN, G. et al. Lateral dominance and motor unit firing behavior. **Brain Research**, v. 576, n. 1, p. 165–167, 1992. DOI:10.1016/0006-8993(92)90625-J.

KANDEL, E. et al. **Principles of Neuroscience**. 5th. ed. [s.l.] McGraw Hill Professional, 2013.

KAUT, O. et al. Postural Stability in Parkinson's Disease Patients Is Improved after Stochastic Resonance Therapy. **Parkinson's Disease**, v. 2016, p. 1–7, 2016.

DOI:10.1155/2016/7948721.

KEENAN, K. G.; VALERO-CUEVAS, F. J. Experimentally Valid Predictions of Muscle Force and EMG in Models of Motor-Unit Function Are Most Sensitive to Neural Properties. **Journal of Neurophysiology**, v. 98, n. 3, p. 1581–1590, 2007. DOI:10.1152/jn.00577.2007.

KIEHN, O.; EKEN, T. Prolonged firing in motor units: evidence of plateau potentials in human motoneurons? **Journal of Neurophysiology**, v. 78, n. 6, p. 3061–3068, 1997.

KOUZAKI, M. et al. Subthreshold electrical stimulation reduces motor unit discharge variability and decreases the force fluctuations of plantar flexion. **Neuroscience Letters**, v. 513, n. 2, p. 146–150, 2012. DOI:10.1016/j.neulet.2012.02.020.

KURITA, Y. et al. Wearable Sensorimotor Enhancer for a Fingertip Based on Stochastic Resonance Effect. **IEE Transactions on human-machine systems**, v. 43, n. 3, p. 333–337, 2013.

KURITA, Y. et al. Surgical Grasping Forceps with Enhanced Sensorimotor Capability via the Stochastic Resonance Effect. **IEEE/ASME Transactions on Mechatronics**, v. 21, n. 6, p. 2624–2634, 2016. DOI:10.1109/TMECH.2016.2591591.

LAIDLAW, D. H. et al. Steadiness is reduced and motor unit discharge is more variable in old adults. **Muscle & Nerve**, v. 23, n. 4, p. 600–612, 2000. DOI:10.1002/(SICI)1097-4598(200004)23:4<600::AID-MUS20>3.0.CO;2-D.

LAKSHMINARAYANAN, K. et al. Application of vibration to wrist and hand skin affects fingertip tactile sensation. **Physiological Reports**, v. 3, n. 7, p. e12465, 2015. DOI:10.14814/phy2.12465.

LEMON, R. N. Descending Pathways in Motor Control. **Annual Review of Neuroscience**, v. 31, n. 1, p. 195–218, 2008.

DOI:10.1146/annurev.neuro.31.060407.125547.

LI, K. et al. Coordination of digit force variability during dominant and non-dominant sustained precision pinch. **Experimental Brain Research**, v. 233, n. 7, p. 2053–2060, 2015. DOI:10.1007/s00221-015-4276-y.

LODHA, N.; CHRISTOU, E. A. Low-Frequency Oscillations and Control of the Motor Output. **Frontiers in Physiology**, v. 8, n. February, p. 1–9, 2017. DOI:10.3389/fphys.2017.00078.

MAGALHAES, F. H.; KOHN, A. F. Vibratory noise to the fingertip enhances balance improvement associated with light touch. **Experimental Brain Research**, v. 209, n. 1, p. 139–151, 2011. DOI:10.1007/s00221-010-2529-3.

MANJARREZ, E. et al. Stochastic resonance in human electroencephalographic activity elicited by mechanical tactile stimuli. **Neuroscience Letters**, v. 324, n. 3, p. 213–216, 2002. DOI:10.1016/S0304-3940(02)00212-4.

MANJARREZ, E. et al. Stochastic resonance within the somatosensory system: effects of noise on evoked field potentials elicited by tactile stimuli. **Journal of Neuroscience**, v. 23, n. 6, p. 1997–2001, 2003.

MARCHAND-PAUVERT, V. et al. Handedness-related asymmetry in transmission in a system of human cervical premotoneurons. **Experimental Brain Research**, v. 125, n. 3, p. 323–334, 1999. DOI:10.1007/s002210050688.

MARTINEZ-VALDES, E. et al. High-density surface electromyography provides reliable estimates of motor unit behavior. **Clinical Neurophysiology**, v. 127, n. 6, p. 2534–2541, 2016. DOI:10.1016/j.clinph.2015.10.065.

MATTHEWS, P. B. C. Relationship of firing intervals of human motor units to the trajectory of post-spike after-hyperpolarization and synaptic noise. **Journal of**

**Physiology**, v. 492, n. 2, p. 597–628, 1996. DOI:10.1113/jphysiol.1996.sp021332.

MCDONNELL, M. D.; ABBOTT, D. What is stochastic resonance? Definitions, misconceptions, debates, and its relevance to biology. **PLoS computational biology**, v. 5, n. 5, p. e1000348, 2009. DOI:10.1371/journal.pcbi.1000348.

MCDONNELL, M. D.; WARD, L. M. The benefits of noise in neural systems: bridging theory and experiment. **Nature Reviews Neuroscience**, v. 12, n. 7, p. 415–426, 2011. DOI:10.1038/nrn3061 nrn3061 [pii].

MENDEZ-BALBUENA, I. et al. Improved Sensorimotor Performance via Stochastic Resonance. **Journal of Neuroscience**, v. 32, n. 36, p. 12612–12618, 2012. DOI:10.1523/JNEUROSCI.0680-12.2012.

MILNER-BROWN, H. S. et al. The contractile properties of human motor units during voluntary isometric contractions. **Journal of Physiology**, v. 228, n. 2, p. 285–306, 1973.

MOON, H. et al. Force control is related to low-frequency oscillations in force and surface EMG. **PLoS ONE**, v. 9, n. 11, p. e109202, 2014. DOI:10.1371/journal.pone.0109202.

MORITZ, C. T. et al. Discharge Rate Variability Influences the Variation in Force Fluctuations Across the Working Range of a Hand Muscle. **Journal of Neurophysiology**, v. 93, n. 5, p. 2449–2459, 2005. DOI:10.1152/jn.01122.2004.

MOSIER, E. M. et al. The influence of prolonged vibration on motor unit behavior. **Muscle and Nerve**, v. 55, n. 4, p. 500–507, 2017. DOI:10.1002/mus.25270.

MOSS, F. Stochastic resonance and sensory information processing: a tutorial and review of application. **Clinical Neurophysiology**, v. 115, n. 2, p. 267–281, 2004. DOI:10.1016/j.clinph.2003.09.014.

MULAVARA, A. P. et al. Improving balance function using vestibular stochastic resonance: optimizing stimulus characteristics. **Experimental brain research**, v. 210, n.

2, p. 303–12, 2011. DOI:10.1007/s00221-011-2633-z.

NAGAMORI, A. et al. Cardinal features of involuntary force variability can arise from the closed-loop control of viscoelastic afferented muscles. **PLOS Computational Biology**, v. 14, n. 1, p. e1005884, 2018. DOI:10.1371/journal.pcbi.1005884.

NAITO, E. et al. Dominance of the Right Hemisphere and Role of Area 2 in Human Kinesthesia. **Journal of Neurophysiology**, n. September 2004, p. 1020–1034, 2011. DOI:10.1152/jn.00637.2004.

NAKASHIMA, K. et al. Cutaneous effects on presynaptic inhibition of flexor Ia afferents in the human forearm. **The Journal of physiology**, v. 426, p. 369–80, 1990.

NEGRO, F. et al. Fluctuations in isometric muscle force can be described by one linear projection of low-frequency components of motor unit discharge rates. **Journal of Physiology**, v. 587, n. Pt 24, p. 5925–5938, 2009. DOI:jphysiol.2009.178509 [pii]\n10.1113/jphysiol.2009.178509.

NEGRO, F. et al. The human motor neuron pools receive a dominant slow-varying common synaptic input. **Journal of Physiology**, v. 594, n. 19, p. 5491–5505, 2016. DOI:10.1113/JP271748.

NEGRO, F.; FARINA, D. Linear transmission of cortical oscillations to the neural drive to muscles is mediated by common projections to populations of motoneurons in humans. **Journal of Physiology**, v. 589, n. Pt 3, p. 629–637, 2011a. DOI:10.1113/jphysiol.2010.202473jphysiol.2010.202473 [pii].

NEGRO, F.; FARINA, D. Decorrelation of cortical inputs and motoneuron output. **Journal of Neurophysiology**, v. 106, n. 5, p. 2688–2697, 2011b. DOI:10.1152/jn.00336.2011.

NOVAK, T.; NEWELL, K. M. Physiological tremor (8–12Hz component) in isometric force control. **Neuroscience Letters**, v. 641, p. 87–93, 2017.

DOI:10.1016/j.neulet.2017.01.034.

OFORI, E. et al. Visuomotor and audiomotor processing in continuous force production of oral and manual effectors. **Journal of motor behavior**, v. 44, n. 2, p. 87–96, 2012.

DOI:10.1080/00222895.2012.654523.

OLDFIELD, R. C. The assessment and analysis of handedness: The Edinburgh inventory. **Neuropsychologia**, v. 9, n. 1, p. 97–113, 1971. DOI:10.1016/0028-3932(71)90067-4.

PIERROT-DESEILLIGNY, E.; BURKE, D. **The Circuitry of the Human Spinal Cord**. Cambridge: Cambridge University Press, 2012. DOI:10.1017/CBO9781139026727.

PINCUS, S. M. Approximate entropy as a measure of system complexity. **Proceedings of the National Academy of Sciences**, v. 88, n. 6, p. 2297–2301, 1991.

DOI:10.1073/pnas.88.6.2297.

PRIORI, A. et al. Human handedness and asymmetry of the motor cortical silent period. **Experimental Brain Research**, v. 128, n. 3, p. 390–396, 1999.

DOI:10.1007/s002210050859.

PRIPLATA, A. et al. Noise-Enhanced Human Balance Control. **Physical Review Letters**, v. 89, n. 23, p. 238101, 2002. DOI:10.1103/PhysRevLett.89.238101.

PRIPLATA, A. A. et al. Vibrating insoles and balance control in elderly people. **The Lancet**, v. 362, n. 9390, p. 1123–1124, 2003. DOI:10.1016/S0140-6736(03)14470-4.

PRIPLATA, A. A. et al. Noise-enhanced balance control in patients with diabetes and patients with stroke. **Annals of Neurology**, v. 59, n. 1, p. 4–12, 2006.

DOI:10.1002/ana.20670.

PROCHAZKA, A.; ELLAWAY, P. Sensory systems in the control of movement. **Comprehensive Physiology**, v. 2, p. 2615–2627, 2012.

DOI:dx.doi.org/10.1002/cphy.c100086.

PROSKE, U.; ALLEN, T. The neural basis of the senses of effort, force and heaviness. **Experimental Brain Research**, v. 237, n. 3, p. 589–599, 2019. DOI:10.1007/s00221-018-5460-7.

PROSKE, U.; GANDEVIA, S. C. The Proprioceptive Senses: Their Roles in Signaling Body Shape, Body Position and Movement, and Muscle Force. **Physiological Reviews**, v. 92, n. 4, p. 1651–1697, 2012. DOI:10.1152/physrev.00048.2011.

SAINBURG, R. L. Evidence for a dynamic-dominance hypothesis of handedness. **Experimental Brain Research**, v. 142, n. 2, p. 241–258, 2002. DOI:10.1007/s00221-001-0913-8.

SAMOUDI, G. et al. Effects of stochastic vestibular galvanic stimulation and LDOPA on balance and motor symptoms in patients with Parkinson's disease. **Brain Stimulation**, v. 8, n. 3, p. 474–480, 2015. DOI:10.1016/j.brs.2014.11.019.

SATO, M. Response of Pacinian corpuscles to sinusoidal vibration. **The Journal of Physiology**, v. 159, p. 391–409, 1961. DOI:10.1113/jphysiol.1961.sp006817.

SCHMIED, A. et al. Human spinal lateralization assessed from motoneurone synchronization: dependence on handedness and motor unit type. **The Journal of Physiology**, v. 480, n. 2, p. 369–387, 1994. DOI:10.1113/jphysiol.1994.sp020367.

SEMMLER, J. G.; NORDSTROM, M. A. Influence of handedness on motor unit discharge properties and force tremor. **Experimental Brain Research**, v. 104, n. 1, p. 115–125, 1995. DOI:10.1007/BF00229861.

SEMMLER, J. G.; NORDSTROM, M. A. Motor unit discharge and force tremor in skill- and strength-trained individuals. **Experimental Brain Research**, v. 119, n. 1, p. 27–38, 1998. DOI:10.1007/s002210050316.



SEO, N. J. et al. Effect of remote sensory noise on hand function post stroke. **Frontiers in human neuroscience**, v. 8, n. 934, p. 1–19, 2014. DOI:10.3389/fnhum.2014.00934.

SHERRINGTON, C. S. Remarks on some Aspects of Reflex Inhibition. **Proceedings of the Royal Society B: Biological Sciences**, v. 97, n. 686, p. 519–545, 1925. DOI:10.1098/rspb.1925.0017.

SLIFKIN, A. B.; NEWELL, K. M. Noise, Information Transmission, and Force Variability. **Journal of Experimental Psychology**, v. 25, n. 3, p. 837–851, 1999.

SLIFKIN, A. B.; NEWELL, K. M. Variability and noise in continuous force production. **Journal of Motor Behavior**, v. 32, n. 2, p. 141–150, 2000. DOI:10.1080/00222890009601366.

SOSNOFF, J. J.; NEWELL, K. M. Intermittent visual information and the multiple time scales of visual motor control of continuous isometric force production. **Perception & Psychophysics**, v. 67, n. 2, p. 335–44, 2005.

TAN, U. The H-reflex recovery curve from the wrist flexors: Lateralization of motoneuronal excitability in relation to handedness in normal subjects. **International Journal of Neuroscience**, v. 48, n. 3–4, p. 271–284, 1989a. DOI:10.3109/00207458909002170.

TAN, Ü. Lateralization of the Hoffmann Reflex from the Long Flexor Thumb Muscle in Right-and Left-Handed Normal Subjects. **International Journal of Neuroscience**, v. 48, n. 3–4, p. 313–315, 1989b. DOI:10.3109/00207458909002176.

TASK, A.; HONDA, H. Rightward superiority of eye movements in a bimanual. **The Quarterly Journal of Experimental Psychology Section A**, v. 34, n. 4, p. 499–513, 1982. DOI:10.1080/14640748208400833.

TENAN, M. S. et al. The effect of imperceptible Gaussian tendon vibration on the

Hoffmann reflex **Neuroscience Letters**, 2019. DOI:10.1016/j.neulet.2019.05.018.

THOMPSON, C. K. et al. Robust and accurate decoding of motoneuron behaviour and prediction of the resulting force output. **Journal of Physiology**, v. 596, n. 14, p. 2643–2659, 2018. DOI:10.1113/JP276153.

TOLEDO, D. R. et al. Improved proprioceptive function by application of subsensory electrical noise: effects of aging and task-demand. **Neuroscience**, n. July, 2017. DOI:10.1016/j.neuroscience.2017.06.045.

TRENADO, C. et al. Broad-band Gaussian noise is most effective in improving motor performance and is most pleasant. **Frontiers in Human Neuroscience**, v. 8, n. February, p. 22, 2014a. DOI:10.3389/fnhum.2014.00022.

TRENADO, C. et al. Suppression of Enhanced Physiological Tremor via Stochastic Noise: Initial Observations. **PLoS ONE**, v. 9, n. 11, p. e112782, 2014b. DOI:10.1371/journal.pone.0112782.

TRENADO, C. et al. Enhanced corticomuscular coherence by external stochastic noise. **Frontiers in Human Neuroscience**, v. 8, n. May, p. 1–10, 2014c. DOI:10.3389/fnhum.2014.00325.

WATANABE, R.; KOHN, A. Nonlinear frequency-domain analysis of the transformation of cortical inputs by a motoneuron pool-muscle complex. **IEEE Transactions on Neural Systems and Rehabilitation Engineering**, v. 4320, n. c, p. 1–1, 2017. DOI:10.1109/TNSRE.2017.2701149.

WATANABE, R. N. et al. Influences of premotoneuronal command statistics on the scaling of motor output variability during isometric plantar flexion. **Journal of Neurophysiology**, v. 110, n. 11, p. 2592–606, 2013. DOI:10.1152/jn.00073.2013.

WATANABE, R. N.; KOHN, A. F. Fast Oscillatory Commands from the Motor Cortex Can

Be Decoded by the Spinal Cord for Force Control. **The Journal of Neuroscience**, v. 35, n. 40, p. 13687–13697, 2015. DOI:10.1523/JNEUROSCI.1950-15.2015.

XU, L. et al. Does vibration superimposed on low-level isometric contraction alter motor unit recruitment strategy? **Journal of Neural Engineering**, v. 15, n. 6, p. 066001, 2018. DOI:10.1088/1741-2552/aadc43.

YADAV, V.; SAINBURG, R. L. Limb dominance results from asymmetries in predictive and impedance control mechanisms. **PLoS ONE**, v. 9, n. 4, 2014. DOI:10.1371/journal.pone.0093892.

## ATTACHMENTS

---

**TERMO DE CONSENTIMENTO LIVRE E ESCLARECIDO****AVALIAÇÃO DO FENÔMENO DE RESSONÂNCIA ESTOCÁSTICA NO CONTROLE NEUROFISIOLÓGICO DA FORÇA MUSCULAR EM SUJEITOS COM A DOENÇA DE PARKINSON****Prof. Dr. Leonardo Abdala Elias****Número do CAAE: 59961616.8.0000.5404**

Você está sendo convidado a participar como voluntário de uma pesquisa. Este documento, chamado Termo de Consentimento Livre e Esclarecido, visa assegurar seus direitos como participante e é elaborado em duas vias, uma que deverá ficar com você e outra com o pesquisador.

Por favor, leia com atenção e calma, aproveitando para esclarecer suas dúvidas. Se houver perguntas antes ou mesmo depois de assiná-lo, você poderá esclarecê-las com o pesquisador. Se preferir, pode levar este Termo para casa e consultar seus familiares ou outras pessoas antes de decidir participar. Não haverá nenhum tipo de penalização ou prejuízo se você não aceitar participar ou retirar sua autorização em qualquer momento.

**Justificativa e objetivos:**

A doença do Parkinson é uma patologia que afeta o controle da força e pode ser acompanhada por um tremor estático e/ou de ação. Nós queremos avaliar se uma vibração aplicada na ponta do dedo indicador é capaz de promover uma melhoria no controle da força nos sujeitos com a doença de Parkinson e, para fins de comparação, em sujeitos saudáveis. Este fenômeno é denominado ressonância estocástica e existem indícios de seu efeito no desempenho motor de seres humanos. Esperamos que os resultados deste projeto possam aumentar o entendimento sobre os mecanismos neurofisiológicos por trás do tremor fisiológico e parkinsoniano.

**Procedimentos:**

Participando do estudo você está sendo convidado a: participar de uma única avaliação com visita previamente agendada, de aproximadamente 2h, no Laboratório de Pesquisa em Neuroengenharia na Faculdade de Engenharia Elétrica e de Computação, situado no próprio campus da UNICAMP. O estudo contempla a avaliação da força exercida por um músculo da mão (primeiro interósseo dorsal), com e sem a presença de uma vibração na ponta do dedo indicador. A atividade deste músculo será registrada por meio da eletromiografia de superfície e intramuscular (com fios finos). A primeira é uma técnica não invasiva e indolor, onde são fixados eletrodos de superfície com fita *Transpore* (hipoalergênica) na pele limpa com álcool 70%. A segunda, no entanto, necessita do auxílio de uma agulha (260µm de diâmetro) para a inserção dos eletrodos de fios finos (50µm de diâmetro). O conjunto agulha+fios serão esterilizados antes de serem inseridos no músculo. Em seguida, a agulha será removida e os fios permanecerão no músculo durante a execução da tarefa, mas são imperceptíveis. O procedimento para esta última técnica causará pouco desconforto, porém, a manutenção dos fios durante a realização das tarefas é indolor. Depois de esclarecer quaisquer dúvidas serão iniciadas as tarefas de força constante de abdução do dedo indicador, com 1min de descanso entre cada repetição, para evitar a fadiga da musculatura. Durante a execução de algumas tarefas, você poderá sentir uma vibração indolor na ponta do dedo indicador. Você participará de um dos grupos do estudo, que são: grupo controle (jovem ou idoso/meia idade) e grupo com a doença de Parkinson. É importante ressaltar que este estudo não vai interferir no tratamento da doença de Parkinson, e que os remédios deverão ser mantidos nos horários regulares. Caso você seja do grupo de Parkinson, os experimentos serão realizados logo após o atendimento no Ambulatório de Neurologia do Hospital das Clínicas da UNICAMP.

Rubrica do pesquisador: \_\_\_\_\_ Rubrica do participante: \_\_\_\_\_

**Desconfortos e riscos:**

Você **não** deve participar deste estudo se: apresentar patologias neurológicas, musculares, esqueléticas, degenerativas e cognitivas.

Todas as avaliações e equipamentos utilizados neste estudo são seguros e não oferecem nenhum dano ou risco previsíveis aos voluntários. Todos os membros da equipe de pesquisadores têm experiência prévia nas técnicas de registro e análises que serão utilizadas neste estudo.

**Benefícios:**

Não haverá benefícios diretos aos participantes desta pesquisa. Espera-se que esta pesquisa possa oferecer mais recursos para o entendimento das causas neurofisiológicas envolvidas no tremor fisiológico e parkinsoniano, além de aumentar exemplos na literatura da ocorrência do fenômeno da ressonância estocástica no sistema sensorio-motor humano.

**Acompanhamento e assistência:**

Após o encerramento das avaliações do estudo, não será realizado o acompanhamento ou novas intervenções. Não se espera nenhuma intercorrência durante a realização dos experimentos. Porém, caso os voluntários sintam quaisquer desconfortos decorrentes da realização das tarefas propostas, a médica e o fisioterapeuta da equipe de pesquisadores darão suporte para que os sintomas sejam minimizados.

**Sigilo e privacidade:**

Você tem a garantia de que sua identidade será mantida em sigilo e nenhuma informação será dada a outras pessoas que não façam parte da equipe de pesquisadores. Na divulgação dos resultados desse estudo, seu nome não será citado.

**Ressarcimento e indenização:**

Não haverá qualquer despesa e nem gratificações financeiras para a sua participação no estudo. Se sua participação no estudo ocorrer fora do horário que você habitualmente frequenta o campus da UNICAMP, para suas atividades estudantis ou laborais, serão ressarcidos os gastos referentes ao transporte e à alimentação. Além disso, garantimos também o ressarcimento dos gastos de transporte e alimentação de seus acompanhantes. Você terá a garantia ao direito a indenização diante de eventuais danos decorrentes da pesquisa.

**Contato:**

Em caso de dúvidas sobre a pesquisa, você poderá entrar em contato com o pesquisador responsável **Leonardo Abdala Elias**, no **Laboratório de Pesquisa em Neuroengenharia da Faculdade de Engenharia Elétrica e de Computação da UNICAMP**, situado na **Rua João Pandiá Calógeras, 110, CEP: 13 083-870, Cidade Universitária, Campinas-SP**, telefone: **(19) 3521-3756**, e-mail: **leoelias@fee.unicamp.br**.

Em caso de denúncias ou reclamações sobre sua participação e sobre questões éticas do estudo, você poderá entrar em contato com a secretaria do Comitê de Ética em Pesquisa (CEP) da UNICAMP das 08:30hs às 11:30hs e das 13:00hs às 17:00hs na Rua: Tessália Vieira de Camargo, 126; CEP 13083-887 Campinas – SP; telefone (19) 3521-8936 ou (19) 3521-7187; e-mail: [cep@fcm.unicamp.br](mailto:cep@fcm.unicamp.br).

**O Comitê de Ética em Pesquisa (CEP).**

O papel do CEP é avaliar e acompanhar os aspectos éticos de todas as pesquisas envolvendo seres humanos. A Comissão Nacional de Ética em Pesquisa (CONEP), tem por objetivo desenvolver a regulamentação sobre proteção dos seres humanos envolvidos nas

Rubrica do pesquisador: \_\_\_\_\_ Rubrica do participante: \_\_\_\_\_

pesquisas. Desempenha um papel coordenador da rede de Comitês de Ética em Pesquisa (CEPs) das instituições, além de assumir a função de órgão consultor na área de ética em pesquisas

**Consentimento livre e esclarecido:**

Após ter recebido esclarecimentos sobre a natureza da pesquisa, seus objetivos, métodos, benefícios previstos, potenciais riscos e o incômodo que esta possa acarretar, aceito participar:

Nome do(a) participante: \_\_\_\_\_

\_\_\_\_\_ Data: \_\_\_\_/\_\_\_\_/\_\_\_\_.

(Assinatura do participante ou nome e assinatura do seu RESPONSÁVEL LEGAL)

**Responsabilidade do Pesquisador:**

Asseguro ter cumprido as exigências da resolução 466/2012 CNS/MS e complementares na elaboração do protocolo e na obtenção deste Termo de Consentimento Livre e Esclarecido. Asseguro, também, ter explicado e fornecido uma via deste documento ao participante. Informo que o estudo foi aprovado pelo CEP perante o qual o projeto foi apresentado. Comprometo-me a utilizar o material e os dados obtidos nesta pesquisa exclusivamente para as finalidades previstas neste documento ou conforme o consentimento dado pelo participante.

\_\_\_\_\_ Data: \_\_\_\_/\_\_\_\_/\_\_\_\_.  
(Assinatura do Pesquisador)

Rubrica do pesquisador: \_\_\_\_\_ Rubrica do participante: \_\_\_\_\_

23/07/2019

RightsLink Printable License

<b>SPRINGER NATURE LICENSE TERMS AND CONDITIONS</b>	
Jul 23, 2019	
<p>This Agreement between Carina Germer ("You") and Springer Nature ("Springer Nature") consists of your license details and the terms and conditions provided by Springer Nature and Copyright Clearance Center.</p>	
License Number	4634790000127
License date	Jul 23, 2019
Licensed Content Publisher	Springer Nature
Licensed Content Publication	Medical & Biological Engineering & Computing
Licensed Content Title	Sinusoidal vibrotactile stimulation differentially improves force steadiness depending on contraction intensity
Licensed Content Author	Carina Marconi Germer, Luciana Sobral Moreira, Leonardo Abdala Elias
Licensed Content Date	Jan 1, 2019
Type of Use	Thesis/Dissertation
Requestor type	academic/university or research institute
Format	electronic
Portion	full article/chapter
Will you be translating?	no
Circulation/distribution	<501
Author of this Springer Nature content	yes
Title	Evaluation of the effects of sinusoidal vibrotactile stimulation on the neurophysiological control of muscle force
Institution name	University of Campinas
Expected presentation date	Sep 2019